Structure–function analysis of RNA polymerase II: use of RNA as a template and site-directed mutagenesis in *S. cerevisiae*

Elisabeth Lehmann
aus Dresden

2010

Dissertation zur Erlangung des Doktorgrades der Fakultät für Chemie und Pharmazie der Ludwig-Maximilians-Universität München

Structure–function analysis of RNA polymerase II: use of RNA as a template and site-directed mutagenesis in *S. cerevisiae*

Elisabeth Lehmann
aus Dresden

2010

Erklärung

Diese Dissertation wurde im Sinne von §13 Abs. 3 bzw. 4 der Promotionsordnung vom 29. Januar 1998 (in der Fassung der vierten Änderungssatzung vom 26. November 2004) von Herrn Prof. Dr. Patrick Cramer betreut.

Ehrenwörtliche Versicherung

Diese Dissertation wurde selbständig, ohne unerlaubte Hilfe erarbeitet.

München, am

_____

Elisabeth Lehmann

Dissertation eingereicht am: 03. Dezember 2010

Erstgutachter: Prof. Dr. Patrick Cramer

Zweitgutachter: Prof. Dr. Dietmar Martin

Tag der mündlichen Prüfung: 31. Januar 2011

Acknowledgements

I would like to thank all former and current members of the Cramer lab for the great working environment and always being open for questions.

Bei meiner Familie bedanke ich mich für die permanente Unterstützung, auch während meines Studiums.

Summary

During this work structural and functional analysis of RNA polymerase II (Pol II) was conducted. RNA polymerase II is the enzyme performing DNA transcription by synthesising messenger RNAs in the nucleus of eukaryotic cells. Human cells can be infected by hepatitis B virus together with its satellite hepatitis D virus (HDV). The complementary RNA genome and antigenome of HDV are replicated by direct transcription from each other without a reverse transcription step involving DNA. As HDV does not encode for a polymerase and its replication does not rely on hepatitis B virus, human host RNA polymerase was implicated to perform HDV replication. As a dedicated RNA-dependent RNA polymerase was not known in humans, DNA-dependent RNA polymerases were hypothesised to perform RNA synthesis from HDV RNA templates. The first part of this work shows that Pol II from budding yeast *Saccharomyces cerevisiae*, which is closely related to human Pol II, indeed has RNA-dependent RNA polymerase activity *in vitro*. The activity is much slower and less processive than the DNA-dependent reaction. It could be a rudimentary activity of Pol II that was used during the theorised time of the "RNA world" earlier in evolution when RNA genomes existed and before DNA became the primary carrier of genetic information.

As Pol II is an elementary enzyme for cellular protein biogenesis it is an interesting object of regulative and mechanistic studies. Directed mutagenesis of Pol II can be used to analyse contributions of residues to enzyme activity both *in vivo* and *in vitro*. As Pol II cannot be reconstituted from recombinantly expressed subunits, mutations have to be introduced endogenously. To facilitate mutagenesis in yeast, a plasmid-based mutagenesis system for the largest subunit Rpb1 was established within the second part of this work. Lethal mutations can be easily identified but corresponding enzymes could not be purified. Pol II mutants that are still capable of keeping cells viable were successfully cloned and purified. Pol II mutants produced based on the system are active in biochemical assays *in vitro*. The system opens up new opportunities to generate various Pol II mutants to address diverse questions in Pol II-related studies.

Publications

Parts of this work have been published or are in the process of publication:

Kashkina E, Anikin M, Brueckner F, Lehmann E, Kochetkov SN, McAllister WT, Cramer P, Temiakov D (2007). Multisubunit RNA polymerases melt only a single DNA base pair downstream of the active site. *J Biol Chem* **282**(30)**:** 21578-21582. Erratum in (2009): *J Biol Chem* **284:** 22500.

Lehmann E, Brueckner F, Cramer P (2007). Molecular basis of RNA-dependent RNA polymerase II activity. *Nature* **450:** 445-449.

Cramer P, Armache KJ, Baumli S, Benkert S, Brueckner F, Buchen C, Damsma GE, Dengl S, Geiger SR, Jasiak AJ, Jawhari A, Jennebach S, Kamenski T, Kettenberger H, Kuhn CD, Lehmann E, Leike K, Sydow JF, Vannini A (2008). Structure of eukaryotic RNA polymerases. *Annu Rev Biophys* **37:** 337-352.

Brueckner F, Armache KJ, Cheung A, Damsma GE, Kettenberger H, Lehmann E, Sydow J, Cramer P (2009). Structure-function studies of the RNA polymerase II elongation complex. *Acta Crystallogr D Biol Crystallogr* **65:** 112-120.

Sydow JF, Brueckner F, Cheung AC, Damsma GE, Dengl S, Lehmann E, Vassylyev D, Cramer P (2009). Structural basis of transcription: mismatch-specific fidelity mechanisms and paused RNA polymerase II with frayed RNA. *Mol Cell* **34:** 710-721.

Ruan W, Lehmann E, Thomm M, Kostrewa D, Cramer P. Evolution of two mechanisms for intrinsic RNA polymerase transcript cleavage. Manuscript in preparation.

Table of contents

1 Introduction

1.1 DNA transcription in eukaryotes

In living organisms genetic information is stored in the form of DNA. Transcription of genes encoded on DNA is performed by a single DNA-dependent RNA polymerase in prokaryotic cells. In the nucleus of eukaryotic cells, DNA is transcribed into RNA by three evolutionarily related but different types of polymerases. The three RNA polymerases show different sensitivities to the inhibitory mushroom toxin α-amanitin. Pol II is inhibited at low concentrations, yeast Pol I is much less sensitive and yeast Pol III activity is not affected by α-amanitin (Schultz & Hall, 1976) contrary to vertebrate Pol I and Pol III (Schwartz *et al.*, 1974). Pol I synthesises the precursor of 18S, 5.8S and 28S rRNA. 5S rRNA and all tRNAs are produced by Pol III. Pol II transcribes protein coding genes into mRNA and also synthesises small nuclear RNAs (Berg *et al.*, 2002). Noncoding RNAs synthesised by Pol IV and Pol V, two additional RNA polymerases found only in plants, play a role in RNA interference (Matzke *et al.*, 2009). After processing of mRNA precursors ribosomes in the cytoplasm translate the mRNA-encoded information and synthesise proteins.

1.2 RNA Pol II from *S. cerevisiae*

Concerning sequence and structure, Pol II is homologous to Pol I and Pol III (Cramer *et al.*, 2008) as well as to prokaryotic (Vassylyev *et al.*, 2002; Zhang Y. *et al.*, 2006) and archaeal RNA polymerases (Kusser *et al.*, 2008). Pol II is strongly conserved from lower to higher eukaryotes. 53 % of the amino acid residues of Pol II from *S. cerevisiae* are identical to the human enzyme (Cramer *et al.*, 2001). At least ten subunits encoded by human genes can replace their counterparts in yeast without loss of cell viability (Woychik, 1998). Thus yeast Pol II is as a good model and research object and is representative of the human enzyme.

1.2.1 Subunit composition and structure determination of Pol II

Pol II has a molecular weight of 514 kDa comprised of twelve subunits (Rpb1–Rpb12, Table 1) and is thus the smallest and simplest one of the three RNA poly-

merases (Cramer *et al.*, 2008). Complete Pol II is formed by the ten-subunit core associated with the peripheral subunits Rpb4/7. Ten of the subunits are essential in yeast; Rpb4 and Rpb9 are not essential and both are positioned at the very outside of the protein complex (Figure 1). The Pol II core alone is sufficient for transcription elongation, while the dissociable Rpb4/7 subcomplex is essential for transcription initiation with only Rpb7 being indispensable (Edwards *et al.*, 1991).

Table 1: *S. cerevisiae* **Pol II subunits.**

Subunit	M_r	Classification	Subunit sharing	Necessity
Rpb1	191.6 kDa	Ten-subunit core	-	Essential
Rpb2	138.8 kDa	Ten-subunit core	-	Essential
Rpb3	35.3 kDa	Ten-subunit core	-	Essential
Rpb4	25.4 kDa	Rpb4/7 subcomplex	-	Dispensable
Rpb5	25.1 kDa	Ten-subunit core	With Pol I and Pol III	Essential
Rpb6	17.9 kDa	Ten-subunit core	With Pol I and Pol III	Essential
Rpb7	19.1 kDa	Rpb4/7 subcomplex	-	Essential
Rpb8	16.5 kDa	Ten-subunit core	With Pol I and Pol III	Essential
Rpb9	14.3 kDa	Ten-subunit core	-	Dispensable
Rpb10	8.3 kDa	Ten-subunit core	With Pol I and Pol III	Essential
Rpb11	13.6 kDa	Ten-subunit core	-	Essential
Rpb12	7.7 kDa	Ten-subunit core	With Pol I and Pol III	Essential

The X-ray structure of the Pol II core complex was solved at 2.8 Å resolution (Cramer *et al.*, 2001), which served as basis for the structure of a core transcribing complex (Gnatt *et al.*, 2001) and many following Pol II structures. By addition of recombinantly expressed Rpb4/7 X-ray crystallographic structure determination led to backbone models of complete Pol II at 4.2 Å and 4.1 Å resolution (Armache *et al.*, 2003; Bushnell & Kornberg, 2003). By solving the structure of the Rpb4/7 subcomplex independently at 2.3 Å the complete Pol II model could be refined to 3.8 Å resulting in the first atomic model of complete Pol II (Armache *et al.*, 2005). This could be used as search model to solve the structure of complete Pol II with bound DNA-RNA strands at 4.0 Å resolution (Kettenberger *et al.*, 2004). Technical improvements of synchrotron hardware and processing programs yielded better quality of data. Up to present the highest resolved structure of a complete Pol II complex containing nucleic acids was obtained during Pol II fidelity studies at 3.2 Å (Sydow *et al.*, 2009).
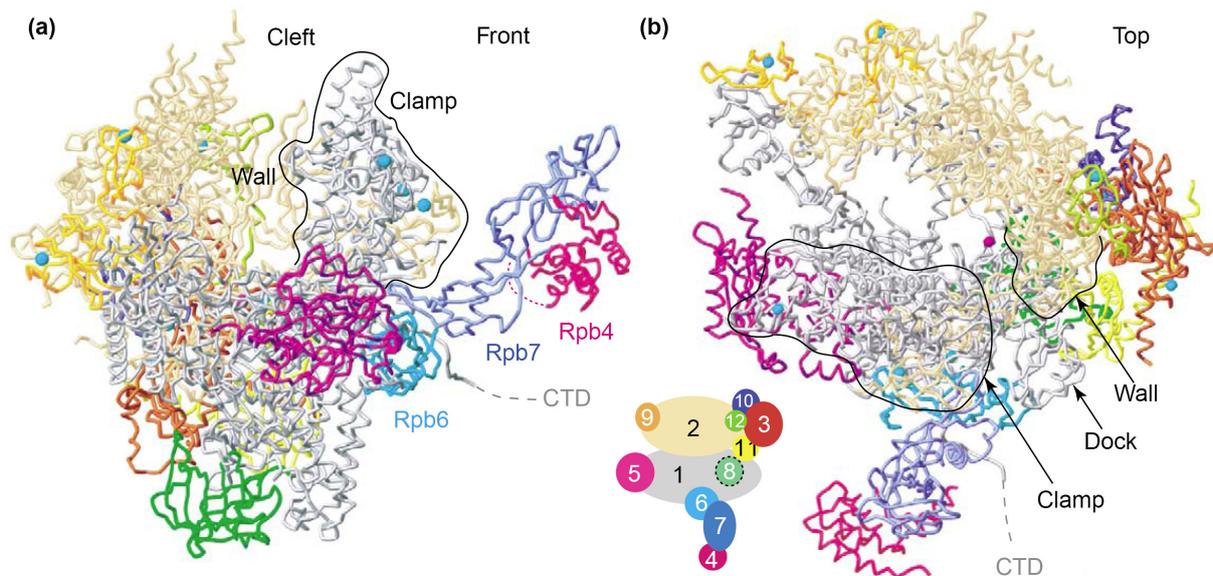
Figure 1: Ribbon model of the complete Pol II (Armache *et al.*, 2003).

The views are from (**a**) the front and from (**b**) the top, respectively. Cyan spheres and a pink sphere depict eight zinc ions and an active site magnesium ion, respectively. The linker to the CTD is indicated as a dashed line. A key to subunit colour is shown in the bottom left corner of (**b**), with subunits Rpb1–Rpb12 numbered 1–12. This Figure is adopted (Cramer, 2004).

The Pol II model reveals that the two main parts of the enzyme primarily formed by the largest subunits Rpb1 and Rpb2 are separated by a deep cleft (Figure 1). The clamp located on one side of the cleft is a mobile element and comprises parts of the subunits Rpb1 and Rpb2 (Cramer *et al.*, 2001). The clamp was observed in two conformations thus polymerase can adopt an open state as found in core Pol II structures (Cramer *et al.*, 2000) or a closed state as in complete Pol II structures (Armache *et al.*, 2003; Bushnell & Kornberg, 2003). Eight Zn^{2+} ions are bound to Pol II contributing to structural stabilisation (Cramer *et al.*, 2001). At the active site two catalytically important Mg^{2+} ions bind. One Mg^{2+} ion (metal A) is stably coordinated by three aspartates within the aspartate loop of Rpb1. The second Mg^{2+} ion (metal B) is delivered with incoming NTPs and thus exchanged between catalytic steps (Cramer *et al.*, 2001).

1.2.2   Structure and activity of the Pol II elongation complex

Synthetic nucleic acid strands with appropriate sequences can be annealed to form complexes stabilised by Watson-Crick base pairs. Constructs resembling nucleic acids associated to a transcribing Pol II complex (Figure 2a) contain a DNA-RNA hybrid upstream of the active site and a DNA-DNA duplex region downstream. These pre-
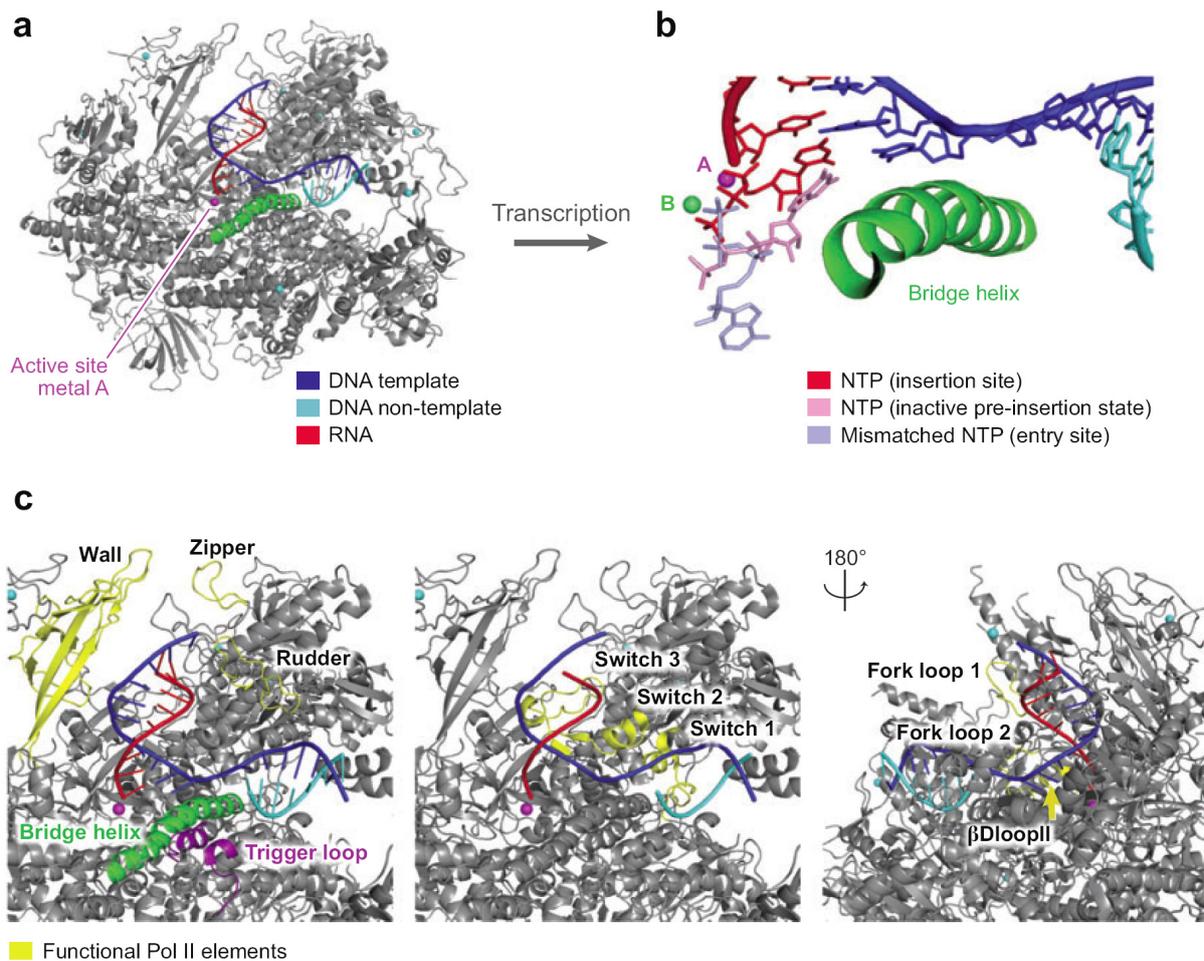
Figure 2: Structure of the Pol II EC.

a, Overview of the EC structure (Kettenberger *et al.*, 2004; Wang *et al.*, 2006; Westover *et al.*, 2004). **b**, Superposition of NTP-binding sites: insertion site (Westover *et al.*, 2004), entry site (Westover *et al.*, 2004) and inactive preinsertion-like state (Kettenberger *et al.*, 2004) are shown in, red, violet and pink, respectively. **c**, Functional Pol II surface elements in the EC.

formed nucleic acid scaffolds can be assembled with purified Pol II *in vitro* and subjected to crystallisation or RNA elongation or cleavage experiments. The surface of the enzyme is generally negatively charged with the exception of the positively charged region covering the cleft, active site and wall (Cramer *et al.*, 2001) (Figure 1). Negatively charged nucleic acids are accommodated in this positively charged cleft during elongation (Figure 2a). At the front of Pol II the DNA-template–non-template duplex enters the cleft. The non-template is displaced from the template strand and only the template reaches the active site (Figure 2a). The template is kinked about 90° and forms an 8–9 bp DNA–RNA hybrid upstream of the active site towards the wall (Figure 2c). The hybrid in the hybrid-binding site of Pol II has a conformation between A- and B-DNA (Gnatt *et al.*, 2001). Conformational rearrangements of switch loops (Figure 2c) allow movement of the clamp to form a tran-

scribing complex. The loops termed rudder, zipper and lid were suggested to be involved in separation of RNA from template DNA at the upstream end of the hybrid (Cramer *et al.*, 2001) (Figure 2c).

RNA synthesis occurs by covalent nucleotide addition to the RNA's 3' end at the catalytic site. It discriminates against dNTPs and only an NTP that can form a Watson-Crick bp with the templating dNTP (+1) is incorporated, with the trigger loop (Figure 2c) playing a role in substrate specificity (Wang *et al.*, 2006). The fidelity of eukaryotic transcription is very high with an estimated nucleotide incorporation error probability of 10^{-5} (de Mercoyrol *et al.*, 1992).

After an NTP has bound to the insertion site (Figure 2b) the mobile trigger loop (Figure 2c) folds and closes the active site (Wang *et al.*, 2006). Covalent bond formation between the incoming nucleotide and the RNA 3'-OH is catalysed by the two Mg^{2+} ions (metal A and B, Figure 2b) at the active site and inorganic pyrophosphate is released. This leaves Pol II in the pre-translocated state. Upstream translocation of nucleic acids relative to the enzyme involves a conformational change in the bridge helix, which is contacted by the trigger loop (Brueckner *et al.*, 2009). The enzyme's conformation is then in the post-translocated state with a free nucleotide insertion site and another nucleotide can be added by repeating the nucleotide addition cycle.

1.2.3   The transcription cycle

In vivo transcription of genes can be divided into three phases: initiation, elongation and termination. Initiation covers recruitment of polymerase to DNA and formation of a stable elongation complex which translocates along DNA during the elongation phase. The polymerase is released from the DNA in the termination phase.

Many Pol II promoters contain a TA-rich element which is bound by TBP, a subunit of TFIID. Other factors can interact with alternative elements such as TFIIB, which interacts with TFIIB recognition elements. TFIID is formed by TBP together with TBP-associated factors that can apparently interact with Initiator and downstream promoter elements (Sikorski T. W. & Buratowski, 2009) (Table 2). The binding of TBP introduces an approximately 90° kink in DNA (Kim J. L. *et al.*, 1993a; Kim Y. *et al.*, 1993b), which serves as a saddle for binding of further factors. TFIIB bridges between the TBP-DNA complex and Pol II (Kostrewa *et al.*, 2009) and thus recruits

complete Pol II with TFIIF to the promoter. TFIIE can then bind and melts the promoter and recruits TFIIH which has DNA-dependent ATPase, helicase and kinase activities (Lee & Young, 2000). The Mediator, a huge multiprotein complex was found to promote transcription initiation by transmitting stimulatory effects from activators to the basal transcription machinery (Sikorski T. W. & Buratowski, 2009).

Table 2: Protein complexes involved in Pol II preinitiation complex formation. This table is adapted (Sikorski T. W. & Buratowski, 2009).

Protein Complex	Number of subunits	Functions
TFIIA	2–3	Functions to counteract repressive effects of negative cofactors; acts as a coactivator by interacting with activators and components of the basal initiation machinery
TFIIB	1	Stabilizes TFIID-promoter binding; aids in recruitment of TFIIF/Pol II to the promoter; directs accurate start site selection
TFIID	14 (TBP and TBP Associated Factors)	Nucleates PIC assembly either through TBP binding to TATA sequences or TAF binding to other promoter sequences; coactivator activity through direct interaction of TAFs and gene specific activators
TFIIE	2	Helps recruit TFIIH to promoters; stimulates helicase and kinase activities of TFIIH; binds ssDNA and is essential for promoter melting
TFIIF	2–3	Tightly associates with Pol II; enhances affinity of Pol II for TBP-TFIIB-promoter complex; necessary for recruitment of TFIIE/TFIIH to the PIC; aids in start site selection and promoter escape; enhances elongation efficiency
TFIIH	10	ATPase/helicase necessary for promoter opening and promoter clearance; helicase activity for transcription coupled DNA repair; kinase activity required for phosphorylation of Pol II CTD; facilitates transition from initiation to elongation
Mediator	≥ 24	Bridges interaction between activators and basal factors; stimulates both activator dependent and basal transcription; required for transcription from most Pol II dependent promoters

As transcription starts, short RNA products are synthesised and released by Pol II during the abortive initiation phase. After promoter clearance processive RNA elongation follows. Transitions between states are uniform for transcribed genes (Mayer *et al.*, 2010) and involve formation of specific phosphorylation patterns at the heptapetide repeats of the CTD of Rpb1 (Buratowski, 2009). The CTD is thus recognised by and serves as binding platform for different mRNA processing factors, such as the

capping enzyme that adds a 7-methylguanine triphosphate cap to the RNA's 5' end (Lee & Young, 2000). In parallel the RNA is elongated by Pol II and after passing the poly(A) site cleavage frees the nascent mRNA that can then be modified and exported into the cytoplasm to be translated. Release from the product RNA and template DNA leads to Pol II termination that requires Rat1 and other factors (Dengl & Cramer, 2009). Free Pol II with an unphosphorylated CTD can then be recruited to another promoter, reinitiating the transcription cycle.

1.3 Functional studies of Pol II by site-directed mutagenesis

Site-directed mutagenesis allows for targeted studies *e.g.* of the precise contribution of single or multiple amino acid residues in enzyme-catalysed reactions. Mutagenesis studies are highly valuable to understand mechanisms of RNA polymerase function in detail. Archaeal RNA polymerases can be recombinantly expressed in *E. coli* and reconstituted from single subunits, enabling fast and easy studies of mutants (Naji *et al.*, 2007; Werner & Weinzierl, 2002). Pol II in contrast could not be obtained by assembly from recombinantly expressed subunits. Purified Pol II enzymes bearing mutations can only be expressed endogenously. Thus mutations have to be introduced in the host organism. In yeast mutations can be introduced genomically, but an easier strategy is to use a plasmid-based approach, which additionally allows for identification of lethal mutations.

For Rpb2 (Table 1), a mutagenesis system was established allowing the introduction of mutations in Rpb2 and its galactose-inducible overexpression in *S. cerevisiae* (Domecq *et al.*, 2010). The largest subunit Rpb1 mainly forms the active site region (Figure 1) and contains many functional elements of Pol II (Figure 2c) such as the zipper, lid, rudder, switch 2, active site aspartate loop, bridge helix, switch 1, switch 5 (Cramer *et al.*, 2001), trigger loop (Wang *et al.*, 2006), clamp coiled coil (Kostrewa *et al.*, 2009) and F loop (Miropolskaya *et al.*, 2009). As Rpb1 covers a large portion of the Pol II surface and contains the CTD (1.2.3) it is of great importance when studying Pol II interactions with external factors and transcriptional regulation. Thus a mutagenesis system of Rpb1 would open up new possibilities to study catalytic mechanisms as well as binding and effects of other factors on Pol II.

1.4 Implications for additional RdRP activity of Pol II and its role in HDV replication

Chemically DNA is very similar to RNA. However, the presence of a 2'-OH group at the sugar of every base leads to another energetically more favourable sugar pucker of RNA. This is the basis for an RNA double strand to adopt A-DNA conformation while DNA generally exists as B-DNA under physiological conditions (Berg *et al.*, 2002). A free DNA-RNA hybrid adopts a conformation very similar to A-DNA (Horton & Finzel, 1996). This suggests itself that Pol II can possibly bind an RNA–RNA duplex in A-DNA conformation with only minor structural rearrangements in a similar manner as a DNA-RNA hybrid that is tightly bound to the enzyme during the process of transcription (Gnatt *et al.*, 2001). *In vitro* an RNA–RNA duplex can be accommodated in the enzyme's hybrid binding site (Kettenberger *et al.*, 2006). It was also discovered that Pol II can synthesise RNA using homopolymeric RNAs as template (Dezelee *et al.*, 1974). Stimulated by TFIIS, Pol II can cleave RNA and perform 3' terminal NTP addition in the absence of DNA *in vitro* (Johnson & Chamberlin, 1994). *In vivo* there is also evidence that eukaryotic RNA polymerases contribute to RNA-dependent RNA synthesis as *e.g.* in plants Pol II was implicated in the replication of viroids (Rackwitz *et al.*, 1981).

Infection of the human hepatitis B virus can be accompanied by infection of a satellite virus HDV that causes hepatitis D. The HDV genome is a circular, highly self-complementary single-stranded RNA, which is the template for synthesis of the RNA antigenome and vice versa (Chao, 2007). Human Pol I and Pol II were predicted to play a role in the RNA-dependent replication of the RNA genome and antigenome of HDV as it does not include a reverse transcription step into DNA and there is no viral encoded polymerase (Lai, 2005). HDV RNA can be transcribed at least partially by Pol II *in vitro* (Filipovska & Konarska, 2000). In contrast to plant viroids, which do not code for polypeptides, HDV encodes for the protein HDAg. It is essential for HDV replication but is not a replicase itself (Filipovska & Konarska, 2000) and was found to bind to RNA Pol II and to stimulate transcription (Yamaguchi *et al.*, 2001). 5'-capping and 3'-polyadenylation are modifications that are only observed for Pol II transcripts as they are CTD-dependent (Lee & Young, 2000). HDAg mRNA was observed in 5'-capped and 3'-polyadenylated states suggesting that its transcription templated by the genomic RNA strand of HDV is catalysed by Pol II (Gudima *et al.*,

2000). HDV replication is sensitive to α-amanitin at concentrations specifically inhibiting Pol II (MacNaughton *et al.*, 1991; Moraleda & Taylor, 2001). As sensitivities to α-amanitin of genomic and antigenomic strand replication differ, other polymerases than Pol II might as well be involved in HDV replication (Macnaughton *et al.*, 2002; Modahl *et al.*, 2000). A nucleolus-associated polymerase is also involved in HDV replication as immunofluorescence staining showed that genomic and antigenomic RNAs of HDV were found to occur at different intranuclear locations (Li *et al.*, 2006).

Overall these results suggest Pol II to be one of several activities that is responsible for HDV replication and transcription. New RdRPs have been recently discovered in human (Maida *et al.*, 2009) and being involved in RNAi in Drosophila (Lipardi & Paterson, 2009). The detailed contribution of these RdRPs and Pol II within RdRP-involving processes in eukaryotes is currently not clear.

1.5 RNA polymerase-catalysed cleavage of product RNA

The major function of RNA polymerases is to catalyse RNA synthesis by 3' terminal NMP incorporation under release of pyrophosphate using NTPs as substrates (1.2.2). The back reaction comprising pyrophosphorolysis and release of an NTP is energetically unfavourable. However RNA cleavage can be catalysed by Pol II involving an attacking H_2O molecule and is used during proofreading of transcription. As hydrolysis is a reaction distinct from pyrophosphorolysis and the reaction mechanism can be influenced by stimulatory factors, Pol II has a tunable active site (Sosunov *et al.*, 2003). During the process of transcription the net reaction is NTP incorporation resulting in RNA elongation. However Pol II can encounter obstacles on the DNA during the process of gene transcription and become arrested. In the process of backtracking Pol II translates upstream on the DNA template while the RNA 3' end is extruded through the enzyme's pore (Cramer *et al.*, 2008). Reactivation of arrested Pol II requires cleavage and release of the 3' RNA. A free 3' end realigned at the active centre can then be used again as a substrate for elongation.

1.5.1 Contribution of cleavage stimulatory factors

Complete Pol II alone can perform dinucleotide cleavage when assembled with a 9 bp hybrid including a mismatched 3' nucleotide *in vitro* (Sydow *et al.*, 2009). Pol II

lacking the non-essential subunit Rpb9 was shown to have similar intrinsic cleavage activities at mild alkaline conditions as wild-type Pol II (Weilbaecher *et al.*, 2003). However, Rpb9 was implicated to play a role in this divalent cation-dependent weak intrinsic cleavage activity but its mechanism of action is still uncharacterised (Nesser *et al.*, 2006). A strong cleavage activity of Pol II can be observed upon stimulation with TFIIS (Izban & Luse, 1992). In the Pol II-TFIIS complex TFIIS inserts a hairpin into the pore. Two adjacent carboxylic acid residues, the DE motif, at the hairpin's tip coordinate metal B and a water molecule, which serves as the nucleophilic attacking moiety in RNA hydrolysis (Kettenberger *et al.*, 2003). Arrested Pol II lacking Rpb9 responds weakly to stimulation by TFIIS when testing read-through at transcription pause sites on DNA (Awrey *et al.*, 1997). Both TFIIS and Rpb9 are not essential but a double-knock out is lethal in certain genetic backgrounds suggesting a redundant function. Consistently, both TFIIS and Rpb9 were found to play a role in Pol II transcriptional fidelity (Koyama *et al.*, 2007; Nesser *et al.*, 2006) but detailed understanding of their contributions *in vivo* is still missing.

In Pol I and Pol III subunits A12.2 and C11, respectively are homologous to Rpb9 in Pol II. The C-terminus of A12.2 and C11 is related as well to the C-terminus of TFIIS, especially the two key acidic residues aspartate and glutamate are conserved in TFIIS, A12.2 and C11 but not in Rpb9, which contains residues aspartate and threonine instead. Pol I has a strong intrinsic cleavage activity that depends on subunit A12.2 (Kuhn *et al.*, 2007) in analogy to the cleavage activity of Pol III (Whitehall *et al.*, 1994) that depends on C11 (Chedin *et al.*, 1998). The Pol II structural model was fitted to an electron microscopic density of Pol III at 9.9 Å resolution. At the position of the N-terminal domain of Rpb9 density was observed that was assigned to the homologous N-terminal domain of C11. As no additional density nearby could be assigned to the C11 C-terminal domain high flexibility was suggested (Fernández-Tornero *et al.*, 2010). In contrast to Rpb9, A12.2 and C11 thus seem to act as built-in cleavage stimulatory factors in Pol I and Pol III whose function in the Pol II system is conducted by the dissociable factor TFIIS.

1.5.2 Role of functional polymerase elements in cleavage

The RNA cleavage activity of eukaryotic RNA polymerases can be stimulated by external factors (1.5.1) or internal elements that transmit information to the active cen-

tre. Functional elements near the active centre must then be directly involved in the cleavage procedure. The trigger loop is important for catalysis of NTP addition (Wang *et al.*, 2006) (1.2.2) and a contribution to RNA hydrolysis seems plausible. However, in case of *E. coli* RNA polymerase intrinsic as well as factor-stimulated cleavage does not depend on refolding of the trigger loop, *i.e.* formation of trigger helices that form a metastable three helix bundle with the bridge helix (Zhang J. *et al.*, 2010). But the trigger loop is not indispensable as a histidine residue in the trigger loop was found to be essential for RNA hydrolysis in studies with RNA polymerase of *Thermus aquaticus* and this role was suggested to be conserved among bacteria (Yuzenkova & Zenkin, 2010). The F loop, which is directly adjacent to the N-terminus of the bridge helix can contact the folded trigger loop, thus stabilising it in this conformation (Miropolskaya *et al.*, 2009). Although it is essential for the RNA elongation activity of bacterial RNA polymerases the F loop does not play an essential role in RNA hydrolysis by *Thermus aquaticus* RNA polymerase (Miropolskaya *et al.*, 2009).

1.6 Aim of this work

Based on the crystal structure of Pol II in complex with the FC* inhibitor RNA (Kettenberger *et al.*, 2006), the question arose if Pol II can perform RNA templated nucleotide incorporation. Initial experiments with artificial RNA elongation scaffolds were promising (Lehmann, 2006). The RNA elongation and RNA hydrolysis activity of Pol II using artificial RNA–RNA scaffolds were characterised more in detail in this work, including visualisation of the RdRP elongation complex in a crystal structure. The possibilities and limits of Pol II's RdRP activity within the process of HDV replication were studied. As *in vitro* setups allow for well-defined compositions of reaction mixtures containing only purified components, their results can complement former experiments using cell extracts or indirect assignments by α-amanitin resistance. This work's *in vitro* studies on HDV replication should serve as a useful basis for targeted experiments *in vivo e.g.* to find further stimulatory factors and thus to gain further insights into the mechanism of HDV replication and in turn spreading of the virus. Detailed understanding of the HDV replication mechanism and contribution of involved factors is necessary to find targets for drugs that can successfully decrease human pathogenic HDV propagation.

As Pol II cannot be reconstituted from recombinantly expressed subunits an Rpb1 mutagenesis system in *S. cerevisiae* was developed within this work. To facilitate mutagenesis a strain containing plasmid-encoded Rpb1 was created. Although methods for gene knock-out, plasmid-transformation and sporulation are established in yeast, the challenge of this project was the huge size of this particular target gene, which makes all amplification and cloning steps technically more demanding than for a small gene. A well-established mutagenesis system in yeast that can be used for easy and convenient production of Rpb1-mutated Pol II complexes and that can be reproduced for other Pol II subunits was developed.

2 Materials and Methods

2.1 Materials

2.1.1 Bacterial and yeast strains

Table 3: *E. coli* strains.

Name	Description	Source
BL21-CodonPlus (DE3)-RIL	*E. coli* B F$^-$ *ompT hsdS*(r$_B^-$ m$_B^-$) *dcm$^+$* Tet^r *gal* λ(DE3) *endA* Hte [*argU ileY leuW* Cam^r]	Stratagene
XL1-Blue	*recA1 endA1 gyrA96 thi-1 hsdR17 supE44 relA1 lac* [F' *proAB lacI^{q}ZΔM15* Tn*10* (Tet^r)]	Stratagene

Table 4: *S. cerevisiae* strains.

Name	Description	Source
CB010*Δrpb4*	MATa *pep4*::HIS3, *prb1*::LEU2, *prc1*::HISG, *can1*, *ade2*, *trp1*, *ura3*, *his3*, *leu2-3,112*, *rpb4*::URA3	(Edwards *et al.*, 1990), (Fu *et al.*, 1999)
BJ5464	MATα *ura3-52 trp1 leu2-Δ1 his3-Δ200 pep4*::HIS3 *prb1-Δ1.6R can1 GAL*	ATCC-LGC Standards
BJ5465	MATa *ura3-52 trp1 leu2-Δ1 his3-Δ200 pep4*::HIS3 *prb1-Δ1.6R can1 GAL*	ATCC-LGC Standards
BJ5626	MATα/MATa *ura3-52/ura3-52 trp1/+ +/leu2-Δ1 his3-Δ200/his3-Δ200 pep4*::HIS3/*pep4*::HIS3 *prb1-Δ1.6R/prb1-Δ1.6R can1/can1 GAL/GAL*	ATCC-LGC Standards
BJ5464 Rpb3 His-Bio	BJ5464 His-Bio tag introduced at 5'end of Rpb3 gene, use of URA3 selection marker	(Kireeva *et al.*, 2000b)
BJ5464 Rpb3 His-Bio Δ*rpb9*	BJ5464 Rpb3 His-Bio *rpb9*::NatNT2	This study
BJ5626 Δ*rpb1*/+	BJ5626 *rpb1*::kanMX6/Rpb1	This study
BJ5626 Δ*rpb1*/+ pRS316-Rpb1	BJ5626 *rpb1*::kanMX6/Rpb1 pRS316-Rpb1	This study
BJ5626 Δ*rpb1*/+ pRS316-Rpb1 pRS31N-Pep4-Prb1	BJ5626 *rpb1*::kanMX6/Rpb1 pRS316-Rpb1 pRS31N-Pep4-Prb1	This study

Name	Description	Source
BJ5464 *Δrpb1* pRS316-Rpb1	BJ5464 *rpb1*::kanMX6 pRS316-Rpb1	This study
BJ5465 *Δrpb1* pRS316-Rpb1	BJ5465 *rpb1*::kanMX6 pRS316-Rpb1	This study
BJ5464 *Δrpb1* pRS315-Rpb1	BJ5464 *rpb1*::kanMX6 pRS315-Rpb1	This study
BJ5464 *Δrpb1* pRS315-Rpb1-N-H_{10}	BJ5464 *rpb1*::kanMX6 pRS315-Rpb1-N-$H_{10}(SA)_5$	This study
BJ5464 *Δrpb1* pRS315-Rpb1-C-H_{10}	BJ5464 *rpb1*::kanMX6 pRS315-Rpb1-C-H_{10}	This study
BJ5464 *Δrpb1* pRS316-Rpb1 pRS315-Rpb1-Δlid1-C-H_{10}	BJ5464 *rpb1*::kanMX6 pRS316-Rpb1 pRS315-Rpb1-Δlid1-C-H_{10}	This study
BJ5464 *Δrpb1* pRS316-Rpb1 pRS315-Rpb1-Δlid2-C-H_{10}	BJ5464 *rpb1*::kanMX6 pRS316-Rpb1 pRS315-Rpb1-Δlid2-C-H_{10}	This study
BJ5464 *Δrpb1* pRS316-Rpb1 pRS315-Tet-Rpb1-Δlid2-C-H_{10}	BJ5464 *rpb1*::kanMX6 pRS316-Rpb1 pRS315-Tet-Rpb1-Δlid2-C-H_{10}	This study
BJ5464 *Δrpb1* pRS315-Rpb1-FIII-C-H_{10}	BJ5464 *rpb1*::kanMX6 pRS315-Rpb1-FIII-C-H_{10}	This study
BJ5464 *Δrpb1* pRS315-Rpb1-ccc2R-C-H_{10}	BJ5464 *rpb1*::kanMX6 pRS315-Rpb1-ccc2R-C-H_{10}	This study
BJ5464 *Δrpb1* pRS315-Rpb1-ccc7A-C-H_{10}	BJ5464 *rpb1*::kanMX6 pRS315-Rpb1-ccc7A-C-H_{10}	This study
BJ5464 *Δrpb1* pRS315-Rpb1-I756K-C-H_{10}	BJ5464 *rpb1*::kanMX6 pRS315-Rpb1-I756K-C-H_{10}	This study
BJ5464 *Δrpb1* pRS315-Rpb1-D1359K-C-H_{10}	BJ5464 *rpb1*::kanMX6 pRS315-Rpb1-D1359K-C-H_{10}	This study
BJ5464 *Δrpb1* pRS315-Rpb1-G1360Q-C-H_{10}	BJ5464 *rpb1*::kanMX6 pRS315-Rpb1-G1360Q-C-H_{10}	This study
BJ5464 *Δrpb1 Δrpb9* pRS316-Rpb1	BJ5464 *rpb1*::kanMX6 *rpb9*::natNT2 pRS316-Rpb1	This study
BJ5464 *Δrpb1 Δrpb9* pRS315-Rpb1-C-H_{10}	BJ5464 *rpb1*::kanMX6 *rpb9*::natNT2 pRS315-Rpb1-C-H_{10}	This study
BJ5464 *Δrpb1 Δrpb9* pRS315-Rpb1-FIII-C-His	BJ5464 *rpb1*::kanMX6 *rpb9*::natNT2 pRS315-Rpb1-FIII-C-H_{10}	This study
BJ5464 *Δrpb1 Δrpb9* pRS315-Rpb1-I756K-C-H_{10}	BJ5464 *rpb1*::kanMX6 *rpb9*::natNT2 pRS315-Rpb1-I756K-C-H_{10}	This study
BJ5464 *Δrpb1 Δrpb9* pRS315-Rpb1-D1359K-C-H_{10}	BJ5464 *rpb1*::kanMX6 *rpb9*::natNT2 pRS315-Rpb1-D1359K-C-H_{10}	This study
BJ5464 *Δrpb1 Δrpb9* pRS315-Rpb1-G1360Q-C-H_{10}	BJ5464 *rpb1*::kanMX6 *rpb9*::natNT2 pRS315-Rpb1-G1360Q-C-H_{10}	This study
BJ5464 *Δrpb1 Δdst1* pRS315-Rpb1-C-H_{10}	BJ5464 *rpb1*::kanMX6 *dst1*::Trp1 pRS315-Rpb1-C-H_{10}	This study

Name	Description	Source
BY4741	MATa *his3-Δ1 leu2-Δ0 met15-Δ0 ura3-Δ*	Euroscarf
BY4742	MATα *his3-Δ1 leu2-Δ0 lys2-Δ0 ura3-Δ0*	Euroscarf
BY4743	MATα/MATa *his3-Δ1*/*his3-Δ1 leu2-Δ0*/*leu2-Δ0*; *met15-Δ0*/MET15; LYS2/*lys2-Δ0*; *ura3-Δ0*/*ura3-Δ0*	Euroscarf
BY4743 *Δrpb1*/+	BY4743 *rpb1*::kanMX6/Rpb1	This study
BY4743 *Δrpb1*/+ pRS316-Rpb1	BY4743 *rpb1*::kanMX6/Rpb1 pRS316-Rpb1	This study
BY4741 *Δrpb1* pRS316-Rpb1	BY4741 *rpb1*::kanMX6 pRS316-Rpb1	This study
BY4742 *Δrpb1* pRS316-Rpb1	BY4742 *rpb1*::kanMX6 pRS316-Rpb1	This study

2.1.2 Plasmids

Table 5: Bacterial expression plasmid.

Name	Backbone	Insert	Insertion sites[1]	Source
pET-21b(+)-Rpb4/7	pET-21b(+)	Rpb4, Rpb7-C-H_6	NdeI/XhoI	(Sakurai *et al.*, 1999)

Table 6: Plasmids used as templates for cassette amplification by PCR.

Name	Cassette	Source
pFA6a-kanMX6	kanMX6	(Wach *et al.*, 1994)
pFA6a-natNT2	natNT2	(Janke *et al.*, 2004)
pCM251	Tet-on promoter with two copies of *tetO*	(Bellí *et al.*, 1998)

Table 7: Yeast plasmids.

Name	Backbone	Insert	Insertion sites[1]	Source
pRS315	pRS315	-	-	(Sikorski R. S. & Hieter, 1989)
pRS316	pRS316	-	-	(Sikorski R. S. & Hieter, 1989)
pRS315-Rpb1	pRS315	Rpb1[2]	XhoI/SacI	This study
pRS316-Rpb1	pRS316	Rpb1[2]	XhoI/SacI	This study
pRS315-Rpb1-N-H_{10}	pRS315	Rpb1-N-H_{10}-$(SA)_5$[2]	XhoI/SacI	This study

---

[1] The insertion site listed first corresponds to the upstream end of the insert.
[2] The insert corresponds to the ORF with naturally flanking sequences 523 bp upstream and 281 bp downstream.

Name	Backbone	Insert	Insertion sites[1]	Source
pRS315-Rpb1-C-H$_{10}$	pRS315	Rpb1-C-H$_{10}$[2]	XhoI/SacI	This study
pRS315-Rpb1-Δlid1-C-H$_{10}$	pRS315	Rpb1-Δlid1-C-H$_{10}$[2]	XhoI/SacI	This study
pRS315-Rpb1-Δlid2-C-H$_{10}$	pRS315	Rpb1-Δlid2-C-H$_{10}$[2]	XhoI/SacI	This study
pRS315-Tet-Rpb1-Δlid2-C-H$_{10}$	pRS315	Tet-Rpb1-Δlid2-C-H$_{10}$[3]	XhoI/SacI	This study
pRS315-Rpb1-FIII-C-H$_{10}$	pRS315	Rpb1-FIII-C-H$_{10}$[2]	XhoI/SacI	This study
pRS315-Rpb1-CTD-C-H$_{10}$	pRS315	Rpb1-CTD-C-H$_{10}$[2]	XhoI/SacI	This study
pRS315-Rpb1-TEV-C-H$_{10}$	pRS315	Rpb1-TEV-C-H$_{10}$[2]	XhoI/SacI	This study
pRS315-Rpb1-ccc2R-C-H$_{10}$	pRS315	Rpb1-ccc2R-C-H$_{10}$[2]	XhoI/SacI	This study
pRS315-Rpb1-ccc7A-C-H$_{10}$	pRS315	Rpb1-ccc7A-C-H$_{10}$[2]	XhoI/SacI	This study
pRS315-Rpb1-I756K-C-H$_{10}$	pRS315	Rpb1-I756K-C-H$_{10}$[2]	XhoI/SacI	This study
pRS315-Rpb1-D1359K-C-H$_{10}$	pRS315	Rpb1-D1359K-C-H$_{10}$[2]	XhoI/SacI	This study
pRS315-Rpb1-G1360Q-C-H$_{10}$	pRS315	Rpb1-G1360Q-C-H$_{10}$[2]	XhoI/SacI	This study
pRS31N-Pep4-Prb1	pRS31N[4]	Pep4[5], Prb1[6]	BamHI/XhoI, NotI/BamHI	This study

---

[3] The insert corresponds to the ORF with a Tet-on promoter upstream and the naturally flanking sequence 281 bp downstream.

[4] The backbone corresponds to pRS316 with the ura3 ORF replaced by an insertion of the natNT2 sequence at NdeI/NsiI[1] sites.

[5] The insert corresponds to the ORF with naturally flanking sequences 500 bp upstream and 195 bp downstream.

[6] The insert corresponds to the ORF with naturally flanking sequences 500 bp upstream and 200 bp downstream.

2.1.3   Synthetic oligonucleotides

Table 8: DNA oligonucleotide used in RNA elongation experiments.[7]

Name	Sequence[8]	Source
FB-DNA1-EL	TCGAGGTAGCTTGACGCCTGGTCAAA	metabion

Table 9: RNA oligonucleotides used in RNA elongation experiments.[7]

Name	Sequence[8]	Source
KB-RNA1-flu	FAM-UGCAUAAAGACCAGGC[9]	biomers.net
KB-RNA1-blunt-flu	FAM-UUUGACCAGGC[9]	biomers.net
FB-RNA1	UCGAGGUAGCUUGACGCCUGGUCAAA	biomers.net
FB-RNA1-4bp	UCAGGUAGCUGAC GCCUGGUCAAA	biomers.net
FB-RNA1-6bp	UCGAAGGUAGCUUUGACGCCUGGUCAAA	biomers.net
FB-RNA1-ss6	CUUGACGCCUGGUCAAA	biomers.net
FB-RNA1-ss10	GUAGCUUGACGCCUGGUCAAA	biomers.net
FB-RNA1-mut1	UCGAGCGACCUUGACGCCUGGUCAAA	biomers.net
FB-RNA1-mut2	UCGAGGCAGCUUGACGCCUGGUCAAA	metabion
HDV-cleaved-flu	FAM-UAGAGAGAUUUUUUCUCUCGAUUCUCUAUCGGAAU[9]	biomers.net
HDV-AG-clAG-36-flu	FAM-UAGAGAGAUUUUUUCUCUCGAUUCUAGAUCGGAAU[9]	biomers.net
HDV-AG-cl-U-17-flu	FAM-UGAUUCUCUAUCGGAAU[9]	biomers.net
HDV-AG-cl-U-18-flu	FAM-UGAUUCUCUAUCGGAAUC[9]	biomers.net
HDV-AG-cl-UA-19	UGAUUCUCUAUCGGAAUCA	metabion
HDV-cleaved-loopC-FAM	FAM-UAGAGAGAUUUUUCUCUCUCGAUUCUCUAUCGGAAU[9]	metabion
HDV-AG-cl-48-flu	FAM-UAGAGAGAUUUGUGGGGAGCCACUUUUCUCUCGAUUCUCUAUCGGAAU[9]	metabion
RNAfusion1 FC*-HDV	FAM-UCGAGGUAGCUUGACAUUCUCUAUCGGAAU[9]	metabion

---

[7] Oligonucleotides were HPLC-purified, delivered lyophilised and dissolved in TE buffer to a final concentration of 400 µM.
[8] Oligonucleotide sequences are shown in the 5' to 3' direction.
[9] Oligonucleotide labelled with 6-carboxyfluorescein (FAM) at 5' end.

Name	Sequence[8]	Source
RNAfusion2 HDV-EC-tem	UAGAGAGAUUUUUUUCUCUCG GCCUGGUCAAA	metabion
HDV-AG-cl-21-FAM	FAM-CUCGAUUCUCUAUCGGAAUCG[9]	metabion
HDV-AG-cl-27-FAM	FAM-UCUCUCGAUUCUCUAUCGGAAUCGAGA[9]	metabion
HDV-AG-cl-33-FAM	FAM-UUUUCUCUCGAUUCUCUAUCGGAAUCGAGAGAA[9]	metabion
HDV-AG-cl-37-FAM	FAM-UUUUUUCUCUCGAUUCUCUAUCGGAAUCGAGAGAAAA[9]	metabion
HDV-AG-cl-43-art-FAM	FAM-GAUUUUUUUCUCUCGAUUCUCUAUCGGAAUCGAGAGAAAAAAA[9]	metabion
HDV-AG-cl-43-nat-FAM	FAM-GCCACUUUUCUCUCGAUUCUCUAUCGGAAUCGAGAGAAAAGUG[9]	metabion
HDV-AG-uncl-31-flu	FAM-UCUCUCGAUUCUCUAUCGGAAUCUAGAGAGA[9]	biomers.net
HDV-uncl-35-GCCG-FAM	FAM-CUUUGCCCUCGAUUCUCUAUCGGAAUCUAGAGGGC[9]	metabion
HDV-AG-11nont	UAGAGAGAUUU	metabion
HDV-AG-25tem-FAM	FAM-UUUUCUCUCGAUUCUCUAUCGGAAU[9]	metabion
pCPG79 RNA-28-FAM	FAM-GGUCCGGGAUCUGGAUCCAGAUCCCGGA[9]	metabion
HDV-AG-cl-51-bulge-FAM	FAM-AAGGGAGAGCCACUUUUCUAGUAAUUCUCUAUCGGAAUCGAGAGAAAAGUG[9]	metabion

Table 10: DNA oligonucleotides used as PCR primers.[10]

Name	Sequence[8]	Source
1_Sc_Rpb1_310bp_up_f	TCCCTGATCAACTTTCAAGG	Thermo Fisher Scientific
2_Sc_Rpb1_20bp_up_KanMX6_5'_r	CCTTAATAACCCGGGGATCCGGTCTGATTTATATTTTGGGG	Thermo Fisher Scientific
3_Sc_Rpb1_20bp_up_KanMX6_5'_f	CCCCAAAATATAAATCGACCGGATCCCCGGGTTAATTAAGG	Thermo Fisher Scientific
4_Sc_KanMX6_3'_Rpb1_20bp_down_r	CGTAAGGATGATATACTATAGAATTCGAGCTCGTTTAAACTGG	Thermo Fisher Scientific

---

[10] Oligonucleotides were HPLC-purified, delivered lyophilised and dissolved in H_2O to a final concentration of 100 µM.

Name	Sequence[8]	Source
5_Sc_KanMX6_3'_Rpb1_20bp_down_f	CCAGTTTAAACGAGCTCGAATTCTATAGTATATCATCCTTACG	Thermo Fisher Scientific
6_Sc_Rpb1_232bp_down_r	GCTTAGAAGTTGGACGGACG	Thermo Fisher Scientific
7_Sc_Rpb1_500bp_up_XhoI_f	TGCTAGCTCTCGAGAGAGGTATCATAAGAACATCCG	Thermo Fisher Scientific
8_Sc_Rpb1-EagI_down_BamHI_r	AGCTAGCAGGATCCTTACCCTTCAAACGAGCACG	Thermo Fisher Scientific
11_Sc_Rpb1-BspHI_up_f	GTTAGAGAATATTACATTACGTGG	Thermo Fisher Scientific
12_Sc_Rpb1_260bp_down_SacI_r	AGCTAGCAGAGCTCAAGAGCTTAATTGCTAAAAAGG	Thermo Fisher Scientific
17_Sc_Rpb1_R247:D261_r	CAGCAAGTTTAAAGGTTAAATCACGCACCGGTGG	Thermo Fisher Scientific
18_Sc_Rpb1_R247:D261_f	CCACCGGTGCGTGATTTAACCTTTAAACTTGCTG	Thermo Fisher Scientific
19_Sc_Rpb1_P248:D260_r	GCAAGTTTAAAGGTTAAATCATCTGGACGCACCGG	Thermo Fisher Scientific
20_Sc_Rpb1_P248:D260_f	CCGGTGCGTCCAGATGATTTAACCTTTAAACTTGC	Thermo Fisher Scientific
27_Teton_pCM251_PspOMI_f	TGCTAGCTGGGCCCATCCTCGCGCCCCC	Thermo Fisher Scientific
28_Sc_Rpb1_Teton_BamHI_r	GCACTAGAATACTGTTGTCCTACCATACGGATCCCCGAATTG	Thermo Fisher Scientific
29_Sc_Rpb1_Teton_BamHI_f	CAATTCGGGGGATCCGTATGGTAGGACAACAGTATTCTAGTGC	Thermo Fisher Scientific
24_Sc_Rpb1_FIII_r	GAAATGAGGTAAGGTACGATCTTGGAACCC	Thermo Fisher Scientific
25_Sc_Rpb1_FIII_f	GATCGTACCTTACCTCATTTCCCCAAAAATTCGAAATCCCCAG	Thermo Fisher Scientific
26_Sc_Rpb1-BsiWI_down _r	GAGACGTGGCTTCACC	Thermo Fisher Scientific
14_Sc_Rpb1_2485bp_f	AGGTCTTATCGATACCGCCG	Thermo Fisher Scientific
30_Sc_Rpb1_TEV1488_r	ACCTTGAAAGTACAAATTTTCTTTAACGTCAAGATCTGCATTG	Thermo Fisher Scientific
31_Sc_Rpb1_TEV1488_f	GAAAATTTGTACTTTCAAGGTCTGGTTGATTCGGG	Thermo Fisher Scientific

Name	Sequence[8]	Source
32_Sc_Rpb1-BsiWI_up_f	GACGCTATGGCTGGAGG	Thermo Fisher Scientific
33_Sc_Rpb1_9hep_r	GTTCGTCTTGCTTTGGCGAATATGATGGTGACG	Thermo Fisher Scientific
34_Sc_Rpb1_9hep_f	CGTCACCATCATATTCGCCAAAGCAAGACGAAC	Thermo Fisher Scientific
35_Sc_Rpb1_ccc2R_r	GTGGCCTTCTGTTATGCTCTAGTGTTTCCAAAC	Thermo Fisher Scientific
36_Sc_Rpb1_ccc2R_f	GCATAACAGAAGGCCACATCATGCTATTGAAG	Thermo Fisher Scientific
37_Sc_Rpb1_ccc7A_r	CAGCGGCGGCAGCTGCCTCTAGTGTTTCCAAACTAATATTAGC	Thermo Fisher Scientific
38_Sc_Rpb1_ccc7A_f	TGCCGCCGCTGCAGCTGCTATTGAAGAAGCAGAGAG	Thermo Fisher Scientific
39_Sc_Rpb1_I756K_f	GGGTTCATTTAAAAATATCGCG	Thermo Fisher Scientific
40_Sc_Rpb1_I756K_r	CGCGATATTTTTAAATGAACCC	Thermo Fisher Scientific
41_Sc_Rpb1_D1359K_f	GTTATTGCTTCTAAAGGTTCGTATG	Thermo Fisher Scientific
42_Sc_Rpb1_D1359K_r	CATACGAACCTTTAGAAGCAATAAC	Thermo Fisher Scientific
43_Sc_Rpb1_G1360Q_f	ATTGCTTCTGATCAATCGTATGTT	Thermo Fisher Scientific
44_Sc_Rpb1_G1360Q_r	AACATACGATTGATCAGAAGCAAT	Thermo Fisher Scientific
Sc_Rpb1_C-term-H10_f	CACCACCATCACCACCATCACCACCATCACTGATATAGTATATCATCCTTACG	Thermo Fisher Scientific
Sc_Rpb1_C-term-H10_r	GTGATGGTGGTGATGGTGGTGATGGTGGTGTCTGGAATTTTCATTTTCATTAT	Thermo Fisher Scientific
Sc_Rpb1_N-term-H10AS5_f	CACCACCATCACCACCATCACCACCATCACTCAGCGTCAGCGTCAGCGTCAGCGTCAGCGGTAGGACAACAGTATTCTAGTG	Thermo Fisher Scientific
Sc_Rpb1_N-term-H10AS5_r	CGCTGACGCTGACGCTGACGCTGACGCTGAGTGATGGTGGTGATGGTGGTGATGGTGGTGCATGTCTGATTTATATTTTGGGG	Thermo Fisher Scientific
Sc_Pep4_500bp_up_BamHI_f	TGCTAGCTGGATCCCGTTTTCAATATCTTGAGCTCCTCAATTG	Thermo Fisher Scientific
Sc_Pep4_200bp_down_XhoI_r	AGCTAGCACTCGAGCCGCATCATCGGGC	Thermo Fisher Scientific

Name	Sequence[8]	Source
Sc_Prb1_500bp_up_ NotI_f	TGCTAGCTGCGGCCGCCCCGACAAATCAGC CACTAAC	Thermo Fisher Scientific
Sc_Prb1_200bp_down_ BamHI_r	AGCTAGCAGGATCCAAAAACGCAAATATGTA GTAATACGTGG	Thermo Fisher Scientific
pFA6a_S1_NdeI_f	TGCTAGCTCATATGCGTACGCTGCAGGTCG AC	Thermo Fisher Scientific
pFA6a_S2_NsiI_r	AGCTAGCAATGCATATCGATGAATTCGAGCT CG	Thermo Fisher Scientific
Sc_Rpb9_KO_S1_f	CAAAATCTAGCCAAAAGAGCAAGTTAAACTC CCCTTAAAACTGCTATGCGTACGCTGCAGG TCGAC	Thermo Fisher Scientific
Sc_Rpb9_KO_S2_r	CATTTTCTCTCCCTCTGTCATTAATTTTGAAA GTTCGTTGAGCACTCAATCGATGAATTCGAG CTCG	Thermo Fisher Scientific
Mating_type_1	AGTCACATCAAGATCGTTTATGG	Thermo Fisher Scientific
Mating_type_2	GCACGGAATATGGGACTACTTCG	Thermo Fisher Scientific
Mating_type_3	ACTCCACTTCAAGTAAGAGTTTG	Thermo Fisher Scientific

Table 11: DNA oligonucleotides used as sequencing primers.[10]

Name	Sequence[8]	Source
natNT2_outfor	CGCTCTACATGAGCATGCCCTGCCC	Thermo Fisher Scientific
Sc_Rpb9_test_pr_f	AGCAGATTCTAGGTAGAACG	Thermo Fisher Scientific
Sc_Rpb9_test_pr_r	CATACGTGAAGATAAGTCCC	Thermo Fisher Scientific
9_Sc_Rpb1-EagI_up_f	AATGATATTGCTGGTCAACC	Thermo Fisher Scientific
10_Sc_Rpb1- BspHI_down_BamHI_r	AGCTAGCA GGATCCTTGGACTTGGTACTTT ACGG	Thermo Fisher Scientific
13_Sc_Rpb1_1704bp_f	CACCTGCAATTATCAAGCCC	Thermo Fisher Scientific
14_Sc_Rpb1_2485bp_f	AGGTCTTATCGATACCGCCG	Thermo Fisher Scientific
15_Sc_Rpb1_854bp_f	CTAGAGCATAACGGTGCTCC	Thermo Fisher Scientific

Name	Sequence[8]	Source
16_Sc_Rpb1_3734bp_f	CGTTGTCGTGTTGTTCGTCC	Thermo Fisher Scientific
45_Sc_Rpb1_Xba1_down_r	GCGCAGCATCCATACC	Thermo Fisher Scientific
M13uni (-21)	TGTAAAACGACGGCCAGT	Provided by sequencing company
M13rev (-29)	CAGGAAACAGCTATGACC	Provided by sequencing company

2.1.4 Media

Table 12: Media for *E. coli* cultivation.

Name	Description[11]
LB	1 % (w/v) Bacto tryptone, 0.5 % (w/v) yeast extract, 8.6 mM NaCl, 2.6 mM NaOH, plates contained 1.5 % (w/v) agar
ZY	1 % (w/v) tryptone, 0.5 % (w/v) yeast extract, used with 5052 and NPS (Table 13)

Table 13: Additives for *E. coli* media.

Name	Stock solution[11]	Applied concentration
50 × 5052	25 % (w/v) glycerol, 2.5 % (w/v) glucose, 10 % (w/v) α-lactose	0.5 % (w/v) glycerol, 0.05 % (w/v) glucose, 0.2 % (w/v) α-lactose
20 × NPS	0.5 M $(NH_4)_2SO_4$, 1 M KH_2PO_4, 1 M Na_2HPO_4	25 mM $(NH_4)_2SO_4$, 50 mM KH_2PO_4, 50 mM Na_2HPO_4
Ampicillin	10 % (w/v) ampicillin	0.1 % (w/v) ampicillin
Tetracycline	1.25 % (w/v) tetracycline in EtOH	0.00125 % (w/v) tetracycline
IPTG	1 M IPTG	2 mM IPTG

---

[11]If not specified, chemicals used to prepare buffers and solutions had *p.a.* quality and were produced by one of the following companies: Bio-Rad, Fluka, Invitrogen, Merck, Riedel-de Haën, Roth, Sigma-Aldrich or VWR. If not stated otherwise buffers and mixtures were aqueous solutions.

Table 14: Media for *S. cerevisiae* cultivation.

Name	Description[11]
YP	1.5 % (w/v) yeast extract, 2 % (w/v) peptone
YPD	YP, 2 % (w/v) glucose, plates contained 2 % (w/v) agar
YPD, clonNAT plates	YPD plates, 0.01 % (w/v) clonNAT
YPD, G-418 plates	YPD plates, 0.04 % (w/v) G-418 (~0.3 U/l G-418)
SC -Leu	0.69 % (w/v) YNB, 0.069 % (w/v) CSM -Leu, 2 % (w/v) glucose
SC -His plates	0.69 % (w/v) YNB, 0.077 % (w/v) CSM -His, 2 % (w/v) agar, 2 % (w/v) glucose
SC -Leu plates	0.69 % (w/v) YNB, 0.069 % (w/v) CSM -Leu, 2 % (w/v) agar, 2 % (w/v) glucose
SC -Trp plates	0.69 % (w/v) YNB, 0.074 % (w/v) CSM -Trp, 2 % (w/v) agar, 2 % (w/v) glucose
SC -Ura plates	0.69 % (w/v) YNB, 0.077 % (w/v) CSM -Ura, 2 % (w/v) agar, 2 % (w/v) glucose
SC -Ura, clonNAT plates	0.69 % (w/v) YNB, 0.077 % (w/v) CSM -Ura, 2 % (w/v) agar, 2 % (w/v) glucose, 0.01 % clonNAT
SC -Leu, -Ura plates	0.69 % (w/v) YNB, 0.067 % (w/v) CSM -Leu, -Ura, 2 % (w/v) agar, 2 % (w/v) glucose
5-FOA plates	0.69 % (w/v) YNB, 0.077 % (w/v) CSM -Ura, 0.002 % (w/v) uracil, 0.1 % (w/v) 5-FOA, 2 % (w/v) agar, 2 % (w/v) glucose
Sporulation plates	100 mM NaOAc, 25.5 mM KCl, 2.9 mM $MgSO_4 \cdot 7\ H_2O$, 20.5 mM NaCl, 1.5 % (w/v) agar

Table 15: Additives and components for *S. cerevisiae* media.

Name	Source	Stock solution[11]	Applied concentration
Ampicillin	Roth	10 % (w/v) ampicillin	0.005 % (w/v) ampicillin
Tetracycline	Roth	1.25 % (w/v) tetracycline in EtOH	0.00125 % (w/v) tetracycline
Antifoam C emulsion	Sigma-Aldrich	100 % (v/v) antifoam C emulsion	0.1 % (v/v) antifoam C emulsion
ClonNAT	Werner Bio-Agents	10 % (w/v) clonNAT	0.01 % (w/v) clonNAT
G-418	Formedium	20 % (w/v) G-418 (~150 U/l G-418)	0.04 % (w/v) G-418 (~0.3 U/l G-418)
6-azauracil	Sigma-Aldrich	100 mg/ml in DMSO	50–200 µg/ml
YNB	Formedium	-	0.69 % (w/v) YNB

Name	Source	Stock solution[11]	Applied concentration
CSM -His	Formedium	-	0.077 % (w/v) CSM -His
CSM -Leu	Formedium	-	0.069 % (w/v) CSM -Leu
CSM -Trp	Formedium	-	0.074 % (w/v) CSM -Trp
CSM -Ura	Formedium	-	0.077 % (w/v) CSM -Ura
CSM -Leu, -Ura	Formedium	-	0.067 % (w/v) CSM -Leu, -Ura

2.1.5 Buffers, markers, solutions and enzymes

Table 16: General buffers, dyes, markers and solutions.

Name	Description[11] or source
100 × PI	60 µM leupeptin, 200 µM pepstatin A, 98 mM PMSF, 211 mM benzamidine; in EtOH
4 × stacking gel buffer	0.5 M Tris-HCl, 0.4 % SDS (w/v), pH 6.8
4 × separation gel buffer	3 M Tris-HCl, 0.4 % SDS (w/v), pH 8.85
Tris-glycine running buffer	25 mM Tris, 250 mM glycine, 0.1 % (w/v) SDS
MES running buffer	50 mM MES, 50 mM Tris, 0.1 % (w/v) SDS, 1 mM EDTA
5 × SDS loading dye	25 % (v/v) glycerol, 7.5 % (w/v) SDS, 250 mM Tris-Cl (pH 6.8 at 20 °C), 0.5 % (w/v) bromophenol blue, 12.5 % (v/v) β-mercaptoethanol
1 × SDS loading dye	5 % (v/v) glycerol, 1.5 % (w/v) SDS, 50 mM Tris-Cl (pH 6.8 at 20 °C), 0.1 % (w/v) bromophenol blue, 2.5 % (v/v) β-mercaptoethanol
Broad range molecular weight marker	Bio-Rad
Coomassie stain	50 % (v/v) ethanol, 7 % (v/v) acetic acid, 0.125 % (w/v) Coomassie Brilliant Blue R-250
Destain	7 % (v/v) acetic acid, 5 % (v/v) ethanol
Ethidium bromide solution 1 %	Roth
SYBR Safe DNA gel stain, 10,000 × concentrate in DMSO	Invitrogen
TBE	90 mM Tris, 90 mM boric acid, 2 mM EDTA (pH 8.0)
6 × DNA loading dye	Fermentas
Gene Ruler 1 kb DNA ladder 0.1 µg/µl	Fermentas

Table 17: Buffers used for preparation of chemically competent *E. coli* cells.

Name	Description[11]
TFB-I	30 mM KOAc (pH 5.8 at 22 °C), 50 mM $MnCl_2$, 100 mM RbCl, 10 mM $CaCl_2$, 15 % (v/v) glycerol
TFB-II	10 mM MOPS (pH 7.0 at 4 °C), 75 mM $CaCl_2$, 10 mM RbCl, 15 % (v/v) glycerol

Table 18: Buffers used for Pol II purification via immunoaffinity chromatography.

Name	Description[11]
3 × freezing buffer	150 mM Tris-Cl (pH 7.9 at 4 °C), 3 mM EDTA, 30 µM $ZnCl_2$, 30 % (v/v) glycerol, 3 % (v/v) DMSO, 30 mM DTT, 3 × PI
Heparin column storage buffer	50 mM NaOAc, 20 % (v/v) ethanol
HSB150	50 mM Tris-Cl (pH 7.9 at 4 °C), 150 mM KCl, 1 mM EDTA, 10 µM $ZnCl_2$, 10 % (v/v) glycerol, 10 mM DTT, 1 × PI
HSB600	50 mM Tris-Cl (pH 7.9 at 4 °C), 600 mM KCl, 1 mM EDTA, 10 µM $ZnCl_2$, 10 % (v/v) glycerol, 10 mM DTT, 1 × PI
TEZ0	50 mM Tris-Cl (pH 7.5 at 20 °C), 1 mM EDTA, 10 µM $ZnCl_2$, 1 mM DTT, 1 × PI
TEZ250	10 % (v/v) 10 × TEZ0, 250 mM $(NH_4)_2SO_4$, 1 mM DTT, 1 × PI
TEZ250-azide	10 % (v/v) 10 × TEZ0, 250 mM $(NH_4)_2SO_4$, 0.02 % azide
TEZ500	10 % (v/v) 10 × TEZ0, 500 mM $(NH_4)_2SO_4$, 1 mM DTT, 1 × PI
TEZ500-glycerol	10 % (v/v) 10 × TEZ0, 500 mM $(NH_4)_2SO_4$, 50 % (v/v) glycerol, 1 mM DTT
TEZ500-ethylene glycol	10 % (v/v) 10 × TEZ0, 500 mM $(NH_4)_2SO_4$, 70 % (v/v) ethylene glycol
Pol II buffer	5 mM HEPES (pH 7.25 at 20 °C), 40 mM $(NH_4)_2SO_4$, 10 µM $ZnCl_2$, 10 mM DTT

Table 19: Buffers used for Pol II purification via Ni-NTA affinity chromatography.

Name	Description[11]
3 × freezing buffer	150 mM Tris-Cl (pH 7.9 at 4 °C), 3 mM EDTA, 30 µM $ZnCl_2$, 30 % (v/v) glycerol, 3 % (v/v) DMSO, 30 mM DTT, 3 × PI
HSB150/0	50 mM Tris-Cl (pH 7.9 at 4 °C), 150 mM KCl, 1 mM EDTA, 10 µM $ZnCl_2$, 10 % (v/v) glycerol, 10 mM DTT, 1 × PI
HSB0/0	50 mM Tris-Cl (pH 7.9 at 4 °C), 1 mM EDTA, 10 µM $ZnCl_2$, 10 % (v/v) glycerol, 2.5 mM DTT, 1 × PI
HSB1000/7	50 mM Tris-Cl (pH 7.9 at 4 °C), 1000 mM KCl, 1 mM EDTA, 10 µM $ZnCl_2$, 7 mM imidazole, 10 % (v/v) glycerol, 2.5 mM DTT, 1 × PI

Name	Description[11]
Ni buffer0	20 mM Tris-HCl (pH 7.9 at 4 °C), 150 mM KCl, 10 µM $ZnCl_2$, 2.5 mM DTT, 1 × PI
Ni buffer7	20 mM Tris-HCl (pH 7.9 at 4 °C), 150 mM KCl, 10 µM $ZnCl_2$, 7 mM imidazole, 2.5 mM DTT, 1 × PI
Ni buffer50	20 mM Tris-HCl (pH 7.9 at 4 °C), 150 mM KCl, 10 µM $ZnCl_2$, 50 mM imidazole, 2.5 mM DTT, 1 × PI
Ni buffer100	20 mM Tris-HCl (pH 7.9 at 4 °C), 150 mM KCl, 10 µM $ZnCl_2$, 100 mM imidazole, 2.5 mM DTT, 1 × PI
Ni buffer200	20 mM Tris-HCl (pH 7.9 at 4 °C), 150 mM KCl, 10 µM $ZnCl_2$, 200 mM imidazole, 2.5 mM DTT, 1 × PI
Ni buffer300	20 mM Tris-HCl (pH 7.9 at 4 °C), 150 mM KCl, 10 µM $ZnCl_2$, 300 mM imidazole, 2.5 mM DTT, 1 × PI
MonoQ0	20 mM Tris-acetate (pH 7.9 at 4 °C), 0.5 mM EDTA, 10 µM $ZnCl_2$, 10 % glycerol, 10 mM DTT
MonoQ150	20 mM Tris-acetate (pH 7.9 at 4 °C), 0.5 mM EDTA, 10 µM $ZnCl_2$, 10 % glycerol, 150 mM KOAc, 10 mM DTT
MonoQ2000	20 mM Tris-acetate (pH 7.9 at 4 °C), 0.5 mM EDTA, 10 µM $ZnCl_2$, 10 % glycerol, 2 M KOAc, 10 mM DTT (pH 7.9 at 4 °C)
Pol II buffer	5 mM HEPES (pH 7.25 at 20 °C), 40 mM $(NH_4)_2SO_4$, 10 µM $ZnCl_2$, 10 mM DTT

Table 20: Buffers used for Rpb4/7 purification.

Name	Description[11]
Rpb4/7 freezing buffer	50 mM Tris (pH 7.0 at 4 °C), 150 mM NaCl, 10 % glycerol, 10 mM β-mercaptoethanol, 1 × PI
Buffer0	50 mM Tris (pH 7.5 at 4 °C), 150 mM NaCl, 10 mM β-mercaptoethanol, 1 × PI
Buffer10	50 mM Tris (pH 7.5 at 4 °C), 150 mM NaCl, 10 mM imidazole, 10 mM β-mercaptoethanol, 1 × PI
Buffer20	50 mM Tris (pH 7.5 at 4 °C), 150 mM NaCl, 20 mM imidazole, 10 mM β-mercaptoethanol, 1 × PI
Buffer50	50 mM Tris (pH 7.5 at 4 °C), 150 mM NaCl, 50 mM imidazole, 10 mM β-mercaptoethanol, 1 × PI
Buffer200	50 mM Tris (pH 7.5 at 4 °C), 150 mM NaCl, 200 mM imidazole, 10 mM β-mercaptoethanol, 1 × PI
Salt buffer	50 mM Tris (pH 7.5 at 4 °C), 2 M NaCl, 10 mM β-mercaptoethanol, 1 × PI
SourceQ0	20 mM Tris (pH 7.5 at 4 °C), 1 mM EDTA, 10 mM DTT

Name	Description[11]
SourceQ100	20 mM Tris (pH 7.5 at 4 °C), 100 mM NaCl, 1 mM EDTA, 10 mM DTT
SourceQ2000	20 mM Tris (pH 7.5 at 4 °C), 2 M NaCl, 1 mM EDTA, 10 mM DTT
Pol II buffer	5 mM HEPES (pH 7.25 at 20 °C), 40 mM $(NH_4)_2SO_4$, 10 µM $ZnCl_2$, 10 mM DTT

Table 21: Buffers used for crystallisation.

Name	Description[11]
Pol II buffer	5 mM HEPES (pH 7.25 at 20 °C), 40 mM $(NH_4)_2SO_4$, 10 µM $ZnCl_2$, 10 mM DTT
NH_4OAc–$Mg(OAc)_2$ mother solution	50 mM HEPES (pH 7.0 at 20 °C), 140, 170 or 200 mM NH_4OAc, 150 mM $Mg(OAc)_2$, 3.5, 4.0, 4.5 or 5.0 % (w/v) PEG 6000, 5 mM TCEP
NH_4OAc–$Mg(OAc)_2$ cryo solution	50 mM HEPES (pH 7.0 at 20 °C), 140, 170 or 200 mM NH_4OAc, 150 mM $Mg(OAc)_2$, 3.5, 4.0, 4.5 or 5.0 % (w/v) PEG 6000, 5 mM TCEP 20 % (w/v) glycerol
NH_4OAc–NaOAc mother solution	50 mM HEPES (pH 7.0 at 20 °C), 140, 170 or 200 mM NH_4OAc, 300 mM NaOAc, 4.0, 4.5, 5.0, 5.5, 6.0, 6.5, 7.0 % (w/v) PEG 6000, 5 mM TCEP
NH_4OAc–NaOAc cryo solution	50 mM HEPES (pH 7.0 at 20 °C), 200 mM NH_4OAc, 300 mM NaOAc, , 4.0, 4.5, 5.0, 5.5, 6.0, 6.5, 7.0 % (w/v) PEG 6000, 5 mM TCEP, 22 % (w/v) glycerol

Table 22: Buffers, solutions and components used for RNA elongation experiments.

Name	Description[11] or source
TE	TRIS–EDTA Buffer Solution (pH 7.4), *BioChemika Ultra* (Sigma-Aldrich)
TE	20 mM HEPES (pH 7.6 at 20 °C), 60 mM $(NH_4)_2SO_4$, 8 mM $MgSO_4$, 10 µM $ZnCl_2$, 10 % (v/v) glycerol, 10 mM DTT
100 mM ATP	Fermentas
100 mM CTP	Fermentas
100 mM GTP	Fermentas
100 mM UTP	Fermentas
2 × urea loading dye	180 mM Tris, 180 mM boric acid, 4 mM EDTA (pH 8.0), 8 M urea, 0.03 % (w/v) bromophenol blue, 0.03 % (w/v) xylene cyanol FF
2 × urea loading buffer	180 mM Tris, 180 mM boric acid, 4 mM EDTA (pH 8.0), 8 M urea
TBE	90 mM Tris, 90 mM boric acid, 2 mM EDTA (pH 8.0)

Name	Description[11] or source
Rotiphorese NF-Acrylamide/ Bis-solution 40 % (19:1)	Roth
Rotiphorese NF-Urea	Roth

Table 23: Enzymes, buffers and components used for PCR and plasmid cloning.

Name	Source
dNTP mix, 2 mM each	Fermentas
dNTPs (100 mM; 25 mM each dNTP)	Stratagene
DMSO	Stratagene
Herculase II Fusion DNA Polymerase	Stratagene
5 × Herculase II Reaction Buffer	Stratagene
Phusion High-Fidelity DNA polymerase (2 U/μl)	Finnzymes (ordered at New England Biolabs)
Phusion Hot Start High-Fidelity DNA polymerase (2 U/μl)	Finnzymes (ordered at New England Biolabs)
5 × Phusion HF Buffer	Finnzymes (ordered at New England Biolabs)
Pwo SuperYield DNA polymerase (5 U/μl)	Roche
Pwo SuperYield PCR buffer	Roche
Taq DNA Polymerase (recombinant)	Fermentas
10 × *Taq* Buffer with KCl	Fermentas
25 mM MgCl$_2$	Fermentas
ApaI (50,000 U/ml)	New England Biolabs
BamHI (20,000 U/ml)	New England Biolabs
BsiWI (10,000 U/ml)	New England Biolabs
EagI (10,000 U/ml)	New England Biolabs
NsiI (10,000 U/ml)	New England Biolabs
SacI (20,000 U/ml)	New England Biolabs
XhoI (20,000 U/ml)	New England Biolabs
10 × NEBuffer 1, 2, 3 or 4	New England Biolabs
100 × BSA	New England Biolabs
T4 DNA Ligase	New England Biolabs
10 × T4 DNA Ligase Reaction Buffer	New England Biolabs

Table 24: Buffers used for yeast cloning experiments.

Name	Description[11]
TELit	155 mM LiOAc, 10 mM Tris/HCl (pH 8.0), 1 mM EDTA (pH 8.0)
LitSorb	18.2 % (w/v) D-sorbitol in TELit
LitPEG	40 % (w/v) PEG 3350 in TELit
One-step buffer	0.2 M LiOAc, 40 % (w/v) PEG 3350, 100 mM DTT
LiOAc/DTT	0.1 M LiOAc, 30 mM DTT

2.2 Methods

2.2.1 Plasmid cloning and amplification in *E. coli* cells

2.2.1.1 DNA amplification by polymerase chain reaction

PCR primers were designed to have a melting temperature of 50–65 °C and if possible having at least one C or G residue at their 3' ends. If primers contained a restriction enzyme recognition site an eight nucleotide overhang was included in the primer at its 5' end. A typical PCR reaction mixture with a volume of 50 µl contained 100–200 ng template DNA (plasmid or genomic DNA or PCR product), 0.5 µM of each DNA primer, 200 µM dNTPs and the standard concentration of the respective reaction buffer and enzyme (2.1.5, Table 23). For most applications Phusion High Fidelity DNA polymerase (Finnzymes) was best suited. PCR reactions were run in a T3000 Thermocycler (Biometra). Annealing temperature and extension time were adapted to the respective primers and length of desired amplification product according to polymerase supplier's information. 5 µl of the PCR reaction volume were analysed by agarose gel electrophoresis (2.2.3). PCR products were purified following the QIAquick PCR Purification Kit Protocol (QIAGEN).

2.2.1.2 Enzymatic restriction digest

Enzymatic restriction digests were usually performed in a volume of 50 µl. DNA obtained in one PCR reaction (2.2.1.1) or 1–5 µg of plasmid DNA were digested with DNA restriction enzymes (New England Biolabs) according to manufacturer's recommendations. Digested DNA was purified following the QIAquick Gel Extraction Kit Protocol (QIAGEN).

2.2.1.3 Enzymatic plasmid ligation

DNA amounts of insert and plasmid backbone were estimated analysing 1 µl each by agarose gel electrophoresis (2.2.3) and considering the respective length of fragments. Besides T4 DNA Ligase (New England Biolabs) and corresponding buffer the 20 µl ligation reaction mixture contained digested insert and plasmid with 2-10 fold molar excess of insert. For ligation the mixture was incubated for 1 h at 22 °C.

2.2.1.4 Plasmid transformation into *E. coli* cells

2.2.1.4.1 Transformation into chemically competent cells

Chemically competent *E. coli* (2.2.1.7.1) cells were thawed on ice. 1 µl plasmid DNA solution (2.2.1.5) or 10 µl ligation mixture (2.2.1.3) were added to the cell suspension and incubated for 5 min on ice, then incubated for 30 s at 42 °C, incubated for 1 min on ice and then plated on an LB-Amp plate (2.1.4, Table 12, Table 13) for selection. The plate was incubated overnight at 37 °C.

2.2.1.4.2 Transformation into electrocompetent cells

Electrocompetent *E. coli* cells (2.2.2.3.3.2) were thawed on ice. 3–5 µl ligation mixture (2.2.1.3) were added to the cell suspension and incubated for 5 min on ice. The mixture was transferred into a prechilled Gene Pulser cuvette (0.2 cm gap, Bio-Rad) and pulsed with 2.5 kV using a MicroPulser electroporation apparatus (Bio-Rad). 200 µl LB were added, cell suspension was transferred into a 1.5 ml reaction tube and incubated for 30 min at 37 °C, shaking at 600 rpm and plated on an LB-Amp plate for selection. The plate was incubated 20–24 h at 37 °C.

2.2.1.5 Plasmid amplification and isolation

To isolate plasmid DNA from XL1-blue cells (2.1.1, Table 3) 5 ml LB-Amp were inoculated with a single colony from an LB-Amp plate (2.2.1.4, 2.2.1.6) and incubated overnight at 37 °C, shaking at 160 rpm for cell growth. Cells were harvested by centrifugation (10 min, 3,900 × g, 4 °C). Plasmid DNA was isolated according to the QIAprep Miniprep Protocol (QIAGEN). Due to the high yield of pRS plasmids (2.1.2) these plasmids were eluted from the spin columns with 100 µl H_2O.

2.2.1.6 Sequence verification of isolated plasmids by test restriction digest or colony PCR and sequencing

To verify the correct construction of clones it was first checked whether the desired insert was contained in isolated plasmid clones (2.2.1.5). Therefore, a test restriction digest was performed in a volume of 20 µl, containing 1 µl plasmid DNA, 0.3 µl of each restriction enzyme and buffer (2.1.5, Table 23) and incubated for 1 h at the respective temperature. Alternatively for easier analysis of large amounts of clones a colony PCR was performed to amplify the desired insert. The PCR reaction mixture

of 50 µl contained 0.64 µM of each primer, 150 µM dNTPs, 2 % DMSO and 2.5 mM MgCl$_2$, 1.5 U *Taq* DNA polymerase (Fermentas) and 1 × *Taq* Pol buffer + KCl. To add template DNA a colony from the transformation plate (2.2.1.4) was picked with a plastic inoculation loop and dipped into the PCR reaction mixture. Then the same loop was used to streak the cells on an LB-Amp plate that was then incubated overnight at 37 °C. Colony PCR reactions were run as described (2.2.1.1.) 20 µl of the test restriction digest mixture or 15 µl of the colony PCR mixture were analysed by agarose gel electrophoresis (2.2.3). After colony PCR only plasmid clones known to contain the desired insert were then subjected to plasmid amplification and isolation (2.2.1.5). A clone that was positively tested to contain the insert was then analysed in detail by sequencing the insert and ligation region. Sequencing was performed by Eurofins MWG Operon or at GATC Biotech providing template and primer amounts as requested by the respective company.

2.2.1.7 Preparation of competent *E. coli* cells for plasmid transformation

2.2.1.7.1 Chemically competent *E. coli* cells

500 ml LB with antibiotic (2.1.4, Table 12, Table 13) were inoculated with 10 ml of an overnight culture of the desired strain (2.1.1, Table 3) and incubated at 37 °C, shaking at 160 rpm until an OD$_{600}$ of 0.5 was reached. Cells were cooled on ice for 10 min. In the following the sample was permanently treated on ice or at 4 °C. Cells of 450 ml culture were harvested by centrifugation (10 min, 3,700 × g) and resuspended in 100 ml TFB-I (2.1.5, Table 17). The suspension was centrifuged (10 min at 3,700 × g) resuspended in 8 ml TFB-II (2.1.5, Table 17). Aliquots of 50 µl were frozen in liquid N$_2$ and stored at -80 °C.

2.2.1.7.2 Electrocompetent *E. coli* cells

For better transformation efficiency after ligation electrocompetent XL1-blue cells (2.1.1, Table 3) were prepared. 2 l LB were inoculated with 20 ml of an overnight culture and incubated at 37 °C, shaking at 160 rpm, until an OD$_{600}$ of 0.5 was reached. Cells were cooled on ice for 15 min. In the following the sample was always kept on ice or at 4 °C. Cells were harvested by centrifugation (10 min, 1,000 × g). Cells were resuspended in 800 ml sterile H$_2$O. The suspension was centrifuged (10 min, 1,000 × g) and cells were resuspended in 400 ml sterile H$_2$O. Centrifugation was repeated and cells were resuspended in 20 ml sterile 10 % (v/v) glycerol. After centrifu-

gation (10 min, 5,000 × g) cells were resuspended in 3 ml sterile 10 % (v/v) glycerol. Aliquots of 50 µl were frozen in liquid N_2 and stored at -80 °C.

2.2.2 Vector-based and genomic cloning with *S. cerevisiae* cells

2.2.2.1 General treatment of yeast cultures and storage of strains

Liquid yeast cultures were continuously checked for absence of contaminants using a light microscope (Leica DM LS, Leica). For long-term storage of strains as glycerol stock a mixture of an overnight culture with 25 % (v/v) glycerol was stored at -80 °C. For regular use cells were incubated on appropriate selective plates for cell growth (2.1.4, Table 14, Table 15) and then stored at 4 °C. After 3–4 weeks cells were re-streaked on a fresh plate. After restreaking cells for ten times cells from a glycerol stock were streaked on a fresh plate.

2.2.2.2 Plasmid transformation into *S. cerevisiae* cells and selection of transformants

A pinhead size amount of cells was scraped from a plate and suspended in 1 ml sterile H_2O. Cells were pelleted by centrifugation (1 min, 15,000 × g, room temperature (RT)). Cells were resuspended in 100 µl one-step buffer (2.1.5, Table 24). 0.2 % (w/v) salmon sperm DNA (Sigma-Aldrich) was incubated 10 min at 95 °C and shock-cooled on ice. 10 µl salmon sperm DNA solution was mixed with 2 µl plasmid DNA solution (2.2.1.5). 100 µl cell suspension in one-step buffer were added to the DNA solution. The mixture was incubated 30 min at 45 °C, then 1 ml sterile H_2O was added. Cells were pelleted by centrifugation (10 s, 15,000 × g, RT), resuspended in 100 µl H_2O, plated on a selection plate, which was incubated for two nights at 30 °C.

2.2.2.3 Introduction of genomic mutations in *S. cerevisiae* cells by ho-mologous recombination

2.2.2.3.1 DNA amplification by PCR

DNA to be used for homologous recombination in *S. cerevisiae* was amplified as de-scribed (2.2.1.1) with the following changes: presence of the full recombination se-quence in the primers results in very long primers of 65–70 b that can make a suc-cessful amplification difficult due to formation of secondary structures. In this case a

reduced concentration of 0.025 µM of each primer and 12 ng template plasmid DNA were used in the PCR reaction mixture. For amplification of the GC-rich natNT2 cassette from pFA6a-natNT2 (2.1.2, Table 6) Herculase II Fusion DNA Polymerase (Stratagene) was used in presence of 2 % (v/v) DMSO. To obtain highly concentrated DNA sufficient for transformation and homologous recombination five PCR setups of 50 µl each were run in parallel and pooled. DNA was purified using the QIAquick PCR Purification Kit Protocol (QIAGEN) or alternatively after agarose gel electrophoresis (2.2.3) by the QIAquick Gel Extraction Kit Protocol (QIAGEN).

2.2.2.3.2   Transformation of linear DNA into *S. cerevisiae* cells

2.2.2.3.2.1   Transformation into chemically competent *S. cerevisiae* cells

0.5–5 µg purified DNA (2.2.2.3.1) in a volume not exceeding 10 µl were added to a 50 µl suspension of competent cells (2.2.2.3.3.1). 360 µl LitPEG (2.1.5, Table 24) were added and incubated for 30 min at RT. 47 µl DMSO were added and incubated for 10 min at 30 °C, then 5 min at 37 °C and cells were pelleted by centrifugation (3 min, 350 × g, RT). Cells were resuspended in 1 ml YPD and incubated for 3 h, shaking at 500 rpm for recovery at 30 °C or 24 °C if temperature-sensitivity of the mutant strain might be possible. Centrifugation was repeated; cells were resuspended in 100 µl H_2O and plated on a selective plate. The plate was incubated at 30 °C or 24 °C as before for several days until colonies appeared.

2.2.2.3.2.2   Transformation into electrocompetent *S. cerevisiae* cells

250 ng DNA, solved in H_2O (2.2.2.3.1) was added to 100 µl cell suspension (2.2.2.3.3.2), transferred into a prechilled Gene Pulser cuvette (0.2 cm gap, Bio-Rad) and pulsed with 2.5 kV using a MicroPulser electroporation apparatus (Bio-Rad). 1 ml YPD (30 °C) was added; the cell suspension was transferred to a 2 ml Eppendorf reaction tube and incubated for 1 h at 30 °C, shaking at 350 rpm. After centrifugation (10 s, 350 × g, RT) cells were resuspended in 100 µl H_2O, plated on a selective plate and incubated at 30 °C for 2–3 days.

2.2.2.3.3   Preparation of competent *S. cerevisiae* cells for homologous recombination

2.2.2.3.3.1   Chemically competent *S. cerevisiae* cells

100 ml YPD were inoculated with an overnight culture at a starting OD_{600} of 0.2 and incubated at 30 °C, shaking at 150 rpm until OD_{600} was 0.5–0.7. Cells of 50 ml culture were harvested by centrifugation (5 min, 3,900 × g, 22 °C) and resuspended in 25 ml sterile H_2O. Centrifugation was repeated and cells were resuspended in 5 ml LitSorb (2.1.5, Table 24) and after another centrifugation in 360 µl LitSorb. 0.2 % (w/v) salmon sperm DNA (Sigma-Aldrich) was heated 10 min at 95 °C and shock-cooled on ice. 40 µl salmon sperm DNA were added to the cell suspension. 50 µl aliquots were used immediately for transformation (2.2.2.3.2.1) or alternatively stored at -80 °C.

2.2.2.3.3.2   Electrocompetent *S. cerevisiae* cells

500 ml YPD were inoculated with an overnight culture at a starting OD_{600} of 0.15 and incubated at 30 °C, shaking at 150 rpm until OD_{600} was 0.7–0.8. Cells of 100 ml culture were harvested by centrifugation (5 min, 4,900 × g, 4 °C). In the following the sample was permanently treated on ice or at 4 °C. Centrifugation was repeated to wash cells two times with 50 ml H_2O and then with 50 ml 1 M D-sorbitol. Cells were then resupended in 20 ml LiOAc/DTT (2.1.5, Table 24) and incubated for 30–60 min at 30 °C, shaking at 160 rpm. Then the sample was again permanently treated on ice or at 4 °C. Cells were washed two times with 50 ml 1 M D-sorbitol, including centrifugation as described above. Cells were resuspended in 1 ml 1 M D-sorbitol, centrifuged (1 min, 1,500 × g) and finally a cell pellet of 100 µl volume was resuspended in 50 µl 1 M D-sorbitol.

2.2.2.3.4   Verification of genomic mutation by colony PCR

Clones obtained after transformation (2.2.2.3.2) were verified as successful transformants by colony PCR. A pinhead size amount of yeast cells was suspended in 100 µl 0.02 M NaOH and 50–100 µl soda lime glass beads (Ø = 0.5 mm, BioSpec Products) were added. The suspension was incubated for 5 min at 99 °C, shaking at 1,400 rpm and then centrifuged (15 s, 20,000 × g, RT). 5 µl of the DNA-containing supernatant provided the template for a colony PCR that was set up and run as described (2.2.1.6). Amplification primers were designed such that the presence or size of an

amplification product proved the presence of the genomic mutation at the intended locus.

2.2.2.4 Sporulation of diploid *S. cerevisiae* cells, tetrad dissection and isolation of haploid clones

Diploid *S. cerevisiae* cells were incubated on a sporulation plate (2.1.4, Table 14) at 30 °C for 100–120 h to stimulate sporulation. Cells were scratched from the plate, resuspended in 500 µl H_2O, centrifuged (15 s, 20,000 × g, RT) and washed with 500 µl H_2O. Centrifugation was repeated and cells were resuspended in 100 µl H_2O. 10 µl Glusulase (PerkinElmer) were added and incubated for 3.5–5 min at RT for enzymatic partial digestion of asci. The reaction was stopped by dilution with 500 µl H_2O and incubation on ice. 20 µl cell suspension were added to the boundary area of a YPD plate (2.1.4, Table 14). Tetrads were dissected and spores positioned individually on the plate using an MSM System (Singer Instruments) dissection microscope. The plate was incubated for 3–5 days at 30 °C.

2.2.2.5 Determination of the mating type of *S. cerevisiae* clones

To test the mating type of yeast clones a colony PCR (2.2.2.3.4) was performed using three mating type specific primers (2.1.3, Table 10) together in one reaction. An amplified product of 404 bp or 544 bp indicates Mat α or Mat a, respectively, while a diploid clone can be identified by the amplification of both bands.

2.2.2.6 Plasmid shuffling and viability test

In yeast it is possible to easily replace one gene that is born on a plasmid by another by plasmid shuffling. Therefore the gene of interest was present on a plasmid containing a URA3 selection marker gene (*e.g.* pRS316, 2.1.2, Table 7). A second plasmid with another selection marker (*e.g.* LEU2, pRS315, 2.1.2, Table 7) was transformed into cells (2.2.2.2). Transformants containing both plasmids were selected by growth on SC -Leu, -Ura plates (2.1.4, Table 14). Cells were then grown on an SC -Leu plate (2.1.4, Table 14), selecting only for the second plasmid and eventually allowing loss of the plasmid containing the URA3 marker, then cells were grown on a YPD plate (2.1.4, Table 14). A pin-head size amount of cells from this plate was washed in 500 µl H_2O. After centrifugation (15 s, 20,000 × g, RT) cells were resuspended in 500 µl H_2O. Cell suspensions were vortexed immediately before all follow-

ing pipetting steps. 50 µl cell suspension were diluted to 500 µl with H_2O, thus creating five serial dilutions with a 1:10 ratio. 3 µl of each dilution were spotted on a 5-FOA plate and as control on a YPD plate (2.1.4, Table 14). Plates were incubated two days at 30 °C. Only cells that had lost the plasmid containing the URA3 marker gene can grow on a 5-FOA plate. Provided that this plasmid contained the only copy of an essential gene, cells growing on a 5-FOA plate were rescued by another copy present on the second plasmid, while the first plasmid was lost.

2.2.3 Agarose gel electrophoresis for DNA separation

DNA was analysed by horizontal gel electrophoresis. Gels contained 1 % agarose dissolved in TBE and 1 × SYBR Safe DNA gel stain (2.1.5, Table 16) and were casted and run in PerfectBlue gel systems (Peqlab). 6 × DNA loading dye (2.1.5, Table 16) was added to DNA solutions and gels were run (2.1.5, Table 16) at 15–20 V/cm using TBE as running buffer. DNA was visualised by ultraviolet transillumination at a wavelength of 366 nm in a gel documentation system (Intas).

2.2.4 Cell growth and purification of endogenous *S. cerevisiae* Pol II

2.2.4.1 Fermentation of *S. cerevisiae* cells

The respective *S. cerevisiae* Pol II purification strain (2.1.1, Table 4) was streaked on a YPD plate (2.1.4, Table 14) and incubated for three days at 30 °C. 50 ml YPD-Amp-Tet (2.1.4, Table 14, Table 15) were inoculated with cells from the plate and incubated (10–15 h, 30 °C, shaking at 150 rpm). 500 ml YPD-Amp-Tet were inoculated with 50 ml of the previous culture and incubated (10–15 h, 30 °C, shaking at 150 rpm). 15–17 l YPD-Amp-Tet-antifoam C (pH 6.9, 2.1.4, Table 14, Table 15) were inoculated at an OD_{600} of 0.2–0.25 with the previous culture and incubated in a fermenter (*Laborfermenter Typ* NLF 30 L, Bioengineering) (10–18 h, 30 °C, stirring at 250 rpm, air flow at 20 Nl/h). Typically 200 l YPD-Amp-Tet-antifoam C (pH 6.9) were inoculated at an OD_{600} of 0.2–0.25 with the previous culture and incubated in a fermenter (*Pilot Fermenter Typ* P 300 L, Bioengineering) (10–18 h, 30 °C, stirring at 250 rpm, air flow at 82 Nl/h). Until beginning of 2009 yeast fermentation was carried

out in an analogous fashion using two other fermenters (ISF200 and ABEC, Infors). Cells were harvested at late log or early stationary phase.

2.2.4.1.1   Harvesting of cells from 20 l fermenter

After incubation in the 20 l fermenter cells were harvested by centrifugation (10 min, 5,471 × g, 4 °C). 10–20 g of cells per litre cell culture were usually obtained. Cells were resuspended in 330 ml 3 × freezing buffer (2.1.5, Table 19) per kg of cells at 4 °C. 200 ml aliquots of cell suspension containing ~150 g of cells were frozen in liquid N_2 and stored at -80 °C.

2.2.4.1.2   Harvesting of cells from 200 l fermenter

After incubation in the 200 l fermenter cells were harvested directly using a continuous flow centrifuge (Z41/G, Carl Padberg Zentrifugenbau) (2 × 120 min, 20,000 × rpm, 20–30 °C). 5–15 g of cells per litre cell culture were usually obtained. Cells were treated as described (2.2.4.1.1).

2.2.4.2   Purification of Pol II via immunoaffinity chromatography

Wild type Pol II not containing any affinity tags can be specifically purified via an immunoaffinity step (Edwards *et al.*, 1990). This procedure was used to purify ten-subunit Pol II (Table 1) from the *rpb4* deletion strain CB010Δ*rpb4* (2.1.1, Table 4).

2.2.4.2.1   Cell lysis

3 × 200 ml cell suspension (2.2.4.1) were thawed in a water bath (T < 30 °C). All following steps were performed on ice or at 4 °C. 1 ml 100 × PI (2.1.5, Table 16) was added and the suspension transferred to the metal chamber of a BeadBeater (Bio-Spec Products), containing 200 ml soda lime glass beads (Ø = 0.5 mm, BioSpec Products). Air bubbles were removed stirring gently with a glass rod. The chamber was completely filled up with HSB150 (2.1.5, Table 18) before assembly with the impeller and motor, which was run 60–70 min in cycles being 30 s on and 90 s off. To prevent warming, the lysis chamber was surrounded and covered with salt-ice mix, which was regularly renewed. The lysate was separated from beads filtering through a mesh funnel and washed with HSB150, not exceeding a total volume of 1000 ml. The lysate was centrifuged twice (45 min, 13,689 × g, 4 °C) and filtered through cheesecloth and paper filter to remove the lipid phase of the lysate.

2.2.4.2.2   Heparin affinity chromatography

The following steps were performed at 4 °C. 250 ml Heparin Sepharose 6 Fast Flow (Amersham Biosciences, now GE Healthcare) affinity resin were equilibrated with three cv HSB150 (2.1.5, Table 18) using an Econo Pump (Bio-Rad). The lysate (2.2.4.2.1) was loaded, then washed with three cv HSB150 and eluted with two cv HSB600 (2.1.5, Table 18). The first 100 ml of elution were discarded; the following 400 ml were collected.

2.2.4.2.3 $(NH_4)_2SO_4$ precipitation and redissolving

291 g fine ground $(NH_4)_2SO_4$ per litre were added to the elution fraction and incubated overnight at 4 °C, stirring (80–150 rpm) for protein precipitation. The solution was centrifuged (45 min, 21,859 × g, 4 °C) and the precipitate was dissolved in 40 ml 1 × TEZ0 (2.1.5, Table 18). If necessary 1 × TEZ0 was added to decrease conductivity, which was measured diluting 30 µl to 6 ml with deionised H_2O (Millipore) using a *Konduktometer* (Schott) and should be < 400 µS/cm. Finally the solution was centrifuged (15 min, 34,155 × g, 4 °C) to remove undissolved particles.

2.2.4.2.4   Immunoaffinity chromatography

The immunoaffinity resin contained immobilised antibody 8WG16 (NeoClone) that binds selectively to the C-terminal domain of Rpb1 in its unphosphorylated state. Two columns with each 5 ml resin were equilibrated with three cv TEZ250 lacking DTT and PI followed by one cv TEZ250 (2.1.5, Table 18). The sample was loaded onto one column whose flow-through was directly loaded onto the second column. Columns were closed, equilibrated 10 min at RT, washed with five cv TEZ500 and bound proteins were eluted with TEZ500-glycerol (2.1.5, Table 18). At least 15 1 ml fractions were collected and immediately transferred to ice. Protein content of fractions was qualitatively checked adding 10 µl sample to 200 µl of a 1:5 dilution of Bio-Rad Protein Assay dye reagent concentrate (Bio-Rad) in a microtitre plate and peak fractions were pooled. DTT was added ad 10 mM and the pool stored overnight at 4 °C. Immediately after use, the antibody columns were washed with three cv TEZ500-ethylene glycol, reequilibrated with three cv TEZ250-azide and stored at 4 °C in TEZ250-azide (2.1.5, Table 18).

2.2.4.2.5   Buffer exchange, $(NH_4)_2SO_4$ precipitation and storage

As Pol II was eluted from the immunoaffinity column with 50 % glycerol (2.2.4.2.4), buffer had to be exchanged prior to $(NH_4)_2SO_4$-precipitation. The pooled sample was diluted to 50 ml with Pol II buffer and concentrated using an Amicon Ultra-15 Centrifugal Filter Device, 100,000 MWCO (1,300 × g, 4 °C). After concentrating to ~5 ml, ~10 ml Pol II buffer were added and concentrated further. Alternately protein sample was added and concentrated. Pol II buffer was added repeating the concentration until the conductivity (2.2.4.2.3) of the flow through corresponded to the one of Pol II buffer. The sample was concentrated to 2 mg/ml protein concentration determined as described (2.2.6). For precipitation, 1.13 times the volume of $(NH_4)_2SO_4$ solution (saturated at RT) was added to aliquots of 100–500 µg purified Pol II. Samples were incubated 1–14 h at 4 °C on a rotating wheel and centrifuged (30 min, 16,060 × g, 4 °C). The supernatant was partly removed, leaving a liquid-covered protein precipitate. Samples were frozen in liquid N_2 and stored at -80 °C.

2.2.4.3   Purification of Pol II via Ni-NTA affinity chromatography

2.2.4.3.1   Cell lysis

Cell lysis was performed as described (2.2.4.2.1) with the following exceptions: Typically 2 × 200 ml cell suspension (2.2.4.1) were used per purification. Lysis in the BeadBeater was done for 80 min, the lysate was centrifuged once and filtering through cheesecloth was omitted.

2.2.4.3.2   Ultracentrifugation, $(NH_4)_2SO_4$ precipitation and redissolving

The lysate was subjected to ultracentrifugation (90 min, 76,221 × g, 4 °C) using an SW28 rotor (Beckman-Coulter). The aqueous phase of the supernatant was collected. 291 g fine ground $(NH_4)_2SO_4$ per litre were added to the elution fraction and incubated overnight at 4 °C, stirring (80–150 rpm) for protein precipitation. The solution was centrifuged (2 × 45 min, 34,200 × g, 4 °C) and the precipitate was dissolved in 140 ml HSB0/0 (2.1.5, Table 19) per 100 g of $(NH_4)_2SO_4$ pellet by stirring 1–2 h at 4 °C. Conductivity (2.2.4.2.3) of the protein solution was reduced to the conductivity corresponding to HSB1000/7 (2.1.5, Table 19) by addition of HSB0/0. The sample was centrifuged (10 min, 34,200 × g, 4 °C) and imidazole was added ad 7 mM.

2.2.4.3.3   Ni-NTA affinity chromatography

Ni-NTA Agarose (QIAGEN) was equilibrated with HSB1000/7 (2.1.5, Table 19) not containing DTT. The sample was mixed with 16 ml Ni-NTA Agarose and incubated for 60 min, stirring at 4 °C. The suspension was split into three aliquots and applied each to a gravity flow column. The resin was washed with five cv HSB1000/7 and then three cv Ni buffer7 (2.1.5, Table 19). When eluting hexahistidine-tagged Pol II, three cv each of Ni buffer50 and Ni buffer100 (2.1.5, Table 19) were applied to the column. When eluting decahistidine-tagged Pol II, three cv each of Ni buffer100 and Ni buffer200 (2.1.5, Table 19) were used. Elution fractions were pooled and conductivity was set cooresponding to MonoQ150 by addition of MonoQ0 (2.1.5, Table 19).

2.2.4.3.4   Anion exchange chromatography

The Ni-NTA affinity elution fraction was centrifuged (20 min, 17,211 × g, 4 °C). A Mono Q 10/100 GL (Amersham Biosciences, now GE Healthcare) was equilibrated with MonoQ150 using an ÄKTAexplorer HPLC system (Amersham Biosciences, now GE Healthcare), the sample was loaded and washed with four cv MonoQ150. For elution a linear salt gradient over twelve cv from MonoQ150 to MonoQ2000 (2.1.5, Table 19) was applied. Pol II typically eluted at a conductivity of 50–55 mS/cm and the respective fractions were pooled.

2.2.4.3.5   Buffer exchange, $(NH_4)_2SO_4$ precipitation and storage

After anion exchange chromatography the pooled sample was diluted and buffer was exchanged to Pol II buffer followed by $(NH_4)_2SO_4$ precipitation and storage as described (2.2.4.2.5).

2.2.4.4   Small scale purification of Pol II for test purposes

For a qualitative test Pol II purification was performed in a small scale as described (2.2.4.3) with changes described in the following. Cells were grown in a 2 l culture and harvested as described (2.2.4.1, 2.2.4.1.1). A 50 % (w/v) cell suspension containing 10 g of cells was added to 20 ml soda lime glass beads (Ø = 0.5 mm, Bio-Spec Products) subjected to cell lysis (3 × 4 min rotation at 500 rpm with 1 min pause, 4 °C) using a Pulverisette 6 classic line (Fritsch). During anion exchange a Mono Q 5/50 GL (Amersham Biosciences, now GE Healthcare) was used.

2.2.5 Expression and purification of Rpb4/7

2.2.5.1 Recombinant expression of Rpb4/7 in *E. coli*

The Rpb4/7 expression plasmid pET-21b(+)-Rpb4/7 (2.1.2, Table 5) was transformed (2.2.1.4.1) into BL21-CodonPlus (DE3)-RIL cells (2.1.1, Table 3) and incubated on an LB-Amp plate (2.1.4, Table 12, Table 13). 25 ml LB-Amp medium were inoculated with cells from the transformation plate and incubated for 6 h at 37 °C, shaking at 180 rpm. Expression was performed in auto-inducing medium (Studier, 2005). 2 l ZY-Amp (2.1.4, Table 12, Table 13) were inoculated with the 25 ml preculture and incubated for 3.5 h at 37 °C, shaking at 180 rpm until OD_{600} reached 0.6–0.8. The temperature of the cell culture was decreased quickly on ice and subsequently incubated for 24 h at 20 °C, shaking at 180 rpm. Cells were harvested by centrifugation (20–30 min, 5,471 × g, 4 °C), resuspended in 25 ml Rpb4/7 freezing buffer (2.1.5, Table 20), frozen in liquid N_2 and stored at -80 °C.

2.2.5.2 Purification of Rpb4/7

2.2.5.2.1 Cell lysis

Cells from 8 l expression culture were pooled and lysed using a homogeniser (Emul-siFlex-C5, Avestin). The lysate was cleared by centrifugation (2 × 30 min, 26,891 × g, 4 °C).

2.2.5.2.2 Ni-NTA affinity chromatography

4 × 2 ml Ni-NTA Agarose (QIAGEN) were equilibrated with five cv buffer0 (2.1.5, Table 20). All subsequent steps were carried out at 4 °C. The lysate was loaded twice by gravity flow. The resin was washed with five cv buffer0 then with three cv each of salt buffer, buffer10 and buffer20 (2.1.5, Table 20). Proteins were eluted applying three cv buffer50 and six cv buffer200 (2.1.5, Table 20).

2.2.5.2.3 Anion exchange chromatography

Ni-NTA elution fractions (2.2.5.2.2) were pooled and diluted slowly with SourceQ0 to the conductivity of SourceQ100 (2.1.5, Table 20). The sample was filtered using a Millex-GP, filter pore size 0.22 μm (Millipore). The following steps were performed using an FPLC system (ÄKTApurifier, Amersham Biosciences, now GE Healthcare). The anion exchange column (SOURCE 15Q 16/10, Amersham Biosciences, now GE

Healthcare) was equilibrated with a mixture of 5 % SourceQ2000 and 95 % SourceQ0 (2.1.5, Table 20). Ni-NTA elution fraction was loaded to the column and washed with two cv as before. Elution was performed with a linear salt gradient of 100–1000 mM NaCl (5 %–50 % SourceQ2000) over ten cv. Rpb4/7 eluted at a conductivity of 28–31 mS/cm.

2.2.5.2.4   Size exclusion chromatography

Rpb4/7 containing fractions after anion exchange chromatography (2.2.5.2.3) were pooled and concentrated using an Amicon-Ultra-15 Centrifugal Filer Unit, MWCO 10 kDa (Millipore) to a volume of 5 ml. The protein solution was filtered as before (2.2.5.2.3) and subjected to size exclusion chromatography using a HiLoad 26/60 Superdex 75 pg column (Amersham Biosciences, now GE Healthcare) with Pol II buffer (2.1.5, Table 20) as running buffer. Fractions of interest were pooled and concentrated as before to a concentration of 6 mg/ml. 40 µl aliquots corresponding to 5 nmol Rpb4/7 were frozen in liquid N_2 and stored at -80 °C.

2.2.6   Measurement of protein concentration

Protein concentration of protein solutions was determined according to the Bradford assay (Bradford, 1976). A 1:5 dilution of Bio-Rad Protein Assay dye reagent concentrate (Bio-Rad) was used to measure absorption at a wavelength of 595 nm in a 1 cm plastic cuvette with a BioPhotometer (Eppendorf). Standard absorption values were determined for each batch of reagent using bovine serum albumin (Albumin Fraktion V, Roth).

2.2.7   Denaturing concentration of proteins by trichloroacetic acid precipitation

To visualise proteins by SDS-PAGE from low concentrated protein solutions proteins were concentrated by precipitation with TCA. 6.1 N (= 100 %) TCA was added to the protein solution to a final concentration of 10 % (v/v) TCA. The sample was incubated 30–60 min on ice or alternatively overnight at 4 °C and precipitated protein was pelleted by centrifugation (60 min, 16,100 × g, 4 °C). The pellet was washed with 1 ml acetone, which was equilibrated by incubation at -20 °C in advance. After centrifugation (5 min, 16,100 × g, 4 °C) the pellet was dried by incubating the open reaction

tube for 60 min at RT and dissolved in 6 µl 1 × SDS loading dye (2.1.5, Table 16). If an acidic pH was shown by the solution turning yellow, the solution was neutralised by bringing the surface in contact with the gas phase above a 25 % NH$_3$-solution until the sample solution turned blue.

2.2.8 SDS-PAGE for protein separation

Electrophoretic separation of proteins was conducted by vertical SDS-PAGE. Gels contained 3.75 % (v/v) acrylamide and 15 % (v/v) acrylamide (Rotiphorese Gel 30 (37.5:1), Roth) in the stacking and separating gel, respectively and 1 x stacking or separating gel buffer (2.1.5, Table 16) with 0.01 %–0.05 % TEMED and 0.1%–0.065 % (w/v) APS. Gels were casted and run in Mini-gel systems (Bio-Rad) using Tris-glycine running buffer (2.1.5, Table 16). To achieve better protein separation acrylamide gradient gels (NuPAGE Novex 4–12 % Bis-Tris Gel 1.0 mm, Invitrogen) were run in a Novex Mini Cell (Invitrogen) using MES running buffer (2.1.5, Table 16). 5 × SDS loading dye (2.1.5, Table 16) was added to samples and incubated for 5 min at 95 °C. Gels were stained in Coomassie stain for 20–60 min at RT and destained overnight at RT in destain (2.1.5, Table 16).

2.2.9 X-ray crystallographic analysis of Pol II complexes

2.2.9.1 Nucleic acid scaffold formation by annealing

To form non-covalent nucleic acid complexes, DNA or RNA oligonucleotides (dissolved at 400 µM in TE (2.1.5, Table 22)) were mixed in equimolar amounts and diluted to 100 µM by addition of TE. Annealing was performed in a volume of 25–50 µl in a T3000 Thermocycler (Biometra). At 99 °C lid temperature the solution was heated for 180 s at 95 °C and temperature was subsequently reduced (90 s per -1 °C) to 20 °C.

2.2.9.2 Protein-nucleic acid complex assembly and gel filtration

Typically 500 µg (NH$_4$)$_2$SO$_4$-precipitated Pol II (2.2.4.2, 2.2.4.3) were thawed while centrifuging (15–25 min, 16,060 × g, 4 °C). The precipitate was dissolved in 125 µl Pol II buffer per 100 µg Pol II and the concentration was determined (2.2.6). Typically a twofold molar excess of an annealed nucleic acid scaffold (2.2.9.1) was added and

incubated (10 min, 350 rpm, 20 °C) to assemble a Pol II-nucleic acid complex. Then Rpb4/7 (2.2.5.2) was added in a fivefold molar excess with respect to Pol II and the mixture was incubated (20 min, 350 rpm, 20 °C) for assembly. After centrifuging (10 min, 16,060 × g, 4 °C) stoichiometric complexes were purified by gel filtration in Pol II buffer (2.1.5, Table 21) using a Superose 6 10/300 GL and an ÄKTAexplorer HPLC system (Amersham Biosciences, now GE Healthcare). The solution was concentrated (4,656 × g, 4 °C) using an Ultrafree Centrifugal Filter Unit, 10,000 MWCO (Millipore) to a Pol II concentration of 4 mg/ml. Typically a twofold molar excess of the annealed nucleic acid scaffold (2.2.9.1) was added and the sample was centrifuged (10 min, 16,060 × g, 4 °C) prior to crystallisation.

2.2.9.3   Crystallisation setup, crystal harvesting and freezing

Pol II-nucleic acid complexes were crystallised using the hanging drop method. 500 µl mother solution (2.1.5, Table 21) were added to a reservoir of an EasyXtal Tool (QIAGEN). The drop contained 1.5–2.5 µl Pol II-nucleic acid complex sample and 1 µl of the reservoir solution. Crystallisation plates were incubated at 20 °C. Crystals formed after 5–7 days. Crystals were transferred to 200 µl mother solution at 20 °C. The glycerol concentration was increased to 20 or 22 % (v/v) glycerol in five steps with 4 % or 4.4 % increments per hour by exchanging the solvent to a respective mixture of mother and cryo solution (2.1.5, Table 21). After 20 min the solvent was replaced by a solution of the last condition containing additionally 2–10 µM annealed nucleic acid scaffold. Crystals were transferred to 8 °C in a polystyrene box and then incubated overnight at 8 °C. Crystals were then mounted to cryo loops, plunged into liquid N_2 and kept at liquid N_2 until taking measurements.

2.2.9.4   X-ray diffraction measurement using synchrotron radiation

Crystals were exposed to synchrotron radiation at the Swiss Light Source (SLS) at beamline X06SA. Crystals were cooled by a gaseous N_2 cryo stream and exposed to $6–11 \times 10^{11}$ photons/s with wavelengths of 0.9–1.1 Å. Crystals were oscillated in 0.25° increments and exposed 0.5–1.5 s per frame when recording data sets and X-ray diffraction was detected with a MarMosaic 225 CCD (MarResearch) or a PILATUS 6M pixel detector (DECTRIS).

2.2.9.5   Data processing, refinement and model building

Recorded data sets were visualised, integrated and scaled using the HKL package (Otwinowski & Minor, 1997) or XDS (Kabsch, 1993). Initial phases were obtained by molecular replacement using the program Phaser of the CCP4 software suite (Potterton *et al.*, 2003) using the complete 12-subunit Pol II (Armache *et al.*, 2005) as search model. Rigid body refinement using three rigid groups for Pol II (clamp, core without clamp, Rpb4/7), refined phases and electron density maps were then calculated using CNS version 1.2 (Brünger *et al.*, 1998). Manual model building and superpositioning of structures was performed using O (Jones *et al.*, 1991) or Coot (Emsley & Cowtan, 2004) by fitting the active-site aspartate loops. For initial model building initial F_o-F_c electron density maps were used. Refinement of atom coordinates and B factors was performed with CNS version 1.2 and monitored with the free R factor excluding the same 2 % set of reflections from calculation as in refinement of the complete Pol II EC (Brueckner *et al.*, 2007; Kettenberger *et al.*, 2004). Figures were prepared with PyMOL (DeLano, 2002).

2.2.10 *In vitro*-RNA elongation and cleavage experiments with Pol II

2.2.10.1 Nucleic acid scaffold formation by annealing

Nucleic acid complexes were formed by annealing as described (2.2.9.1).

2.2.10.2 Protein-nucleic acid complex assembly

$(NH_4)_2SO_4$-precipitated Pol II (2.2.4.2, 2.2.4.3) was thawed as described (2.2.9.2). The precipitate was dissolved in TB (2.1.5, Table 22) to a final protein concentration of 0.5–1.4 µg/µl (corresponding to 1–3 µM Pol II). Remaining Pol II not used for assembly was frozen in liquid N_2 and stored at -80 °C until use, then thawed on ice and treated the same as freshly dissolved polymerase. For assembly, typically 2.5 pmol Pol II per reaction were mixed with annealed nucleic acid elongation construct (2.2.9.1, diluted to 5 µM in TB). The mixture was incubated (typically 20 min, 20 °C, shaking at 350 rpm) for assembly.

2.2.10.3 RNA elongation assay

The *in vitro* product RNA elongation reaction was performed in TB in a volume of 7.5–25 µl per reaction. Typically Pol II was assembled (2.2.10.2) with a twofold molar excess of nucleic acids. The reaction was started adding 1 mM of the substrate ribonucleotides (2.1.5, Table 22). If not stated otherwise, the mixture was incubated (20 min, 28 °C) in a thermomixer for elongation. The reaction was stopped by addition of one reaction volume 2 × urea loading buffer (2.1.5, Table 22), incubation for 5 min at 95 °C and immediate cooling on ice.

2.2.10.4 RNA cleavage assays

The *in vitro* RNA cleavage reaction was performed in TB in a volume of 7.5–25 µl per reaction. Typically a twofold molar excess of Pol II was assembled (2.2.10.2) with nucleic acids. The reaction was started adding equimolar amounts of TFIIS with respect to Pol II and incubated (60 min, 28 °C) for cleavage. The reaction was stopped as described (2.2.10.3).

2.2.10.5 Polyacrylamide gel electrophoresis for RNA separation

To visualise RNAs after elongation or cleavage assays typically a fraction of the stopped reaction mixture (2.2.10.3, 2.2.10.4) containing one 1 pmol fluorescently labelled RNA was loaded onto a denaturing polyacrylamide gel (10–20 % acrylamide (nonfluorescent), 7 M urea (nonfluorescent), 1 × TBE (2.1.5, Table 22)). To cast and run gels either 1.0 mm cassettes and an XCell *SureLock* Mini-Cell (Invitrogen) or alternatively a Sequi-Gen GT electrophoresis cell (Bio-Rad) was used. To heat gels, they were prerun using 1 × TBE as running buffer. The Mini-Cell was run 20–60 min at RT at 300–400 V and the Sequi-Gen GT cell at 40–50 W until a temperature of 55–60 °C was reached. Samples were loaded and gels were run at the previous conditions for a time ensuring appropriate resolution depending on acrylamide content of the gel and RNA lengths to be separated. Mini gels were transferred to H_2O, directly placed on the glass platen and immediately scanned using the Typhoon 9400 Imager (Amersham Biosciences, now GE Healthcare). From the Sequi-Gen GT cell the glass plate associated with the buffer chamber was removed and the gel covered with a plastic foil to avoid drying. The glass plate attached to the gel was positioned on the glass platen of the Typhoon Imager. FAM labelled RNAs were visualised by a fluorescence scan using the Typhoon 9400 Imager (excitation laser: blue (488 nm),

PMT voltage: 600–700 V, emission filter: 520 nm band-pass filter (520 BP 40), Pixel size: 50–100 µm, focal plane: platen or 3 mm for Mini-Gels or Sequencing gels, respectively).

3   Results and discussion

3.1 Molecular basis of RNA-dependent RNA polymerase II activity

3.1.1   Pol II and artificial minimal RNA–RNA elongation scaffolds

3.1.1.1   Core Pol II can bind and elongate RNA according to template RNA *in vitro*

Structural studies of the transcription EC revealed a B-form DNA duplex entering the downstream polymerase cleft, and a hybrid duplex of DNA template with RNA product above the active site (Gnatt *et al.*, 2001; Kettenberger *et al.*, 2004; Westover *et al.*, 2004) (Figure 3a). During RdRP activity, the hybrid site and the downstream cleft are expected to accommodate A-form RNA duplexes. The downstream cleft can accommodate A-RNA, as observed for the 3' stem of the RNA inhibitor FC∗ (Kettenberger *et al.*, 2006) (Figure 3a). The FC∗ 3' stem overlaps with two DNA template positions downstream of the NTP-binding site (position +2, +3; Figure 3a), suggesting that an RNA template could enter the active site in a similar manner to DNA.
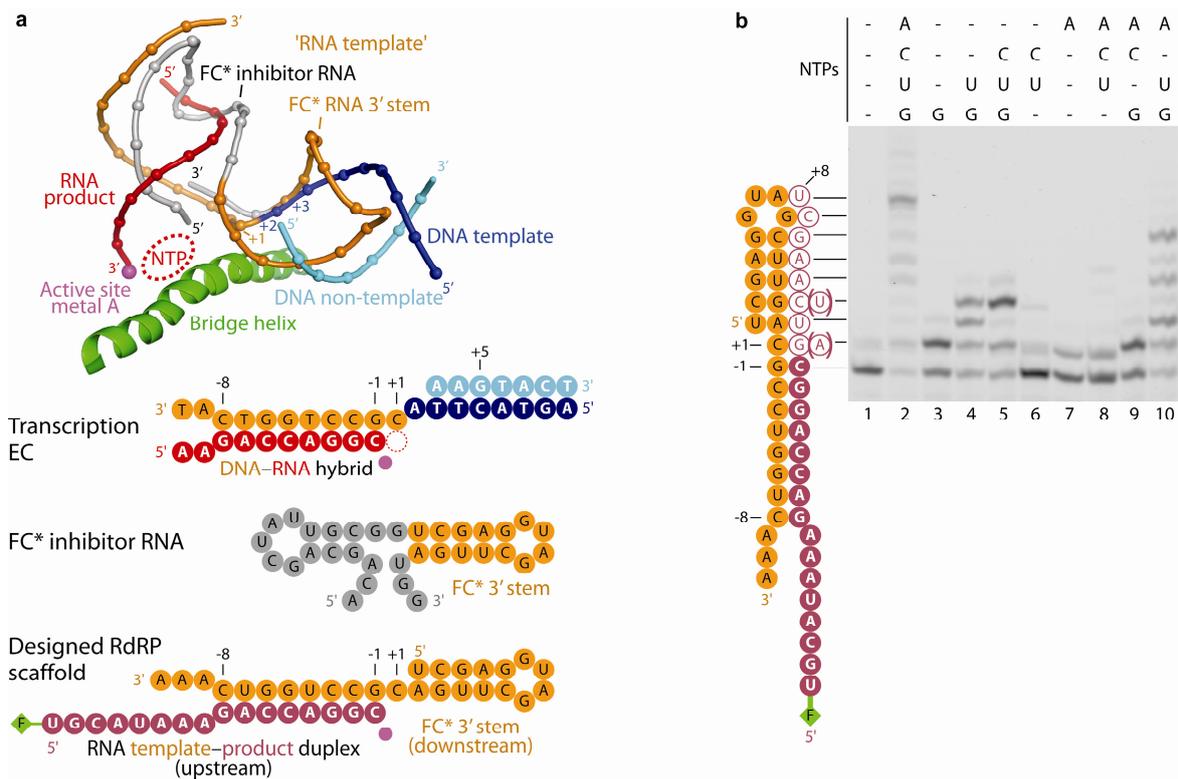
Figure 3: RNA-dependent RNA polymerase II activity.

a, Structure-based design of the RdRP scaffold. Structures of the complete Pol II EC (Kettenberger *et al.*, 2004) and the Pol II–FC* RNA inhibitor complex (Kettenberger *et al.*, 2006; Westover *et al.*, 2004) were superimposed (2.2.9.5). The nucleic acids in the active centre of the two complex structures (EC (Kettenberger *et al.*, 2004) and FC* RNA (Kettenberger *et al.*, 2006)) are shown. The RdRP scaffold derived by combination of a forked RNA template–product duplex with the 3' stem of FC* RNA is shown at the bottom. The RNA product strands are in red (transcription EC) or raspberry (RdRP EC), and the RNA template strand is in orange. The FAM fluorescent label is shown as a green diamond. The same colour code is used throughout. The 5' stem of FC* RNA, which is not used here, is in grey. The nucleotide addition site is denoted +1, and upstream and downstream positions are depicted with negative and positive numbers, respectively. **b**, RNA synthesis by core Pol II with the RdRP scaffold from **a**. Lane 1 shows the fluorescently labelled reactant RNA. In lanes 2–10 the RNA scaffold (2.1.3, Table 9) was incubated with pure Pol II and different types of NTP (2.2.10). Nucleotides incorporated by Pol II RdRP activity are shown as raspberry open circles. UMP misincorporation at position +3 (lane 4) was confirmed by mass spectrometry (Lehmann, 2006).

To test whether Pol II can indeed use an RNA template, we prepared an RNA scaffold that combined the FC∗ 3' stem with a putative RNA template–product duplex (RdRP scaffold; Figure 3a). To monitor potential RNA elongation, the product strand was labelled at the 5' end with FAM. Incubation of this scaffold with core Pol II and NTPs led to RNA elongation (Figure 3b, lanes 1 and 2), indicating the formation of an active RdRP EC. Most RNA was elongated by eight nucleotides, but shorter and longer products were also observed. Mass spectroscopy of the products (Lehmann, 2006) was consistent with RNA-templated synthesis (Table 25). Incubation of the RdRP EC with subsets of NTPs led to products that generally arose from templated nucleotide addition (Figure 3b, lanes 3–10), but the absence of the cognate NTP also permitted misincorporation. At position +1, AMP could be incorporated instead of GMP; at position +3, UMP could replace CMP. Misincorporation did not result from the use of RNA as a template, because a corresponding DNA template (scaffold DdRP; Figure 4a) produced the same product pattern (Figure 4c). These results show the intrinsic RdRP activity of Pol II.
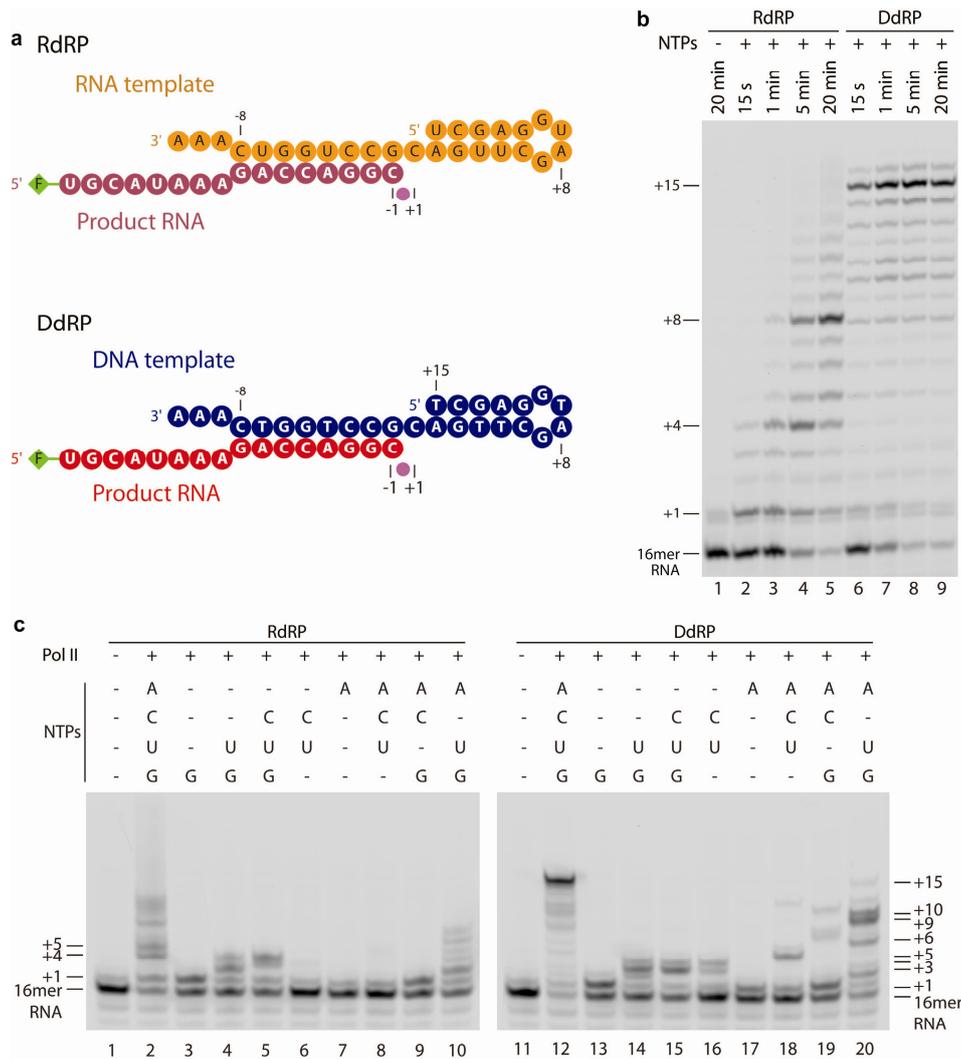
Figure 4: Comparison of incorporation rate and misincorporation events during RNA elongation with scaffolds RdRP and the corresponding scaffold DdRP that comprises a DNA template strand.

a, Scaffolds RdRP and DdRP (2.1.3, Table 8, Table 9) are depicted. The DNA template strand is in blue. **b**, Time courses of RNA synthesis with the RdRP scaffold (lanes 2–5) and the corresponding DNA template-containing scaffold DdRP (lanes 6–9). Lane 1 shows the fluorescently labelled reactant RNA. **c**, RNA synthesis with scaffold RdRP (lane 1–10) and DdRP (lane 11–20). Lane 1 and 11 show the fluorescently labelled reactant RNA. In lanes 2–10 and 11–20, scaffolds were incubated with pure Pol II (2.2.10) and then incubated for 5 min with different types and subsets of NTPs as indicated. Despite the faster rate of synthesis with scaffold DdRP, the pattern of misincorporations is highly similar.

Table 25: Mass spectrometric analysis of RNA species observed after incubation of scaffold RdRP with Pol II and NTPs (compare Figure 3b).

RNA product	Incorporated nucleotides	Theoretical mass[12]	Observed mass
Reactant RNA	-	5664	5663, 5665
+1	G	6009	6009, 6010
+2	GU	6315	6317[13]
+3	GUC	6620	6619[13], 6621[13]
+4	GUCA	6949	6949, 6951
+5	GUCAA	7279	7279
+6	GUCAAG	7624	7624
+7	GUCAAGC	7929	7929
+8	GUCAAGCU	8235	8235, 8236
Template strand	-	8342	8342

---

[12] Calculated with Mongo Oligo Mass Calculator (Rozenski, 1999) and using a molecular weight for 6-FAM of 537.5 Dalton.
[13] Observed after incubations with NTP subsets.

3.1.1.2   Position of RNA duplex bound to complete Pol II revealed in a crystal structure

To unravel the structural basis of the RdRP activity, we determined the crystal structure of the complete Pol II bound to an RdRP scaffold. A scaffold with a 5' extension of six nucleotides sufficed to form an active RdRP EC (Figure 5a, b), and enabled crystallographic analysis at 3.8 Å resolution to be made (Figure 6, Figure 7, Table 26 and 2.2.9). The structure revealed the RNA template–product duplex in the site occupied by the DNA–RNA hybrid during transcription. The RNA product 3' end was bound to the catalytic metal ion A (Figure 6). RNA synthesis occurred at the active site used during transcription, because product RNA was cleaved from the 3' end by TFIIS (Figure 8), which stimulates RNA cleavage at the active site in the EC (Kettenberger *et al.*, 2003), and in a Pol II–RNA complex (Johnson & Chamberlin, 1994). For positions -1 to -5, the structure of the RNA duplex was essentially identical to that of the DNA–RNA hybrid (Kettenberger *et al.*, 2004); however, at the upstream positions -6 to -9, changes in phosphate positions of up to 3 Å resulted in a decreased helical rise (Figure 6b).
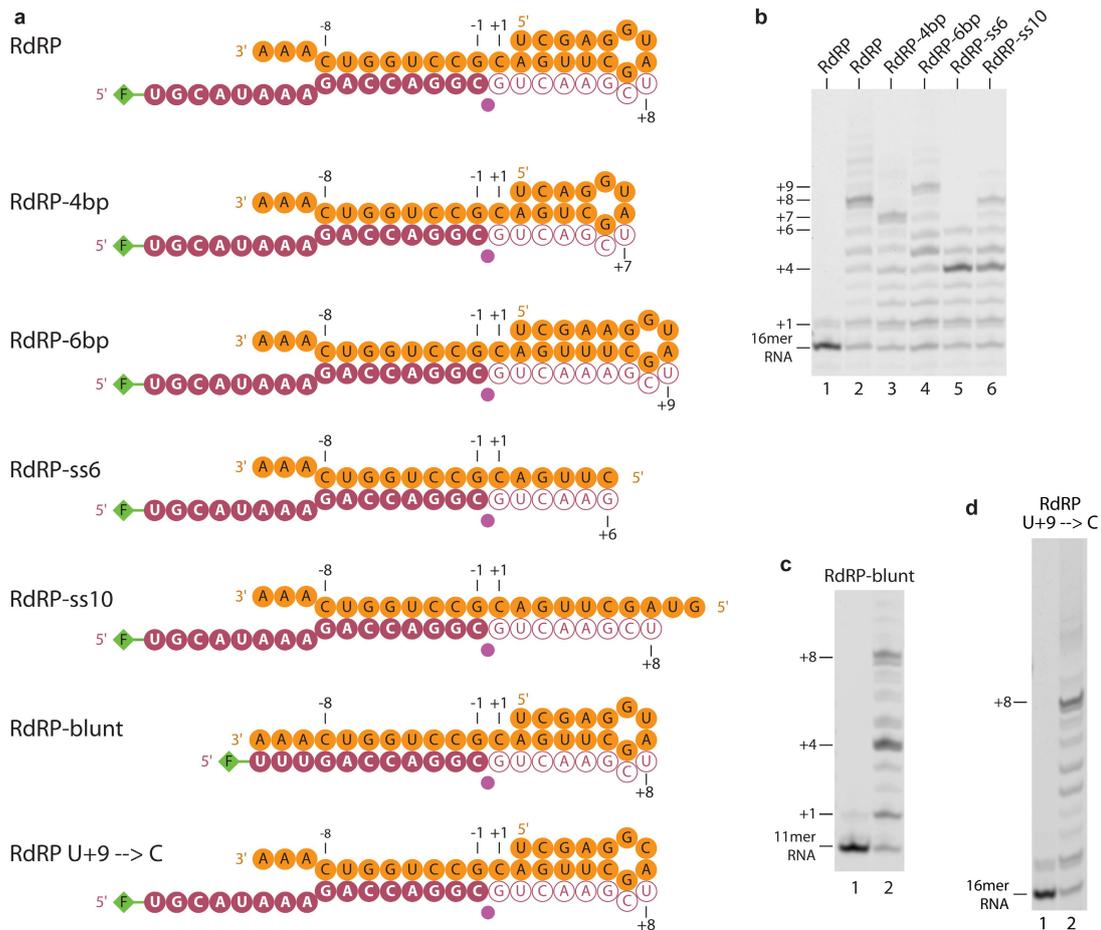
Figure 5: Pol II RdRP activity on alternative artificial scaffolds.

a, Alternative RdRP scaffolds. Nucleotides that are incorporated by Pol II RdRP activity are shown as raspberry open circles. The stalling position is indicated. **b-d**, RNA synthesis with alternative RdRP scaffolds shown in **a**. In lanes 2–6, alternative RNA scaffolds were incubated with pure Pol II and NTPs (2.2.10).
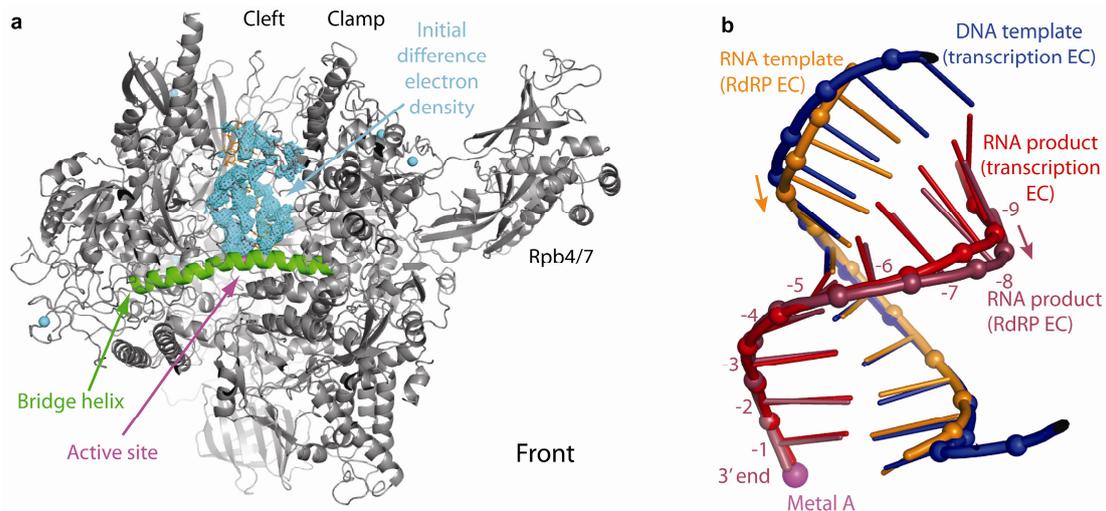
Figure 6: Crystal structure of a Pol II–RdRP complex.

a, Ribbon model of Pol II (grey) with an initial, unbiased difference Fourier electron-density map (cyan, contoured at 2.2 σ).The map was calculated from protein model phases. It reveals the RNA template–product duplex of scaffold RdRP-ss6 (Figure 5a) in the active-centre cleft of Pol II. The bridge helix is in green. The catalytic metal ion A is depicted as a magenta sphere, and Zn^{2+} ions as cyan spheres. The view is related to that in Figure 3a by a 90° rotation around a vertical axis. **b**, Comparison of the RNA template–product duplex in the RdRP EC with the DNA–RNA hybrid duplex in the transcription EC (Kettenberger *et al.*, 2004). Protein structures were superimposed as described (2.2.9.5).
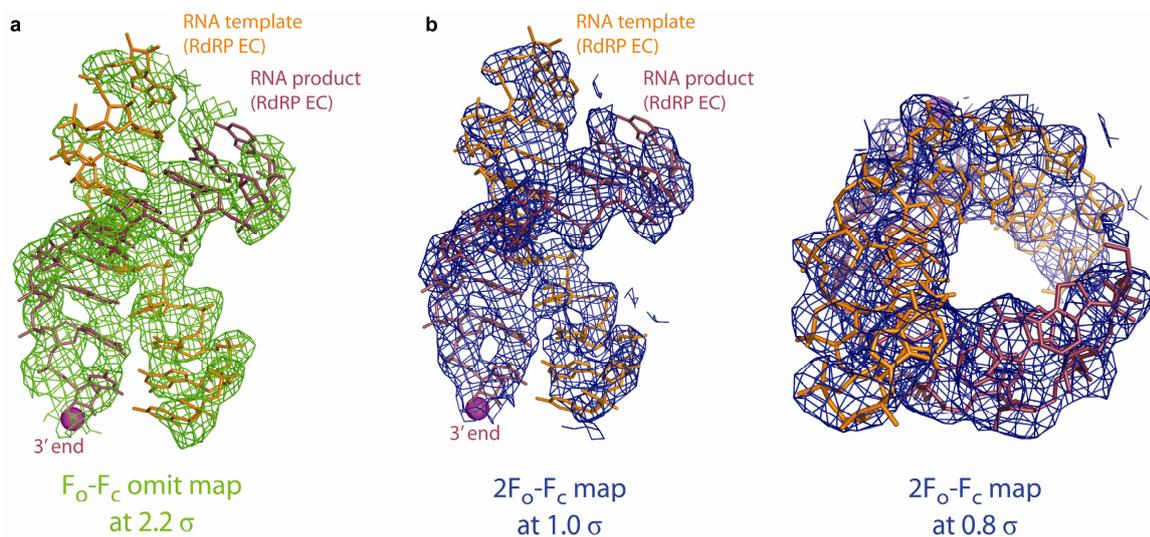
Figure 7: Electron density maps for the RNA template-product duplex in the Pol II RdRP EC.

a, Difference Fourier omit map obtained using phases from the final model with nucleic acids removed. The view is as in Figure 6. The RNAs are shown as stick model. The F_o-F_c map at 2.2 σ is shown as green mesh. **b**, The final observed $2F_o$-F_c electron density map calculated with model phases is shown in blue with the contour level as indicated. Views are related by a 90° rotation around a horizontal axis.

Table 26: Crystallographic data and refinement statistics for the Pol II complexes with the artificial scaffold RdRP-ss6 (Figure 5a and Figure 6) and the HDV-derived 6 bp stem-loop (Figure 12a). Data were collected, processed with program XDS (RdRP-ss6) or DENZO (HDV stem-loop) and refined as described (2.2.9).

Pol II complex	RdRP	HDV
Protein Data Bank accession code	2R92	2R93
Data collection		
Space group	$C222_1$	$C222_1$
Cell dimensions		
a, b, c (Å)	222.7, 393.8, 283.5	223.3, 394.9, 284.1
Wavelength (Å)	1.0716	0.9999
Resolution (Å)	50.0-3.8 (3.94-3.8)[14]	50.0-4.0 (4.14-4.0)[14]
R_{sym}	0.077 (0.335)	0.149 (0.479)
$I/\sigma I$	21.4 (6.8)	12.4 (4.2)
Completeness (%)	99.9 (100.0)	100.0 (99.9)
Redundancy	8.5 (8.5)	8.5 (7.7)
Refinement		
Resolution (Å)	50.0-3.8	50.0-4.0
No. reflections	121,604	104,655
R_{work}/R_{free}	0.212/0.246	0.216/0.241
No. atoms		
Protein	31,207	31,207
Nucleic acid	400	292
Ligand/ion	9	9
B-factors		
Protein	127.4	126.1
Nucleic acid	195.3	166.4
Ligand/ion	111.9	106.7
R.m.s deviations		
Bond lengths (Å)	0.008	0.008
Bond angles (°)	1.47	1.49

---

[14] Highest resolution shell is shown in parenthesis.
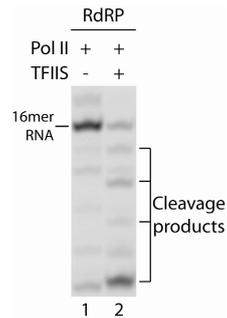
Figure 8: TFIIS-induced 3' RNA cleavage in the RdRP EC (2.2.10.4).
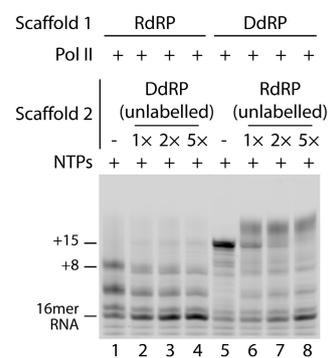
Figure 9: Scaffolds RdRP and DdRP (Figure 5a) compete for Pol II in RNA elongation assays.

Competition assays. Pol II and scaffold 1 were assembled as described (2.2.10.2). Scaffold 2 was added in relative amounts (1, 2, or 5-fold molar excess) with respect to scaffold 1 as indicated, and incubated for 10 min at 20 °C. DdRP and RdRP scaffolds used as scaffolds 2 were identical to scaffolds 1 except that an 11mer product RNA was used, which lacked the five 5' residues and the fluorescent label ("cold" competitors). In control experiments (lanes 1 and 5) transcription buffer was added instead. The mixture was incubated with 1 mM NTPs for 5 min at 28 °C. Without competing scaffold 2 the final product of each reaction is observed (+8 in lane 1, +15 in lane 5), respectively. With increasing amounts of scaffold 2 (lanes 2-4 and 5-8), the final product of the reaction disappears and the reactant RNA remains, indicating competition for Pol II. Competition is observed independent of the order of scaffold addition.

3.1.2 Implications for HDV genome synthesis by Pol II

3.1.2.1 Core Pol II can elongate HDV-derived scaffolds

To investigate the physiological significance of the RdRP activity, we studied a terminal segment of the HDV antigenome (Figure 10a). In cell extracts, this segment directs RNA synthesis that is sensitive to the Pol II inhibitor α-amanitin (Filipovska & Konarska, 2000; Yamaguchi *et al.*, 2001). The reaction involved RNA strand cleavage followed by elongation of the new 3' end (Filipovska & Konarska, 2000;
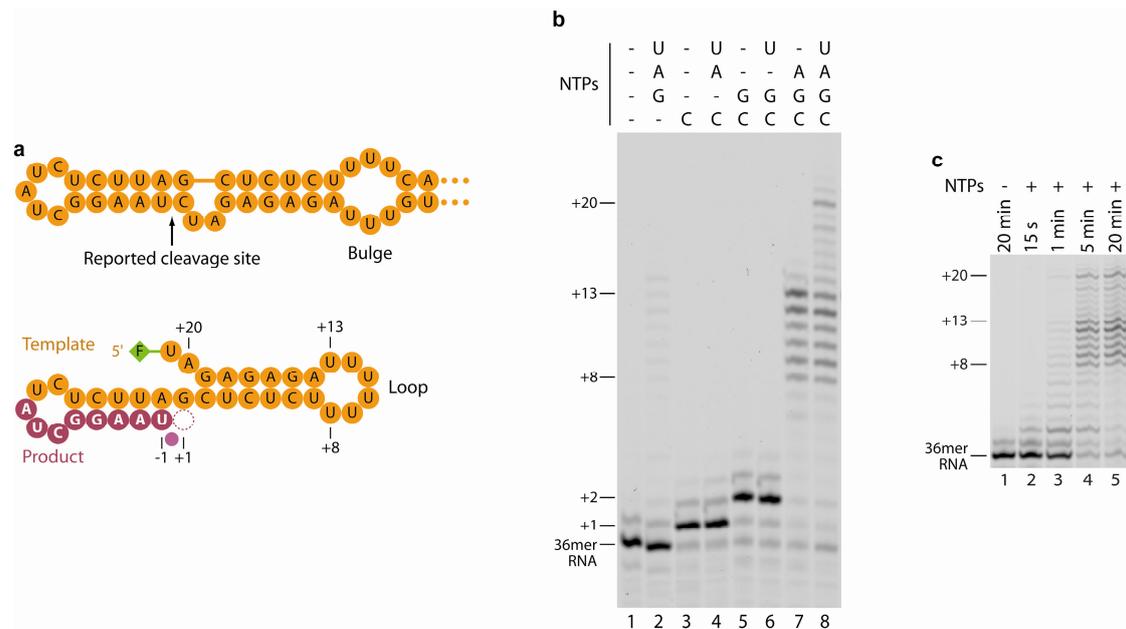
Figure 10: RNA synthesis with HDV RNA-derived scaffolds.

a, Schematic representation of the terminal segment of the HDV antigenome (top) and the HDV-derived scaffold (bottom). **b**, Pol II-dependent RNA synthesis with HDV scaffold. Lanes 2–8 show the elongation products after incubation with various subsets of NTPs as indicated. **c**, Time courses of RNA synthesis with HDV scaffold.

Yamaguchi *et al.*, 2001). The cleaved HDV segment apparently forms an RNA template–product stem-loop and a downstream RNA duplex, which we shortened by replacing a natural bulge with a loop (HDV scaffold; Figure 10a). Incubation of this scaffold with Pol II and NTPs resulted in RNA synthesis up to the end of the template, although synthesis also stopped prematurely (Figure 10b, lane 8). RNA synthesis was strictly dependent on the template. Only cognate NMPs were incorporated at positions +1 and +2 (Figure 10b, lanes 2–6). When UTP was omitted from the reaction, RNA synthesis stopped at position +13 as expected (Figure 10b, lane 7). RNA synthesis was slow, but some final product appeared within 1 min (Figure 10c). These *in vitro* data match the evidence for Pol II-dependent HDV replication *in vivo* (Lai, 2005; Taylor, 2003), and argue for the physiological significance of the RdRP activity of Pol II.

The higher processivity of Pol II on the HDV scaffold than on the RdRP scaffold may originate from the different upstream template–product duplex, which forms a stem-loop instead of a forked end (Figure 11a). We therefore analysed two chimaeric scaffolds that recombine the upstream and downstream regions of the two scaffolds (Figure 11a). Combination of the RdRP upstream region with the HDV downstream region strongly decreased processivity compared with the HDV scaffold (Figure 11b).
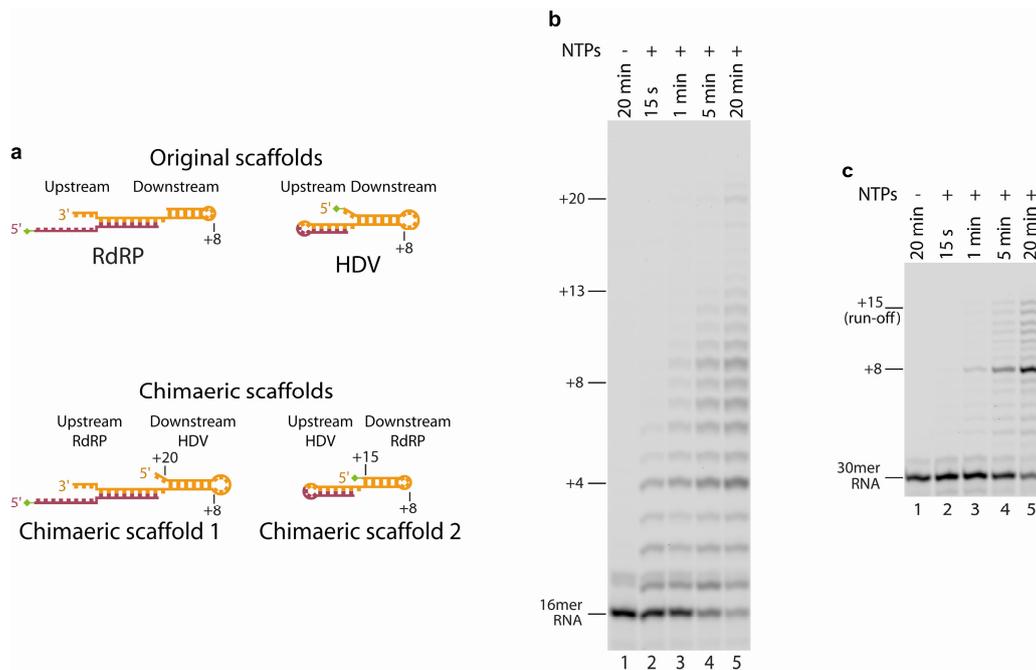
Figure 11: RNA synthesis with chimaeric RdRP–HDV RNA-derived scaffolds.

a, Design of two chimaeric scaffolds that recombine the upstream and downstream regions of the artificial RdRP scaffold (Figure 4a) and the HDV-derived scaffold (Figure 10a). **b-c**, Time courses of RNA synthesis with HDV and with the chimaeric scaffolds 1 (**b**) and 2 (**c**).

In contrast, combination of the HDV upstream stem-loop with the RdRP downstream region enabled run-off synthesis that was not possible with scaffold RdRP (Figure 4a and Figure 11c). Thus, the HDV stem-loop promoted RdRP processivity. Consistently, the stem-loop alone, containing only a two-nucleotide 5' extension, formed a functional RdRP EC (Figure 12a).

3.1.2.2   Pol II can cleave and elongate the HDV-terminal segment

To test whether the RdRP-promoting stem-loop can be formed from the HDV terminal segment *in vitro*, we incubated the segment with pure Pol II–TFIIS complex. This resulted in RNA cleavage at the internal bulge (Figure 13a, b). The bulge apparently connected the two RNA duplexes in a flexible way, to enable positioning of the scissile RNA strand at the active site (Figure 13c). Cleavage produced a 6-bp stem-loop, comparing favourably with the 5-bp stem-loop that forms in extracts (Filipovska & Konarska, 2000). On the addition of NTP, the new 3' end was elongated up to the end of the template (Figure 13a, b, lane 7). Consistently, a corresponding 6-bp stem-loop with a 5' extension supported RdRP activity (Figure 12a). Thus, the Pol II–TFIIS complex can cleave the HDV terminal segment and elongate the new 3' end *in vitro*, which is consistent with models for HDV replication *in vivo*.

3.1.2.3 Crystal structure of Pol II with an HDV-derived RNA stem-loop
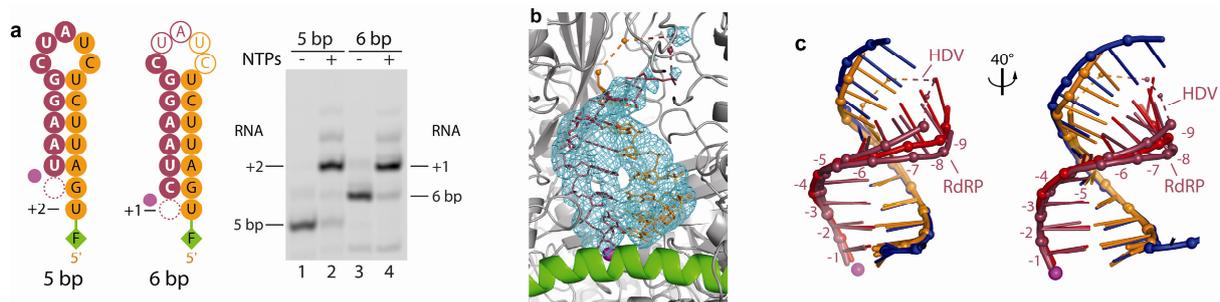
Figure 12: RNA synthesis and crystal structure of Pol II with an HDV-derived stem-loop.

a, HDV-derived terminal stem-loops consisting of 5 or 6 bp enable templated incorporation of the next nucleotide(s). **b**, Difference electron density omit map for the 6-bp HDV stem-loop bound to the hybrid site of complete Pol II (calculated with protein phases only, contoured at 3.0 σ). The disordered loop is indicated with a dashed line. The view is as in Figure 6a. **c**, Superposition of the RNA template–product duplex in the HDV EC and the RdRP EC (Figure 6) on the DNA–RNA hybrid duplex in the transcription EC (Kettenberger *et al.*, 2004).

The 6-bp stem-loop that forms by HDV RNA cleavage *in vitro* (Figure 12a) could be structurally revealed in a complex with Pol II (Figure 12b, c, Table 26 and 2.2.9). The stem-loop bound the hybrid site, and phosphates at positions -1 to -5 occupied the same locations as in the artificial RdRP EC. However, RNA positions -6 and -7 had an increased helical rise (Figure 12c), showing that the hybrid site accommodates
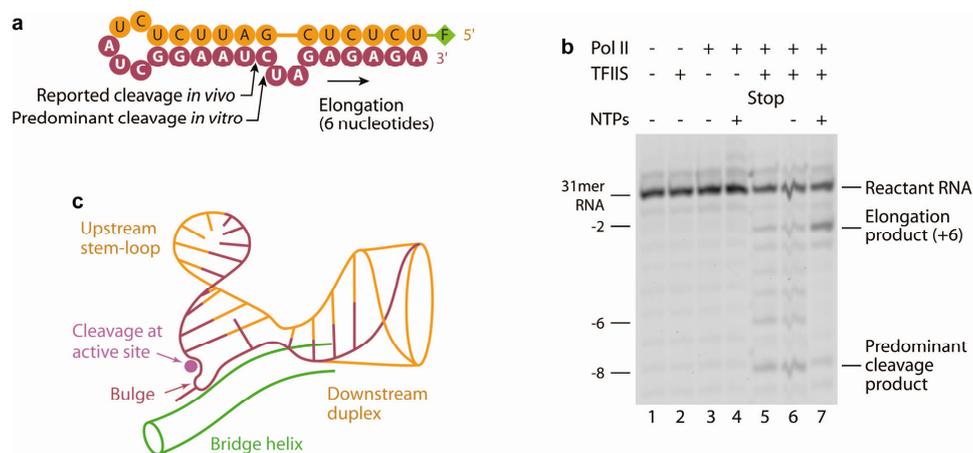
Figure 13: Mechanism of HDV replication initiation.

a, Scaffold based on HDV antigenome before cleavage. **b**, Pure Pol II–TFIIS complex cleaves the HDV antigenome terminal segment (**a**) and elongates the newly formed 3' end on the addition of NTP. For cleavage, Pol II–scaffold complex (625 nM) was incubated with TFIIS (1.25 µM) in transcription buffer for 60 min at 28 °C. For elongation of the cleavage product, the reaction mixture was incubated with 1 mM NTPs at 28 °C for 20 min. For lane 5, the cleavage reaction was stopped after 60 min ('Stop'). **c**, Model of initial interaction of the HDV antigenome terminal segment with the Pol II–TFIIS complex. The stem-loop is placed in accordance with the crystal structure (Figure 12b, c) and the downstream duplex in accordance with the location of the FC* RNA 3' stem. We predict that the HDV bulge passes the bridge helix and active site, where cleavage occurs.
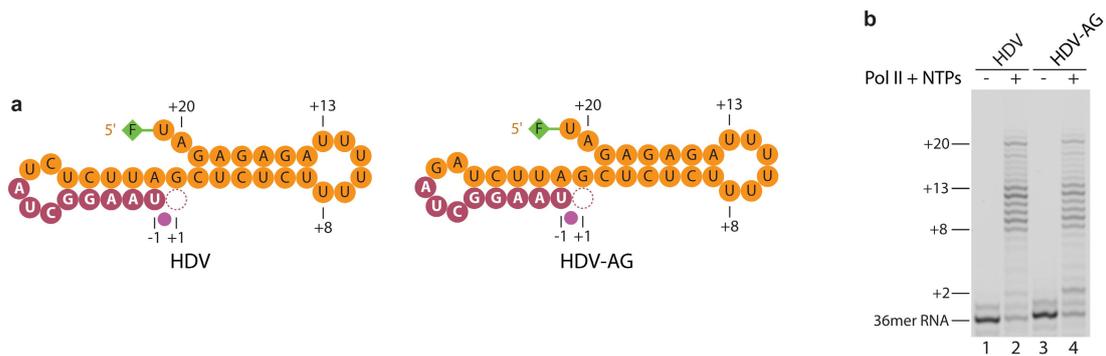
Figure 14: Mutational analysis of the loop in the HDV-derived scaffold.

a, RNA scaffolds HDV and HDV-AG, which contains a CU to AG sequence alteration in the terminal loop. **b**, Comparison of RNA elongation products obtained with RNA scaffolds shown in **a.** Lanes 2 and 4 show elongation products. There are no significant differences in the pattern of elongation products.

various RNA duplexes with upstream ends of different structure. The RNA loop was mobile except for one cytidine residue (Figure 12a, b). Consistently, a double mutation in the loop did not impair activity (Figure 14). Because base-specific Pol II–RNA contacts are absent in both RdRP EC structures, Pol II recognizes the A-RNA stem rather than a particular RNA sequence.

3.1.2.4   Length of elongatable upstream stem-loop is limited

During transcription, upstream template and product strands are separated, whereas the HDV stem-loop probably persists during elongation. Consistently, Pol II readily used stem-loops with 5, 6, 7 or 10 bp as substrates, but not stem-loops with 13, 15 or 18 bp (Figure 12a and Figure 15). Modelling revealed a clash of the polymerase lid with the RNA stem-loop when it reached a length of 10 or 11 bp (Figure 24). The
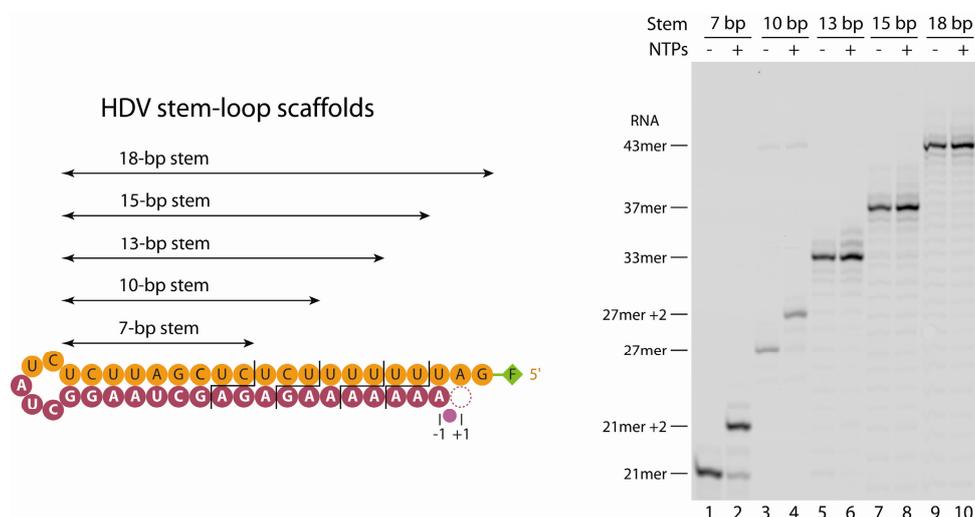
Figure 15: HDV-derived stem-loops of different lengths serve as RdRP scaffolds.
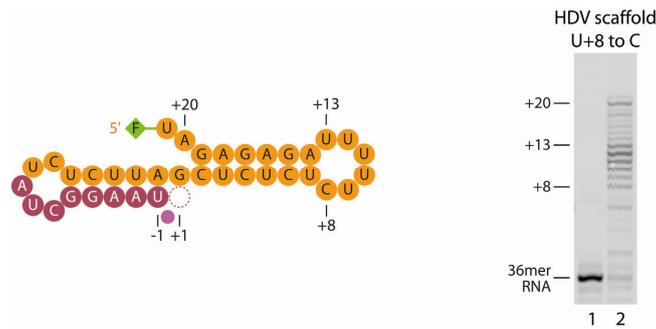
Figure 16: RNA synthesis with an HDV scaffold with U in position 18 mutated to C.

clash may destabilize the RdRP EC and facilitate stalling. This model explains why elongation with the HDV scaffold partly stalled when the stem-loop reached 13–18 bp (Figure 10a, b), and why replacement of the uracil at the downstream position +8 did not influence stalling (Figure 16). The model also explains stalling of the artificial RdRP ECs when a persistent template–product duplex would reach a length of 16 bp (Figure 3b and Figure 5). Similarly, a persistent DNA–RNA hybrid stalls the transcription EC (Kireeva *et al.*, 2000a; Naryshkina *et al.*, 2006; Toulokhonov & Landick, 2006). However, 12-subunit Pol II elongates an RNA scaffold containing a bulge in the stem (Figure 17a) until run-off (+10, Figure 17b). The bulge at positions -10 to -13 was designed at the position probably clashing with the lid loop (Figure 24). Upon addition of nucleotide subsets misincorporation products were weakly observed when the cognate NTP was missing (Figure 17c, lanes 2, 4 and 6). Incorporation of cognate NPTs was highly efficient (Figure 17c, lanes 3, 5 and 7), confirming the secondary structure formation of the RNA as designed (Figure 17a). The limited RdRP processivity *in vitro* is apparently overcome during HDV replication *in vivo* by binding of the HDV-encoded elongation-stimulatory delta antigen to the polymerase clamp (Filipovska & Konarska, 2000; Yamaguchi *et al.*, 2001; Yamaguchi *et al.*, 2007). Clamp movements and/or RNA repositioning would enable the exit of a persistent stem-loop from the cleft.
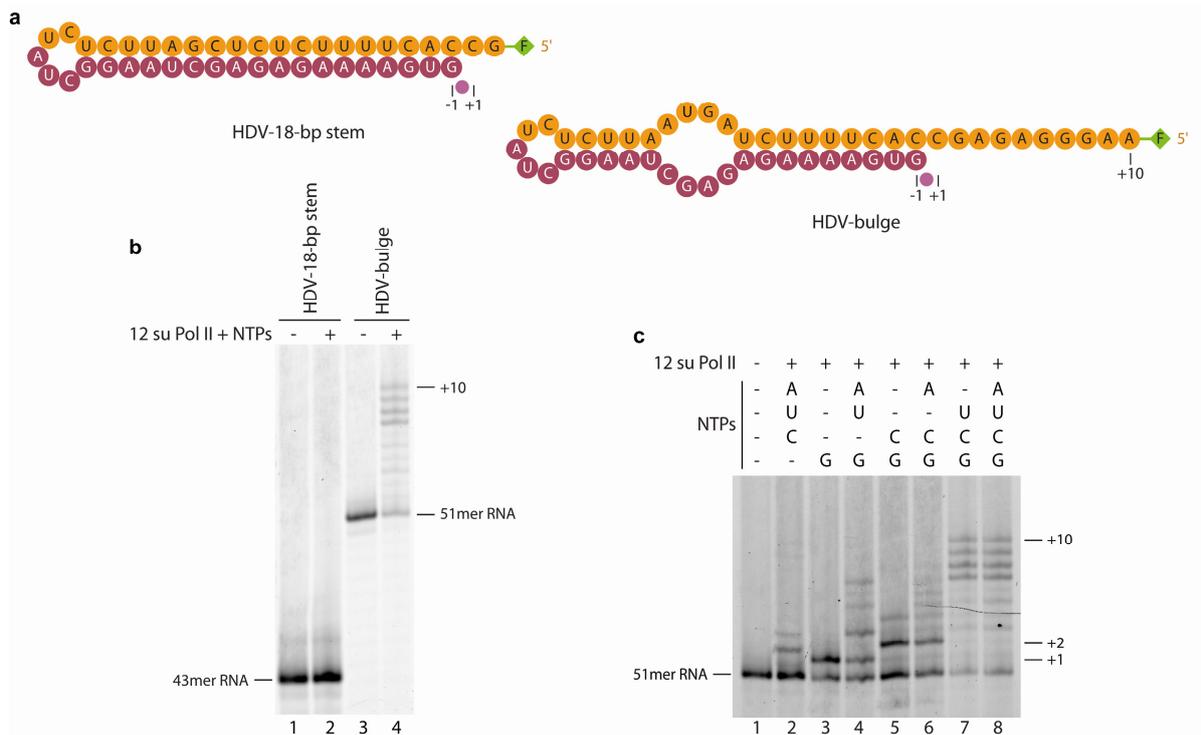
Figure 17: RNA synthesis with an HDV RNA-derived bulge-containing stem-loop.

a, Schematic representation of the HDV-derived 18 bp stem-loop and corresponding scaffold containing a bulge and more templating bases. **b**, Pol II-dependent RNA elongation assay with HDV-18-bp stem and HDV-bulge depicted in (**a**). Lanes 1 and 3 show the fluorescently labelled reactant RNAs. Lanes 2 and 4 show the reaction products after incubation with NTPs. Only the bulged scaffold can be elongated by Pol II. **c**, Pol II-dependent RNA synthesis with HDV-bulge. Lanes 2–8 show the elongation products after incubation with various subsets of NTPs as indicated.

3.1.3 RdRP activity of Pol II remained unrecognised upon previous observations

Our results also explain the previously observed apparently non-templated RNA elongation in a Pol II–RNA complex (Johnson & Chamberlin, 1994). The RNA used for these studies bound Pol II and was cleaved on the addition of TFIIS; cleavage products were elongated by a few nucleotides (Johnson & Chamberlin, 1994). We predict that this RNA formed an 11-bp stem-loop in the hybrid site, and a bulge or a 3' tail at the active site (Figure 18). TFIIS-stimulated cleavage then created a new 3' end at the active site, which was elongated in a templated manner, until a critical template-product length was reached. Consistently, an 11-bp stem-loop resembling a cleaved species (Johnson & Chamberlin, 1994) supported templated nucleotide incorporation (Figure 18). Our results also explain previously observed cleavage and limited re-extension of a short RNA stem-loop by bacterial RNA polymerase (Kashlev
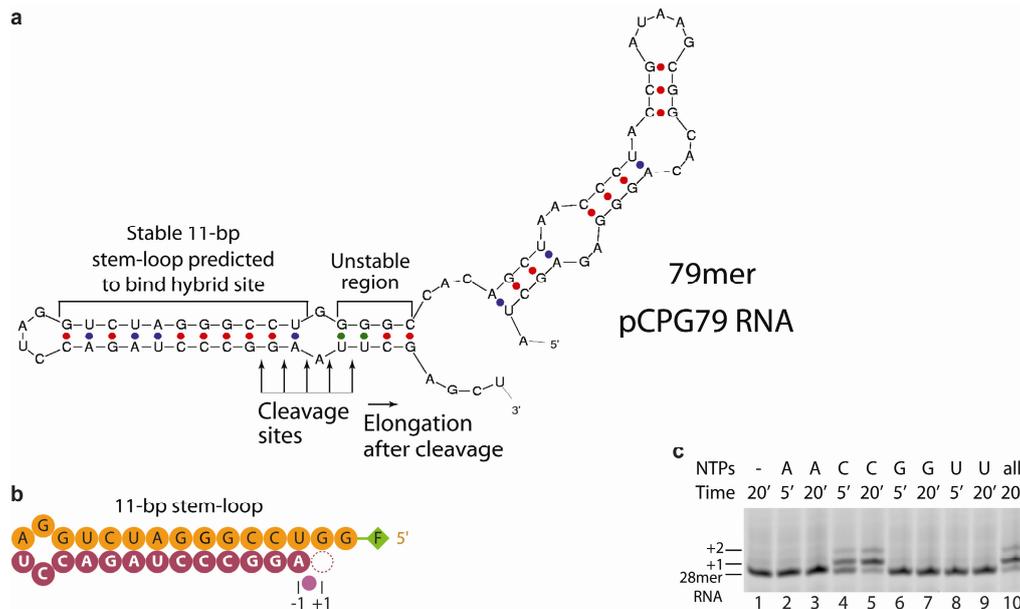
Figure 18: Templated RNA elongation of an 11 bp stem-loop derived from pCPG79 RNA used in previous studies (Armache *et al.*, 2005; Johnson & Chamberlin, 1994).
a, Mfold (Zuker, 2003) secondary structure prediction of pCPG79 RNA. Cleavage sites observed previously by TFIIS-induced cleavage (Johnson & Chamberlin, 1994) are indicated. **b**, RNA scaffold derived from the predicted pCPG79 RNA structure in **a**. The scaffold corresponds to the product obtained after the previously observed RNA cleavage at the central cleavage site (Johnson & Chamberlin, 1994). The scaffold consists of the 3' stem-loop of pCPG79 RNA with an 11 bp stem and a two-nucleotide 5'-overhang. **c**, RNA elongation assay with the scaffold shown in **b**. Reactions were incubated with different NTPs or subsets of NTPs for the time indicated (lanes 2–10). Only CTP leads to addition, indicating GMP-templated RdRP activity.

& Komissarova, 2002). Thus, earlier observations (Johnson & Chamberlin, 1994; Kashlev & Komissarova, 2002) are apparently examples of the RdRP mechanism described here.

3.1.4 Evolutionary progress of RNA polymerase activity from RNA to DNA templates

The RdRP activity of Pol II provides a missing link in molecular evolution, because it supports the prediction that an ancestor of Pol II was the enzyme that replicated early RNA genomes (Poole & Logan, 2005). This is supported by the recent findings that the related bacterial RNA polymerase supports not only RNA synthesis with the non-coding 6S RNA as template (Gildehaus *et al.*, 2007; Wassarman & Saecker, 2006) but also RNA-facilitated RNA cleavage (Zenkin *et al.*, 2006). The early RNA replicase apparently evolved to accept DNA as a template during the transition from RNA to DNA genomes. The early replicase was apparently a common ancestor also of dis-

tinct single-subunit RdRP enzymes, because these show a Pol II-like core protein fold and active site (Salgado *et al.*, 2006). It is possible that the ancient RdRP activity of Pol II, which still replicates HDV, is still used in certain cellular processes, because many organisms lack dedicated single-subunit RdRPs. Given the slow nature and the impaired processivity of the RdRP activity *in vitro*, such processes would require stimulating factors or would be restricted to the generation of smaller RNAs.

3.2 Plasmid-based mutagenesis of Rpb1 in *S. cerevisiae*

3.2.1 Strategy to create yeast strains for Rpb1 mutagenesis

To study mutants of Rpb1, which is an essential protein, we chose to establish a plasmid-based mutagenesis system in *S. cerevisiae* (Figure 19). The advantage of such a system is that the target gene to be mutated is located on a plasmid and mutations are not introduced in the genome. This enables easy identification of mutations that render the protein non-functional und thus yeast cells non-viable. Therefore a strain is needed that carries a genomic knock-out of RPB1 but instead contains the gene on a rescue plasmid, which allows for plasmid shuffling: after transformation of a second plasmid containing the *RPB1* mutant gene of interest, the rescue plasmid can be counter selected via its URA3 marker gene. Cells that do not contain URA3 are positively selected on 5-FOA containing medium. The enzyme encoded by URA3 enables cells to convert 5-FOA to 5-fluorouracil, which inhibits cell growth (Boeke *et al.*, 1984). Only if the Rpb1 mutant is not lethal to the cells, then growth on 5-FOA containing medium occurs (Figure 23). The haploid Δ*rpb1* knock out strain with rescue plasmid can be obtained by sporulation of a rescue-plasmid containing diploid strain with one RPB1 allele knocked-out.
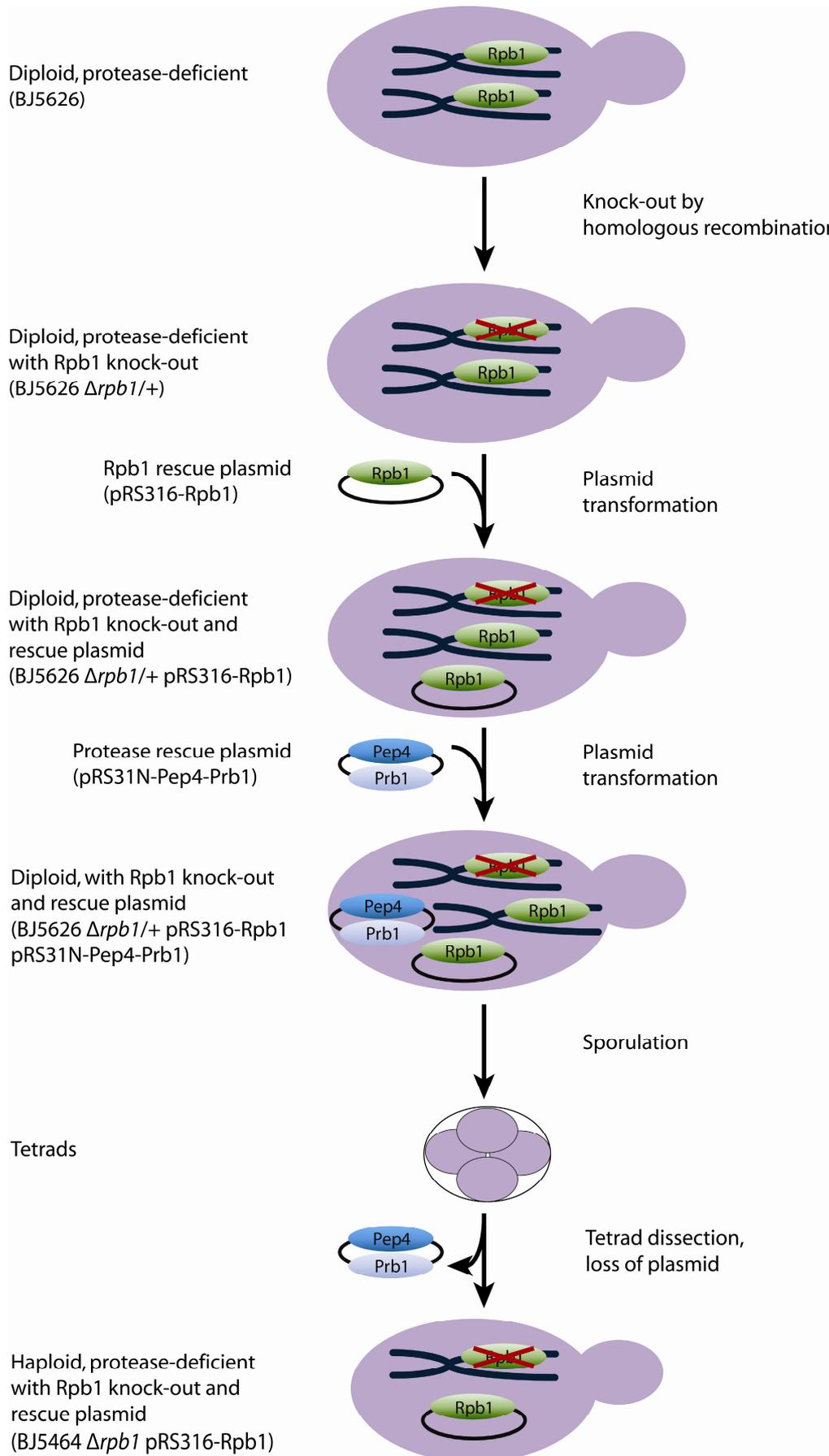
Figure 19: Creation of an Rpb1 mutagenesis strain.

Creation of BJ5464 Δ*rpb1* pRS316-Rpb1 is shown schematically.

3.2.2 Setup of plasmid shuffle strains

The system of Rpb1 mutagenesis was designed such that it would be possible to perform both *in vitro* and *in vivo* studies. For *in vitro* studies with purified Pol II a plasmid shuffling strain was created based on the established Pol II purification strain BJ5464 Rpb3 His-Bio (2.1.1, Table 4 and Figure 19). For *in vivo* analyses like chromatin immunoprecipitation studies a strain was created with a background corresponding to BY4741 or BY4742 (2.1.1, Table 4).

3.2.2.1 Rpb1 knock-out in diploid strains

The kanMX6 cassette was amplified (2.2.1.1) from pFA6a-kanMX6 (2.1.2, Table 6) using the oligonucleotides 3_Sc_Rpb1_20bp_up_KanMX6_5'_f and 4_Sc_KanMX6_3'_Rpb1_20bp_down_r (2.1.3, Table 10) as PCR primers. Flanking regions 310 bp upstream and 232 bp downstream of the RPB1 ORF were amplified using 1_Sc_Rpb1_310bp_up_f with 2_Sc_Rpb1_20bp_up_KanMX6_5'_r and 5_Sc_KanMX6_3'_Rpb1_20bp_down_f with 6_Sc_Rpb1_232bp_down_r (2.1.3, Table 10), respectively using genomic DNA of each BJ5626 and BY4743 as template. Genomic DNA was kindly provided by Heidi Feldmann. A knock-out fragment containing upstream and downstream flanking regions of RPB1 upstream and downstream of the kanMX6-cassette, respectively, was generated in a hybridisation PCR (2.2.1.1) using the three previously amplified fragments as templates with primers 1_Sc_Rpb1_310bp_up_f and 6_Sc_Rpb1_232bp_down_r. The flanking regions direct the locus of insertion of the cassette by homologous recombination into the yeast genome.

In the diploid strains BJ5626 and BY4743 (2.1.1, Table 4) one allele's open reading frame of RPB1 was replaced by the kanMX6 cassette. In case of BJ5626 transformation of DNA for homologous recombination was done by electroporation (2.2.2.3.2.2), which did not work for BY4743, therefore chemical transformation (2.2.2.3.2.1) was applied resulting in strains BJ5626 Δ*rpb1*/+ and BY4743 Δ*rpb1*/+ (2.1.1, Table 4 and Figure 19).

3.2.2.2 Cloning of an Rpb1 rescue plasmid

For construction of the rescue plasmid pRS316-Rpb1 (2.1.2, Table 7) the RPB1 ORF with 523 bp upstream and 281 bp downstream flanking regions from genomic DNA of

BJ5626 and BY4743 was amplified (2.2.1.1) using 7_Sc_Rpb1_500bp_up_XhoI_f with 12_Sc_Rpb1_260bp_down_SacI_r as PCR primers (2.1.3, Table 10). The fragment was inserted into pRS316 at the XhoI and SacI restriction sites. pRS316 has a low copy number in yeast cells.

3.2.2.3   Cloning of a Pep4 and Prb1 rescue plasmid for sporulation

BJ5626 *Δrpb1*/+ pRS316-Rpb1 and BY4743 *Δrpb1*/+ pRS316-Rpb1 (2.1.1, Table 4) were obtained upon transformation (2.2.2.2) of pRS316-Rpb1 into BJ5626 *Δrpb1*/+ and BY4743 *Δrpb1*/+. As BJ5626 *Δrpb1*/+ pRS316-Rpb1 was incompetent to sporulate due to the disruption of the protease genes PEP4 and PRB1 (Zubenko & Jones, 1981) the protease rescue plasmid pRS31N-Pep4-Prb1 (2.1.2, Table 7) was transformed into the strain (Figure 19). PEP4 and PRB1 were amplified using genomic DNA of BY4743 as template with 500 bp upstream and 195 bp or 200 bp downstream, respectively using Sc_Pep4_500bp_up_BamHI_f with Sc_Pep4_200bp_down_XhoI_r or Sc_Prb1_500bp_up_NotI_f with Sc_Prb1_200bp_down_BamHI_r, respectively as PCR primers (2.1.3, Table 10). The natNT2 cassette was amplified from pFA6a-natNT2 (2.1.2, Table 6) using pFA6a_S1_NdeI_f with pFA6a_S2_NsiI_r as PCR primers (2.1.3, Table 10). PEP4 was inserted into pRS316 (2.1.2, Table 7) between the BamHI and XhoI restriction sites, then PRB1 was inserted between the NotI and BamHI restriction site. Then the URA3 marker gene within the pRS316 backbone was removed, inserting the natNT2 cassette between the NdeI and NsiI restriction sites. Thus pRS31N-Pep4-Prb1 contains genes for the proteases Pep4 and Prb1 and carries a clonNAT resistance marker replacing the URA3 prototrophy marker gene of pRS316.

3.2.2.4   Sporulation to obtain haploid Rpb1 mutagenesis strains

BJ5626 Δ*rpb1*/+ pRS316-Rpb1 pRS31N-Pep4-Prb1 and BY4743 Δ*rpb1*/+ pRS316-Rpb1 were subjected to sporulation and dissected (2.2.2.4) and clones with the desired selection markers were selected to obtain haploid strains corresponding to BJ5464 Δ*rpb1* pRS316-Rpb1 and BY4741 Δ*rpb1* pRS316-Rpb1 (2.1.1, Table 4). These strains contain the RPB1 gene on a plasmid with a URA3 marker and can thus be used for plasmid shuffling with 5-FOA (2.2.2.6) after transformation of another (*e.g.* mutant) copy of RPB1 on a second plasmid with a different marker (Figure 23).

3.2.3   Establishment of a His$_{10}$-tag at Rpb1

3.2.3.1   Cloning of N- and C-terminal His$_{10}$-tag at Rpb1 on a plasmid

A possibility to purify Pol II complexes containing mutant Rpb1 even in the presence of wild type Rpb1 was desired. Therefore a His$_{10}$ affinity tag was introduced at Rpb1. Both an N- and C-terminal tag were created, with the N-terminal tag containing a penta(serinylalanine) linker to increase accessibility of the tag during affinity chromatography. The tags were introduced by site-directed mutagenesis using 7_Sc_Rpb1_500bp_up_XhoI_f with Sc_Rpb1_N-term-H$_{10}$AS$_5$_r and Sc_Rpb1_N-term-H$_{10}$AS$_5$_f with 8_Sc_Rpb1-EagI_down_BamHI_r and 11_Sc_Rpb1-BspHI_up_f with Sc_Rpb1_C-term-H$_{10}$_r and Sc_Rpb1_C-term-H$_{10}$_f with 12_Sc_Rpb1_260bp_down_SacI_r (2.1.3, Table 10) for the first PCR step (2.2.1.1) for the N- and C-terminal tags respectively using pRS316-Rpb1 as template. The two respective fragments were used as templates in a second PCR step using 7_Sc_Rpb1_500bp_up_XhoI_f with 8_Sc_Rpb1-EagI_down_BamHI_r and 11_Sc_Rpb1-BspHI_up_f with 12_Sc_Rpb1_260bp_down_SacI_r for the N- and C-terminal fragments, respectively. Fragments were then inserted between the XhoI and EagI or BsiWI and SacI restriction sites of pRS315-Rpb1, to create pRS315-Rpb1-N-H$_{10}$ and pRS315-Rpb1-C-H$_{10}$ (2.1.2, Table 7), respectively.

3.2.3.2   Influence on cell growth of N- and C-terminally tagged Rpb1

The His$_{10}$-tag at Rpb1 should not induce structural changes in Rpb1 that could influence Pol II activity, which might have an effect of yeast growth. Therefore pRS315-
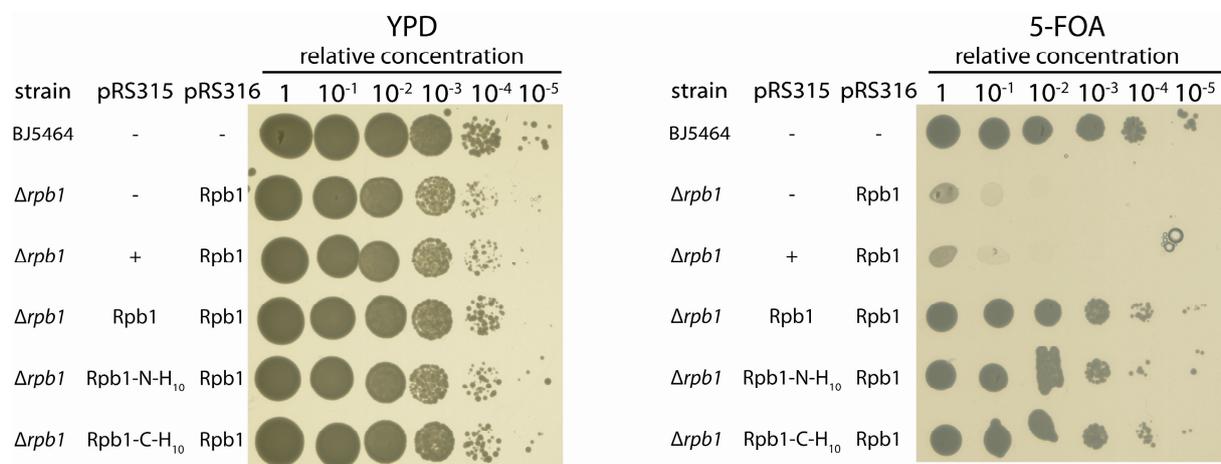
Figure 20: N- or C-terminal His$_{10}$-tag do not influence yeast growth.
Serial dilutions of yeast cells on a YPD plate (left) and a 5-FOA plate (right).

Rpb1-N-H$_{10}$ and pRS315-Rpb1-C-H$_{10}$ were transformed (2.2.2.2) into BJ5464 Δ*rpb1* pRS316-Rpb1 (2.1.1, Table 4). To shuffle plasmids (2.2.2.6) containing His-tagged Rpb1 serial dilutions of yeast cell suspensions were spotted on a YPD and 5-FOA plate (2.1.4, Table 14). Comparing growth of BJ5464 Δ*rpb1* pRS316-Rpb1 with BJ5464 on the YPD plate, the strain containing the only copy of RBP1 on a plasmid grows slightly slower than the corresponding wild type strain BJ5464 (Figure 20). Strains containing plasmid-encoded Rpb1 with a His-tag show the same growth as the control strains without His-tag both on the YPD and the 5-FOA plate. On the 5-FOA plate after loss of pRS316-Rpb1 no growth difference was observed between strains containing N- or C-terminally His-tagged Rpb1. Considering cell growth that is not influenced by the presence and position of the His-tag at Rpb1 both terminal His-tags are equally applicable.

3.2.3.3 Suitability of His-tags for purification via affinity chromatography

To test whether the N- and C-terminal His-tags at Rpb1 are suitable for Pol II purification comprising a Ni-NTA affinity chromatography step, purifications in small scale were performed (2.2.4.4). At the anion exchange step Pol II eluted at a conductivity of 50–60 mS/cm, which is typical also for Rpb3-tagged polymerase. Quantity and qual-
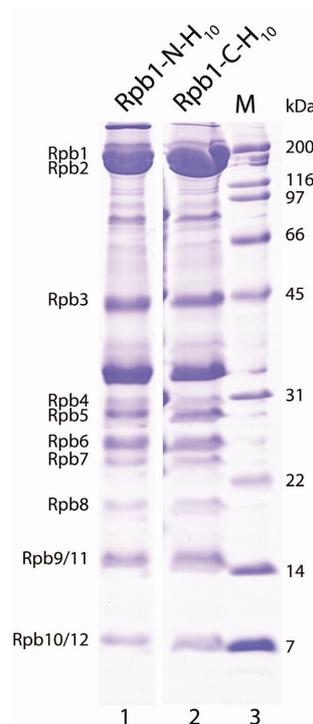
Figure 21: N- and C-terminal His$_{10}$-tag lead to equal purification results.

15 % SDS-PAGE (2.2.8) of the anion exchange elution fractions of Pol II purifications using N- and C-terminal His-tags. M: Marker.

ity of Pol II obtained in this test purification were comparable for both variants (Figure 21). Thus in terms of purification yield and purity both terminal His-tags at Rpb1 are equally useful.

3.2.3.4 Favouritism of the C-terminal His-tag at Rpb1

Neither the N- nor C-terminal His-tag at Rpb1 interfered with growth of yeast (3.2.3.2) nor did they show significant differences for Pol II purification suitability (3.2.3.3). Potential C-terminal degradation of Rpb1 is likely to result in loss of both the C-terminal His-tag and the CTD. Therefore using the C-terminal His-tag ensures that the CTD is entirely intact at the Ni-affinity step during the purification and hence the C-terminal His-tag was preferred to the N-terminal His-tag.

3.2.4 Mutagenesis studies of Rpb1

3.2.4.1 Strategy of plasmid-based mutagenesis

Mutagenesis of RPB1 was performed using a plasmid-based technique. To create the mutagenesis template pRS315-Rpb1-C-H_{10} (2.1.2, Table 7), RPB1 with flanking regions was cut out of pRS316-Rpb1 at the XhoI and SacI restriction sites and sub-
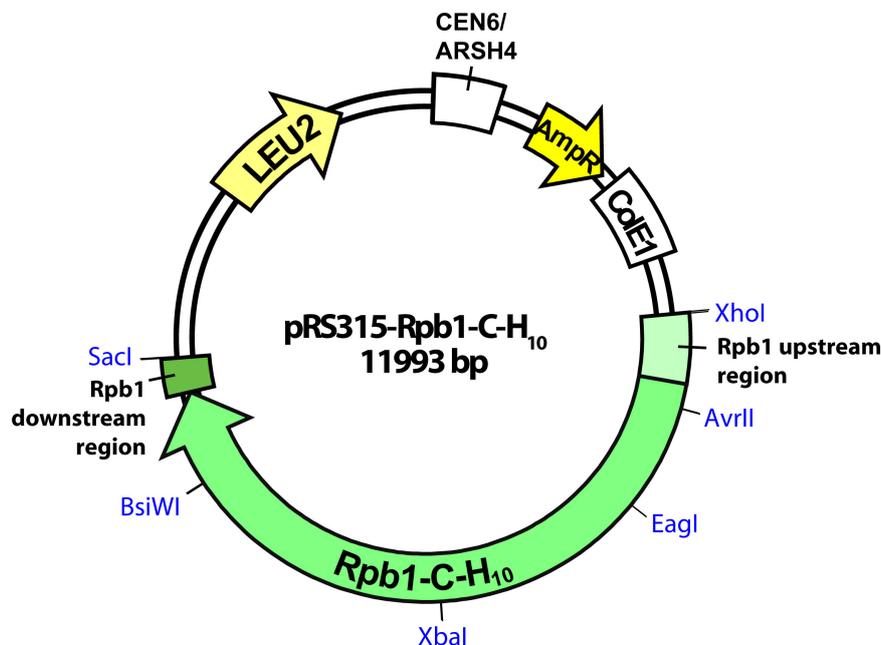
Figure 22: pRS315-Rpb1-C-H_{10} as basis for mutagenesis.

pRS315-Rpb1-C-H_{10} is depicted with the insert Rpb1-C-H_{10} with flanking regions (green) and the yeast and *E. coli* replicative elements CEN6/ARSH4 and ColE1 (white), respectively and selection markers LEU2 and AmpR (yellow), respectively. Single cutter restriction enzymes with recognition sites in and around the RPB1 gene are labelled in blue.

cloned into pRS315 at the same sites to obtain pRS315-Rpb1. The His-tag was introduced as described (3.2.3.1).
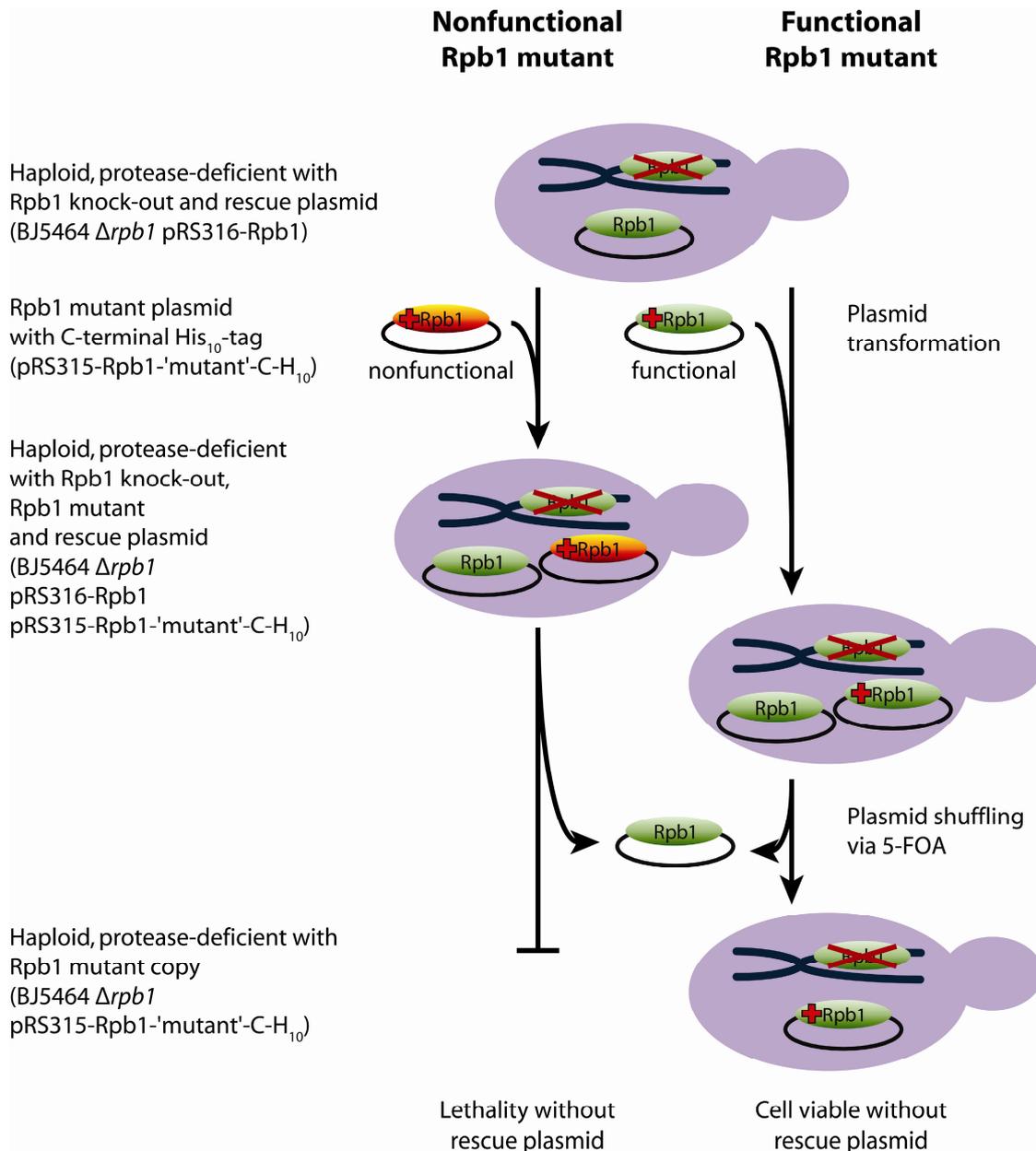
Figure 23: Creation of Rpb1 mutant strains.

Creation of strains containing Rpb1 mutant genes on a plasmid is depicted schematically.

To introduce a mutation in the RPB1 gene only a part of the gene was amplified. Depending on the location of the desired mutation a fragment between two of the single cutter restriction sites (XhoI, AvrII, EagI, XbaI, BsiWI and SacI) in the RPB1 coding region in pRS315-Rpb1-C-H$_{10}$ (Figure 22) was amplified introducing the mutation. In a first PCR step (2.2.1.1) the regions 5' and 3' of the mutation site were amplified separately, using an outer primer outside of the respective restriction enzyme recognition site with a primer containing the desired mutation. The fragments were combined in a second PCR step using only the outer primers to amplify the whole fragment. The fragment containing the mutation was then inserted between the respective restriction sites in pRS315-Rpb1-C-H$_{10}$ (2.1.2, Table 7) to obtain a plasmid encoding mutated and C-terminally His-tagged Rpb1 (Figure 23).

3.2.4.2 Example of a mutation lethal to yeast: Pol II enzymes bearing a lid deletion could not be purified

The lid loop of Pol II plays a role in separation of upstream template DNA and product RNA (1.2.2). Preformed RNA stem-loops with stems longer than 13 bp were not elongated by Pol II in previously described RNA elongation experiments (3.1.2.4, Figure 15) as the RNA probably cannot fit into the hybrid-binding region due to an
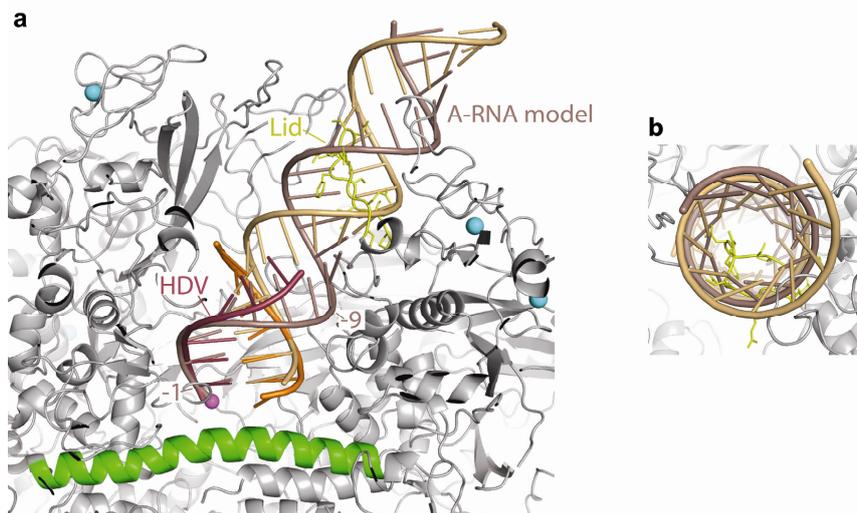
Figure 24: Upstream clash of the lid loop with a modelled HDV RNA duplex.

A rigid 24 bp duplex A-RNA was modelled into the Pol II elongation complex by superpositioning of terminal four base pairs with base pairs -1 to -4 in the HDV elongation complex structure (Figure 12b, c, Table 26). The view is from the front (**a**) and along the helix axis towards the Pol II active site (**b**). HDV product and template strand are shown in raspberry and orange, respectively. Product and template strand of the RNA model are shown in dark-salmon and lightorange, respectively. The lid loop with side chain stick models is shown in yellow.
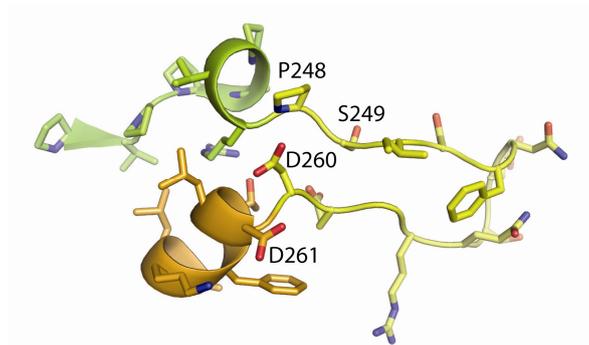
Figure 25: Pol II lid loop and adjacent region.

The lid loop and N- and C-terminal neighbouring regions are depicted in yellow, green and orange, respectively. Important residues are labelled.

upstream clash with the lid loop (Figure 24). To investigate this idea further Pol II enzyme lacking the lid loop was desired for RNA elongation experiments. In *S. cerevisiae* the lid loop comprises residues 248–260 of Rpb1 which are flanked by α-helices (Cramer *et al.*, 2001) (Figure 25). Lid deletion variants within RNA polymerases of other organisms were subjects of previous studies such as a deletion in *E. coli* RNA polymerase corresponding to residues 248–261 in Rpb1 (Toulokhonov & Landick, 2006) or *P. furiosus* RNA polymerase that was reconstituted from recombinantly expressed subunits lacking residues 248–260 of Rpb1 (Naji *et al.*, 2008).

Deletion of residues 248–260 in Rpb1 leads to direct connection of the terminal residues of the adjacent α-helices (Figure 25) which might influence the secondary structure of these regions and thus have secondary effects on Pol II function. Therefore two plasmid variants comprising a deletion of residues 248–260 (pRS315-Rpb1-Δlid1-C-H_{10}, 2.1.2, Table 7) and of residues 249–259 (pRS315-Rpb1-Δlid2-C-
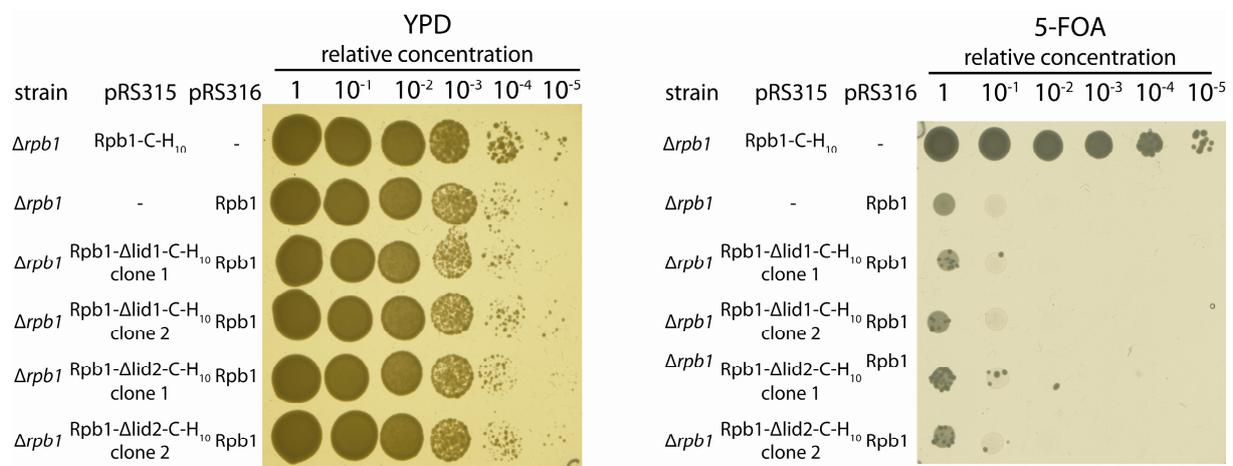
Figure 26: Lid deletion is lethal in *S. cerevisiae*.

Serial dilutions of yeast cells on a YPD plate (left) and a 5-FOA plate (right). Two representative clones each of both lid deletion variants (Δlid1 and Δlid2) cannot grow on a 5-FOA plate.
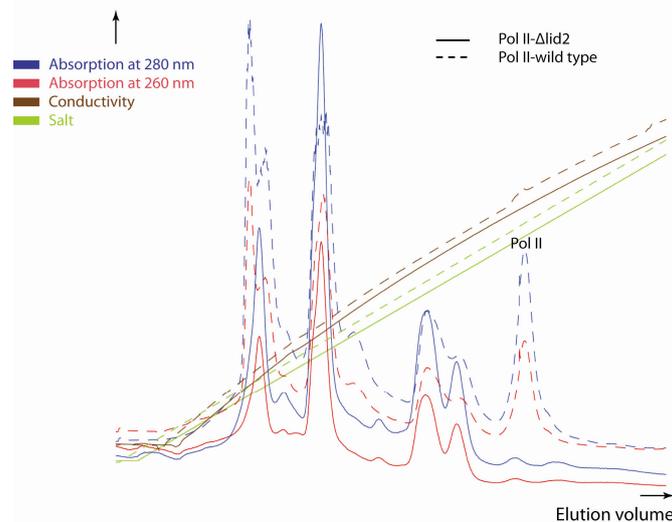
Figure 27: Pol II-Δlid2 could not be isolated by protein purification.

Overlay of anion exchange chromatograms of the last purification step of Pol II-Δlid2 and a representative wild type Pol II purification. Relative absorptions at 280 nm and 260 nm, conductivity and salt in the running buffer are shown as indicated by the colour code. Curves for Pol II-Δlid2 and wild type Pol II are depicted as solid and dashed lines, respectively. The position of the peak containing Pol II is indicated.

H_{10}, 2.1.2, Table 7) that should not induce undesired effects on secondary structures were cloned as described (3.2.4.1). After plasmid shuffling on a 5-FOA-containing plate (2.2.2.6) both lid deletion variants showed a lethal phenotype (Figure 26) confirming an essential role of the Pol II lid loop. Thus to cultivate cells containing a lid deletion variant a rescue copy of wild type RPB1 is required. The His-tag at the mutated copy of Rpb1 allows for selective purification of polymerases containing mutated proteins, while polymerases containing a wild type copy without tag should be separated.

A strain containing the Δlid2 variant and a wild type copy of RPB1 (BJ5464 *Δrpb1* pRS316-Rpb1 pRS315-Rpb1-Δlid2-C-H_{10}, 2.1.1, Table 4) was cultivated by fermentation (2.2.4.1 and 2.2.4.1.1) in SC -Leu medium (2.1.4, Table 14) selective for the plasmid encoding the Δlid2 gene and a purification of Pol II (2.2.4.3) was conducted. Unfortunately Pol II could not be obtained in sufficient amounts for any further studies. The anion exchange chromatogram of the Pol II-Δlid2 purification is generally comparable to a typical wild type Pol II purification chromatogram but the Pol II peak is missing (Figure 27). Cells containing an additional wild type copy of Rpb1 are functionally not dependent on the mutated version of the protein. As Pol II-Δlid2 is not sufficient for yeast cell viability (Figure 26) it is probably non-functional *in vivo* in at least one step of transcription.

When Pol II encounters DNA damages and cannot transcribe further, Rpb1 is ubiquitylated as a first step in transcription-coupled DNA repair (Bregman *et al.*, 1996) and subsequently subjected to proteasomal degradation (Beaudenon *et al.*, 1999; Ratner *et al.*, 1998). Specifically Rpb1 but not the whole Pol II complex is degraded upon DNA damage-inducing UV irradiation (Chen *et al.*, 2007). Ubiquitylation of Pol II does not only occur for polymerases stalled at DNA damage sites but also upon transcriptional arrest independent of DNA damages (Somesh *et al.*, 2005).

As the lid deletion in Pol II is a structurally minor change, a normal assembly and pre-initiation complex formation behaviour can be assumed for Pol II-Δlid2 *in vivo*. The essential role of the lid probably makes an appearance during the processes of transcription initiation or elongation. Thus lid-truncated Pol II might be arrested on DNA with Rpb1-Δlid2 being a subject for degradation. In turn this specific degradation might prevent successful purification of Pol II-Δlid2. A possibility to counteract degradation of Rpb1 is overexpression in yeast that can be induced by removal or addition of antibiotics (Garí *et al.*, 1997). A tetracycline-inducible promoter was amplified from pCM251 (2.1.2, Table 6) and inserted upstream of Rpb1-Δlid2 to create pRS315-Tet-Rpb1-Δlid2-C-H$_{10}$ (2.1.2, Table 7), which encodes Rpb1-Δlid2 under control of the inducible promoter. Preliminary experiments expressing Rpb1-Δlid2 from this plasmid did not indicate phenotypes suggestive of a successful overexpression and stable incorporation of Rpb1-Δlid2 into Pol II complexes. The Rpb1 subunit of Pol II-Δlid2 presented here serves as an example for transcriptionally incompetent Pol II mutants that appear to be quickly degraded while the wild type copy of Rpb1 can rescue cell viability. Hence purification of transcriptionally incompetent mutant Pol II enzymes is currently not possible, unless target protein levels and stability are significantly increased. Consistently a stabilisation could not be achieved by simple overexpression and purification also failed in the case of studies of mutant Rpb2 (Domecq *et al.*, 2010).

3.2.4.3 Example of a functional mutation: Pol II with an F loop mutation was successfully purified

The F loop is an element in bacterial RNA polymerase that is directly adjacent N-terminally to the bridge helix and contacts the trigger loop. It allosterically controls catalysis of nucleotide addition (Miropolskaya *et al.*, 2009). Among eukaryotic RNA

```
                                   Rpb9 interaction
                                   _____
Rpb1 762 SACVGQQSVEGKRIAFGFVDRTLPHFSKDDYSPESKGFVENSYLRGLTP
Rpc1 810 VAVVGQQIISGNRVPDGFQDRSLPHFPKNSKTPQSKGFVRNSFFSGLSP
         * **** :.*:*:. ** **:****.*:. :*:*****.**:: **:*

Rpb1-FIII 762 SACVGQQSVEGKRIAFGFQDRTLPHFPKNSKSPESKGFVENSYLRGLTP
```

Figure 28: Construct design of the Pol III F loop variant in Pol II.

An alignment of Rpb1 (grey) and its Pol III homolog Rpc1 (green) is shown. Five non-conserved residues within the Rpb9 interacting region (orange) were replaced by the corresponding Rpc1 residues to result in Rpb1-FIII.

polymerases there are sequence variations in the region homologous to the F loop in bacterial RNA polymerases. The F loop might be involved in intrinsic cleavage stimulation and its respective residues could contribute to the strong intrinsic cleavage activities observed for Pol I and Pol III, in contrast to Pol II (1.5.1). Within the research project of Wenjie Ruan (Patrick Cramer laboratory), the effect of sequences of the Pol III F loop on RNA cleavage stimulation via interaction with Rpb9 in the context of Pol II was to be studied. Therefore five non-conserved residues of the F loop in Rpb1 were mutated to the corresponding Pol III residues (Figure 28), obtaining Rpb1-FIII.

Cloning of the mutant was performed as described (3.2.4.1) and plasmid shuffling using 5-FOA (2.2.2.6) revealed the FIII mutant to be viable with a growth phenotype comparable to cells without F loop mutation (Figure 29). The variant of Pol II was successfully purified (2.2.4.3) with a yield of 0.6 mg Pol II-FIII per 100 g cells, which is lower than the typical yield for wild type Pol II but a reasonable yield that allows us to conduct functional and crystallographic studies of the mutant enzyme. Upon separation and visualisation of purified Pol II-FIII subunits by SDS-PAGE and Coomassie staining (2.2.8) it was found that one subunit is present in clearly substoichiometric amounts compared with wild type Pol II (Figure 30, lanes 2, 4). To prepare the Rpb9-
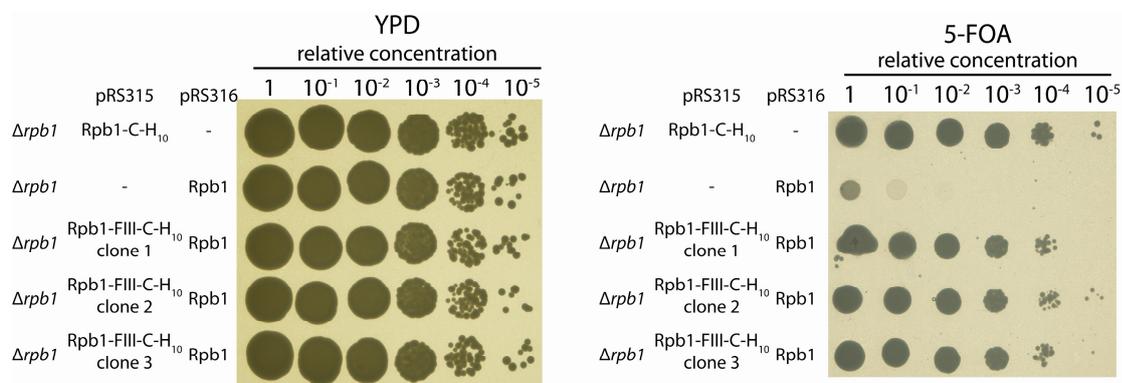
Figure 29: F loop mutation is viable in *S. cerevisiae*.

Serial dilutions of yeast cells on a YPD plate (left) and a 5-FOA plate (right). Three representative clones of both the FIII mutant show the same growth phenotype on a 5-FOA plate.
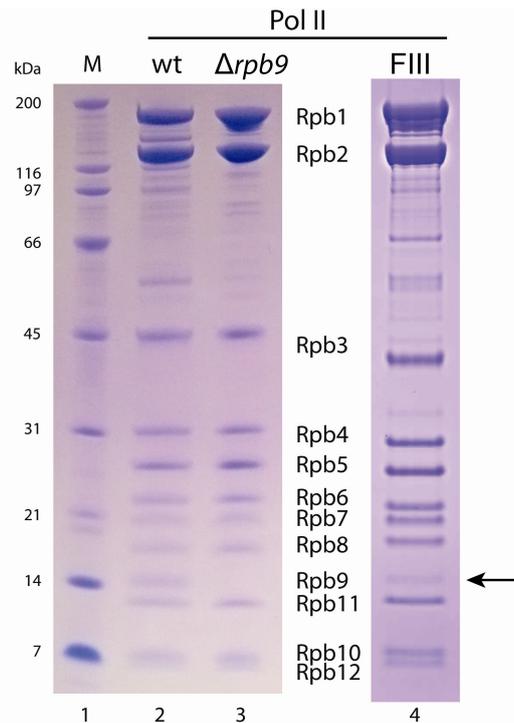
Figure 30: Rpb9 is not stably bound to Pol II-FIII.

4–12 % SDS-PAGE (2.2.8) showing wild type (wt) Pol II, Pol II lacking subunit Rpb9 (*Δrpb9*) and Pol II-FIII. Subunit Rpb9 is present in substoichiometric amounts in Pol II-FIII (arrow). The gel showing Pol II-FIII was conducted by Wenjie Ruan.

deleted strain BJ5464 Rpb3 His-Bio *Δrpb9* (2.1.1, Table 4) the natNT2 cassette was amplified from pFA6a-natNT2 (2.1.2, Table 6) and introduced into BJ5464 Rpb3 His-Bio (2.1.1, Table 4) by homologous recombination (2.2.2.3.3.1) to replace the RPB9 ORF. From this strain Pol II lacking subunit Rpb9 was purified. A comparison of Pol II-*Δrpb9* and Pol II-FIII (Figure 30, lanes 3, 4) confirms that the substoichiometric subunit in Pol II-FIII is Rpb9. It was probably partially lost during the process of purification due to reduced binding affinity of Rpb9 to Pol II comprising the mutated F loop. *In vitro* the functional enzymatic activity of Pol II-FIII was shown in RNA cleavage experiments performed by Wenjie Ruan. Fusion proteins of Rpb9 and its homologous Pol III subunit C11 (1.5.1) were previously found to stimulate a strong cleavage activity in Pol II-*Δrpb9* (Ruan *et al.*, *Manuscript submitted*). Upon incubation of Pol II-FIII with cleavage stimulating Rpb9–C11 fusion proteins (Ruan, *in preparation*) shortened RNA products resulting from RNA dinucleotide cleavage (1.5) are produced (Figure 31).
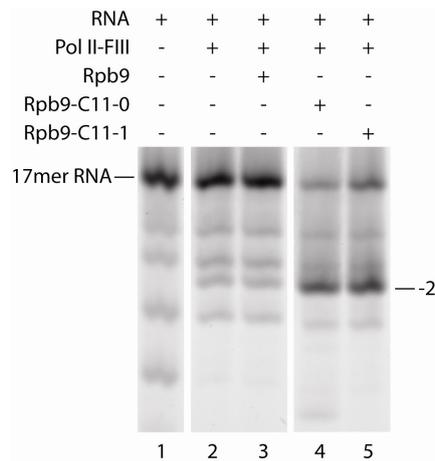
Figure 31: Pol II-FIII is active in stimulated RNA cleavage assays.

An RNA cleavage scaffold containing a G-G mismatch at position +1 was incubated with Pol II-FIII without or with Rpb9 or Rpb9-C11 fusion proteins. The dinucleotide cleavage product is labelled (-2). The bead-based cleavage experiment and the gel depicted here were conducted by Wenjie Ruan essentially as described (Sydow *et al.*, 2009). Details about the experimental procedure, cleavage scaffold and fusion proteins can be found elsewhere (Ruan, *in preparation*).

Pol II-FIII was successfully cloned and purified and its enzymatic activity was confirmed *in vitro*. Pol II-FIII is a functional enzyme bearing a mutation in Rpb1 that stands as an example for other functional Rpb1 mutations that can be produced with this established method.

4 Follow-up experiments and conclusions

Within this work the RdRP activity of purified *S. cerevisiae* Pol II was characterised *in vitro*. Pol II can synthesise RNA in an RNA-templated manner, but the activity is much slower and less processive than the DNA-dependent one. To perform efficient replication of the HDV antigenome human Pol II is probably extrinsically stimulated. HDAg, the only protein encoded by HDV was found to stimulate Pol II transcription activity in nuclear extracts of human cells (Yamaguchi *et al.*, 2001). However it is not clear if other factors are involved in this stimulation. Therefore the effect of recombinantly expressed HDAg on RdRP activity of purified Pol II was tested *in vitro*. Stimulation could not be observed, presumably because yeast and not human Pol II was used or more probably due to the fact that HDAg was recombinantly expressed, thus lacking host-specific posttranslational modifications. This result is consistent with the finding that recombinant HDAg could promote HDV RNA replication only from the genomic but not from the antigenomic strand (Sheu & Lai, 2000). Generally it could be that other factors not related to HDAg can positively stimulate the RdRP activity of Pol II either alone or cooperatively with HDAg. To look for such an activity, yeast nuclear extracts were prepared with the help of Martin Seizl and roughly fractionated. Upon addition of nuclear extract components to a Pol II RdRP assay, stimulation of Pol II could not be observed but rather RNA degradation due to RNases present in all nuclear fractions. Addition of commercial RNase inhibitors could not prevent RNA degradation efficiently without as well inhibiting Pol II activity.

As Pol I and Pol III are closely related to Pol II and as Pol I was already implicated in HDV replication, it seemed likely that they also have RdRP activity *in vitro*. In an *in vitro* RNA elongation assay using the HDV scaffold that is efficiently elongated by Pol II (3.1.2.1, Figure 10) RNA dinucleotide cleavage was observed upon incubation with Pol I (provided by Claus-D. Kuhn) and NTPs, indicating that Pol I can as well bind to the scaffold but its putative RdRP activity is much weaker than its RNA hydrolysis activity. Pol III (provided by Alessandro Vannini) did neither show strong elongation nor any cleavage activity, but definitive conclusions cannot be made from this experiment as Pol III was also very limitedly active in a DdRP control experiment, probably because the Pol III purification protocol was not yet optimised at the time of the experiment (A.V., personal communication). Thus, the roles of RNA polymerases

in HDV replication and in other cellular RdRP-involving processes, in consideration of other non-related RdRPs found recently in human (Maida *et al.*, 2009) and Drosophila (Lipardi & Paterson, 2009) still have to be clarified in detail.

As shown in this work Pol II could not elongate RNA stem-loops with a preformed stem longer than 13 bp. However during elongation of the HDV scaffold, elongation could proceed to the run-off corresponding to production of a stem with at least 25 bp, which would even be much longer during HDV genome synthesis. It seems that a longer nascent stem-loop that is produced by Pol II itself is accommodated within the Pol II complex in a structurally different way than a preformed one. That an RNA containing a bulge can be elongated by Pol II suggests that the bulge can allow bypass of the blocking element in Pol II, presumably the lid loop. How the inhibitory effect of this blocking element is avoided in case of elongation of the HDV scaffold remains unresolved. To clarify whether the lid loop is the blocking element Pol II enzyme containing a lid truncation was desired to be produced. As lid deletion is lethal to yeast cells a rescue copy of Rpb1 must be present to enable cell viability. From such a strain lid-deleted Pol II could not be purified in consistence with results from studies of other lethal Pol II mutant enzymes (Domecq *et al.*, 2010).

An Rpb1 mutagenesis system was established within this work. Mutations can be conveniently introduced by standard cloning procedures on an Rpb1-encoding plasmid. Mutations that cause loss of cell viability can be easily identified by plasmid shuffling. Pol II enzymes comprising lethal mutations could not yet be successfully purified. To be able to inspect all kinds of possible mutations, access to purified enzymes with non-functional mutations *in vivo* is required. Neither endogenous expression nor induced overexpression of the protein containing a non-functional mutation enabled successful purification. Inhibition of cellular degradation of mutant Pol II might be the only possibility to obtain respective mutant enzymes from this mutagenesis system. A strain should be used that is specifically defective in Pol II degradation. The Pol II ubiquitylation pathway would be a suitable target to be disrupted, affecting ubiquitylation-dependent Pol II degradation, while cell growth and protein production capabilities should at best not be negatively affected. Def1 is necessary to degrade Pol II when transcriptionally stalled due to a DNA damage (Woudstra *et al.*, 2002) or otherwise stalled during transcription elongation but does not affect stalled initiation complexes at promoters (Somesh *et al.*, 2005). Upon a

double-knock out of ubiquitin-conjugating enzymes Ubc4 and Ubc5, Rpb1 was neither affected by degradation upon UV irradiation nor by polyubiquitylation upon transcriptional arrest (Somesh *et al.*, 2005). Elc1 is indispensable for formation of polyubiquitin chains at Rpb1 *in vivo* (Ribar *et al.*, 2006) and *in vitro* (Harreman *et al.*, 2009). Thus Def1, Ubc4/Ubc5 and Elc1 are examples for possible candidates whose functions could be disrupted in the Rpb1 mutagenesis yeast strain. Putative defective degradation of mutant Rpb1 could lead to accumulation of Pol II containing mutant Rpb1, being a prerequisite for successful purification. Mutant Rpb1 in such strains could still be degraded by other pathways. Additionally secondary effects could occur, as transcriptionally incompetent Pol II enzymes that cannot be degraded might block the road on DNA hindering read-through of the wild type enzyme, thus leading to inefficient transcription and translation, which could be counterproductive for successful purification with suitable yields. However these effects cannot be predicted and should be approached experimentally. Instead of disturbing enzymatic functions that covalently link ubiquitin to Rpb1 the attachment point at Rpb1 could be removed. Rpb1 residue lysine 695 was found to be a ubiquitylation target in Pol II (Peng *et al.*, 2003) and thus this and/or other residues could be mutated to remove targets for Pol II ubiquitylation in the mutated version of Rpb1 but Pol II complexes containing wild type Rpb1 would not be affected and the general effect on yeast viability should be milder than when disrupting functions of enzymes that might play roles in several cellular processes.

A completely different approach to produce Pol II mutants would be reconstitution of subunits recombinantly expressed in *E. coli*. Although not possible so far in case of Pol II this approach is feasible for archaeal RNA polymerase (Naji *et al.*, 2007; Werner & Weinzierl, 2002). One technical difficulty to express Pol II subunits in *E. coli* is the size of large subunits, which comprise 192 kDa and 139 kDa for Rpb1 and Rpb2, respectively. Although concerning primary sequence archaeal RNA polymerase is highly similar to Pol II, a main difference is the subunit composition as both Rpb1 and Rpb2 correspond to two distinct subunits each in archaeal polymerase namely A' + A'' and B' + B'', respectively (Naji *et al.*, 2007; Werner & Weinzierl, 2002). This split into smaller subunits facilitates expression in *E. coli*. It could be tried to analogously split subunits Rpb1 and Rpb2 to form smaller transcriptional and translational units and to assemble Pol II from 14 subunits. If all domains are properly folded such an enzyme could be transcriptionally active, but little differences in its

activity due to lack of subunit connections should be carefully considered especially in detailed mechanistic studies.

Lethal Pol II mutants cannot be purified and thus cannot be studied in binding or activity assays yet. Mutants that are functional can be cloned and purified using the Rpb1 mutagenesis system established in this work. A mutation in the F loop that was presented here as an example is active in RNA cleavage assays. Furthermore mutations affecting number of CTD repeats, introducing a TEV cleavage site N-terminal of the CTD, clamp coiled coil mutations in the region interacting with Spt4/5 and mutations in the Pol II pore influencing Pol II cleavage activity have successfully been cloned, partially purified and tested for activity, partially by other research group members. The Rpb1 mutagenesis yeast strain designed for array analyses is also in use. In summary, a well-working mutagenesis system for Rpb1 has been established during this work and could already be reproduced for Rpb2 with technical assistance of Stefanie Etzold. Taken together, studies of non-lethal mutations in 64 % of the mass accounting for Pol II, including the active site region and the most important functional elements are now available. Pol II lacking subunit Rpb9, that was also produced during this work can be complemented with recombinant Rpb9 variants, enabling mutant studies of a third subunit of Pol II.

A mutagenesis system of Rpb1 and Rpb2 that is probably generally applicable for all kinds of non-lethal mutations was established. Upon fermentation and purification Pol II mutants can be obtained in reasonable yields. An expansion of the system to have access to purified proteins containing also lethal mutations as suggested above could allow for all variants of mutants thus strengthening the system even more. With the system that is now at hand, binding and mechanistic studies of Pol II concerning many different topics are much faster and easier accessible than before.

5   References

Armache KJ, Kettenberger H, Cramer P. (2003). Architecture of initiation-competent 12-subunit RNA polymerase II. *Proc Natl Acad Sci U S A* **100:** 6964-6968.

Armache KJ, Mitterweger S, Meinhart A, Cramer P. (2005). Structures of complete RNA polymerase II and its subcomplex, Rpb4/7. *J Biol Chem* **280:** 7131-7134.

Awrey DE, Weilbaecher RG, Hemming SA, Orlicky SM, Kane CM, Edwards AM. (1997). Transcription elongation through DNA arrest sites. A multistep process involving both RNA polymerase II subunit RPB9 and TFIIS. *J Biol Chem* **272:** 14747-14754.

Beaudenon SL, Huacani MR, Wang G, McDonnell DP, Huibregtse JM. (1999). Rsp5 ubiquitin-protein ligase mediates DNA damage-induced degradation of the large subunit of RNA polymerase II in Saccharomyces cerevisiae. *Mol Cell Biol* **19:** 6972-6979.

Bellí G, Garí E, Piedrafita L, Aldea M, Herrero E. (1998). An activator/repressor dual system allows tight tetracycline-regulated gene expression in budding yeast. *Nucleic Acids Res* **26:** 942-947.

Berg JM, Tymoczko JL, Stryer L. (2002). *Biochemistry*. 5th edn, WH Freeman.

Boeke JD, LaCroute F, Fink GR. (1984). A positive selection for mutants lacking orotidine-5'-phosphate decarboxylase activity in yeast: 5-fluoro-orotic acid resistance. *Mol Gen Genet* **197:** 345-346.

Bradford MM. (1976). A rapid and sensitive method for the quantitation of microgram quantities of protein utilizing the principle of protein-dye binding. *Anal Biochem* **72:** 248-254.

Bregman DB, Halaban R, van Gool AJ, Henning KA, Friedberg EC, Warren SL. (1996). UV-induced ubiquitination of RNA polymerase II: a novel modification deficient in Cockayne syndrome cells. *Proc Natl Acad Sci U S A* **93:** 11586-11590.

Brueckner F, Hennecke U, Carell T, Cramer P. (2007). CPD damage recognition by transcribing RNA polymerase II. *Science* **315:** 859-862.

Brueckner F, Ortiz J, Cramer P. (2009). A movie of the RNA polymerase nucleotide addition cycle. *Curr Opin Struct Biol* **19:** 294-299.

Brünger AT, Adams PD, Clore GM, DeLano WL, Gros P, Grosse-Kunstleve RW, Jiang JS, Kuszewski J, Nilges M, Pannu NS, Read RJ, Rice LM, Simonson T, Warren GL. (1998). Crystallography & NMR system: A new software suite for

macromolecular structure determination. *Acta Crystallogr D Biol Crystallogr* **54:** 905-921.

Buratowski S. (2009). Progression through the RNA polymerase II CTD cycle. *Mol Cell* **36:** 541-546.

Bushnell DA & Kornberg RD. (2003). Complete, 12-subunit RNA polymerase II at 4.1-A resolution: implications for the initiation of transcription. *Proc Natl Acad Sci U S A* **100:** 6969-6973.

Chao M. (2007). RNA recombination in hepatitis delta virus: implications regarding the abilities of mammalian RNA polymerases. *Virus Res* **127:** 208-215.

Chedin S, Riva M, Schultz P, Sentenac A, Carles C. (1998). The RNA cleavage activity of RNA polymerase III is mediated by an essential TFIIS-like subunit and is important for transcription termination. *Genes Dev* **12:** 3857-3871.

Chen X, Ruggiero C, Li S. (2007). Yeast Rpb9 plays an important role in ubiquitylation and degradation of Rpb1 in response to UV-induced DNA damage. *Mol Cell Biol* **27:** 4617-4625.

Cramer P, Bushnell DA, Fu J, Gnatt AL, Maier-Davis B, Thompson NE, Burgess RR, Edwards AM, David PR, Kornberg RD. (2000). Architecture of RNA polymerase II and implications for the transcription mechanism. *Science* **288:** 640-649.

Cramer P, Bushnell DA, Kornberg RD. (2001). Structural basis of transcription: RNA polymerase II at 2.8 angstrom resolution. *Science* **292:** 1863-1876.

Cramer P. (2004). RNA polymerase II structure: from core to functional complexes. *Curr Opin Genet Dev* **14:** 218-226.

Cramer P, Armache KJ, Baumli S, Benkert S, Brueckner F, Buchen C, Damsma GE, Dengl S, Geiger SR, Jasiak AJ, Jawhari A, Jennebach S, Kamenski T, Kettenberger H, Kuhn CD, Lehmann E, Leike K, Sydow JF, Vannini A. (2008). Structure of eukaryotic RNA polymerases. *Annu Rev Biophys* **37:** 337-352.

de Mercoyrol L, Corda Y, Job C, Job D. (1992). Accuracy of wheat-germ RNA polymerase II. General enzymatic properties and effect of template conformational transition from right-handed B-DNA to left-handed Z-DNA. *Eur J Biochem* **206:** 49-58.

DeLano WL. (2002). The PyMOL Molecular Graphics System. *DeLano Scientific*, San Carlos, CA, USA. http://www.pymol.org.

Dengl S & Cramer P. (2009). Torpedo nuclease Rat1 is insufficient to terminate RNA polymerase II in vitro. *J Biol Chem* **284:** 21270-21279.

Dezelee S, Sentenac A, Fromageot P. (1974). Role of deoxyribonucleic acid-ribonucleic acid hybrids in eukaryotes. Synthetic ribo- and deoxyribopolynucleotides as template for yeast ribonucleic acid polymerase B (or II). *J Biol Chem* **249:** 5978-5983.

Domecq C, Kireeva M, Archambault J, Kashlev M, Coulombe B, Burton ZF. (2010). Site-directed mutagenesis, purification and assay of Saccharomyces cerevisiae RNA polymerase II. *Protein Expr Purif* **69:** 83-90.

Edwards AM, Darst SA, Feaver WJ, Thompson NE, Burgess RR, Kornberg RD. (1990). Purification and lipid-layer crystallization of yeast RNA polymerase II. *Proc Natl Acad Sci U S A* **87:** 2122-2126.

Edwards AM, Kane CM, Young RA, Kornberg RD. (1991). Two dissociable subunits of yeast RNA polymerase II stimulate the initiation of transcription at a promoter in vitro. *J Biol Chem* **266:** 71-75.

Emsley P & Cowtan K. (2004). Coot: model-building tools for molecular graphics. *Acta Crystallogr D Biol Crystallogr* **60:** 2126-2132.

Fernández-Tornero C, Bottcher B, Rashid UJ, Steuerwald U, Florchinger B, Devos DP, Lindner D, Muller CW. (2010). Conformational flexibility of RNA polymerase III during transcriptional elongation. *EMBO J.*

Filipovska J & Konarska MM. (2000). Specific HDV RNA-templated transcription by pol II in vitro. *RNA* **6:** 41-54.

Fu J, Gnatt AL, Bushnell DA, Jensen GJ, Thompson NE, Burgess RR, David PR, Kornberg RD. (1999). Yeast RNA polymerase II at 5 Å resolution. *Cell* **98:** 799-810.

Garí E, Piedrafita L, Aldea M, Herrero E. (1997). A set of vectors with a tetracycline-regulatable promoter system for modulated gene expression in Saccharomyces cerevisiae. *Yeast* **13:** 837-848.

Gildehaus N, Neusser T, Wurm R, Wagner R. (2007). Studies on the function of the riboregulator 6S RNA from E. coli: RNA polymerase binding, inhibition of in vitro transcription and synthesis of RNA-directed de novo transcripts. *Nucleic Acids Res* **35:** 1885-1896.

Gnatt AL, Cramer P, Fu J, Bushnell DA, Kornberg RD. (2001). Structural basis of transcription: an RNA polymerase II elongation complex at 3.3 A resolution. *Science* **292:** 1876-1882.

Gudima S, Wu SY, Chiang CM, Moraleda G, Taylor J. (2000). Origin of hepatitis delta virus mRNA. *J Virol* **74:** 7204-7210.

Harreman M, Taschner M, Sigurdsson S, Anindya R, Reid J, Somesh B, Kong SE, Banks CA, Conaway RC, Conaway JW, Svejstrup JQ. (2009). Distinct ubiquitin ligases act sequentially for RNA polymerase II polyubiquitylation. *Proc Natl Acad Sci U S A* **106:** 20705-20710.

Horton NC & Finzel BC. (1996). The structure of an RNA/DNA hybrid: a substrate of the ribonuclease activity of HIV-1 reverse transcriptase. *J Mol Biol* **264:** 521-533.

Izban MG & Luse DS. (1992). The RNA polymerase II ternary complex cleaves the nascent transcript in a 3'----5' direction in the presence of elongation factor SII. *Genes Dev* **6:** 1342-1356.

Janke C, Magiera MM, Rathfelder N, Taxis C, Reber S, Maekawa H, Moreno-Borchart A, Doenges G, Schwob E, Schiebel E, Knop M. (2004). A versatile toolbox for PCR-based tagging of yeast genes: new fluorescent proteins, more markers and promoter substitution cassettes. *Yeast* **21:** 947-962.

Johnson TL & Chamberlin MJ. (1994). Complexes of yeast RNA polymerase II and RNA are substrates for TFIIS-induced RNA cleavage. *Cell* **77:** 217-224.

Jones TA, Zou JY, Cowan SW, Kjeldgaard M. (1991). Improved Methods for Building Protein Models in Electron-Density Maps and the Location of Errors in These Models. *Acta Crystallogr A* **47:** 110-119.

Kabsch W. (1993). Automatic Processing of Rotation Diffraction Data from Crystals of Initially Unknown Symmetry and Cell Constants. *J Appl Crystallogr* **26:** 795-800.

Kashlev M & Komissarova N. (2002). Transcription termination: primary intermediates and secondary adducts. *J Biol Chem* **277:** 14501-14508.

Kettenberger H, Armache KJ, Cramer P. (2003). Architecture of the RNA polymerase II-TFIIS complex and implications for mRNA cleavage. *Cell* **114:** 347-357.

Kettenberger H, Armache KJ, Cramer P. (2004). Complete RNA polymerase II elongation complex structure and its interactions with NTP and TFIIS. *Mol Cell* **16:** 955-965.

Kettenberger H, Eisenfuhr A, Brueckner F, Theis M, Famulok M, Cramer P. (2006). Structure of an RNA polymerase II-RNA inhibitor complex elucidates transcription regulation by noncoding RNAs. *Nat Struct Mol Biol* **13:** 44-48.

Kim JL, Nikolov DB, Burley SK. (1993a). Co-crystal structure of TBP recognizing the minor groove of a TATA element. *Nature* **365:** 520-527.

Kim Y, Geiger JH, Hahn S, Sigler PB. (1993b). Crystal structure of a yeast TBP/TATA-box complex. *Nature* **365:** 512-520.

Kireeva ML, Komissarova N, Kashlev M. (2000a). Overextended RNA:DNA hybrid as a negative regulator of RNA polymerase II processivity. *J Mol Biol* **299:** 325-335.

Kireeva ML, Komissarova N, Waugh DS, Kashlev M. (2000b). The 8-nucleotide-long RNA:DNA hybrid is a primary stability determinant of the RNA polymerase II elongation complex. *J Biol Chem* **275:** 6530-6536.

Kostrewa D, Zeller ME, Armache KJ, Seizl M, Leike K, Thomm M, Cramer P. (2009). RNA polymerase II-TFIIB structure and mechanism of transcription initiation. *Nature* **462:** 323-330.

Koyama H, Ito T, Nakanishi T, Sekimizu K. (2007). Stimulation of RNA polymerase II transcript cleavage activity contributes to maintain transcriptional fidelity in yeast. *Genes Cells* **12:** 547-559.

Kuhn CD, Geiger SR, Baumli S, Gartmann M, Gerber J, Jennebach S, Mielke T, Tschochner H, Beckmann R, Cramer P. (2007). Functional architecture of RNA polymerase I. *Cell* **131:** 1260-1272.

Kusser AG, Bertero MG, Naji S, Becker T, Thomm M, Beckmann R, Cramer P. (2008). Structure of an archaeal RNA polymerase. *J Mol Biol* **376:** 303-307.

Lai MM. (2005). RNA replication without RNA-dependent RNA polymerase: surprises from hepatitis delta virus. *J Virol* **79:** 7951-7958.

Lee TI & Young RA. (2000). Transcription of eukaryotic protein-coding genes. *Annu Rev Genet* **34:** 77-137.

Lehmann E. (2006). Cocrystallisation of yeast RNA polymerase II with mouse B2 RNA and studies of RNA-directed RNA synthesis by RNA polymerase II. *Master thesis*, Ludwig-Maximilians-Universität München.

Li YJ, Macnaughton T, Gao L, Lai MM. (2006). RNA-templated replication of hepatitis delta virus: genomic and antigenomic RNAs associate with different nuclear bodies. *J Virol* **80:** 6478-6486.

Lipardi C & Paterson BM. (2009). Identification of an RNA-dependent RNA polymerase in Drosophila involved in RNAi and transposon suppression. *Proc Natl Acad Sci U S A* **106:** 15645-15650.

MacNaughton TB, Gowans EJ, McNamara SP, Burrell CJ. (1991). Hepatitis delta antigen is necessary for access of hepatitis delta virus RNA to the cell transcriptional machinery but is not part of the transcriptional complex. *Virology* **184:** 387-390.

Macnaughton TB, Shi ST, Modahl LE, Lai MM. (2002). Rolling circle replication of hepatitis delta virus RNA is carried out by two different cellular RNA polymerases. *J Virol* **76:** 3920-3927.

Maida Y, Yasukawa M, Furuuchi M, Lassmann T, Possemato R, Okamoto N, Kasim V, Hayashizaki Y, Hahn WC, Masutomi K. (2009). An RNA-dependent RNA polymerase formed by TERT and the RMRP RNA. *Nature* **461:** 230-235.

Matzke M, Kanno T, Daxinger L, Huettel B, Matzke AJ. (2009). RNA-mediated chromatin-based silencing in plants. *Curr Opin Cell Biol* **21:** 367-376.

Mayer A, Lidschreiber M, Siebert M, Leike K, Soding J, Cramer P. (2010). Uniform transitions of the general RNA polymerase II transcription complex. *Nat Struct Mol Biol* **17:** 1272-1278.

Miropolskaya N, Artsimovitch I, Klimasauskas S, Nikiforov V, Kulbachinskiy A. (2009). Allosteric control of catalysis by the F loop of RNA polymerase. *Proc Natl Acad Sci U S A* **106:** 18942-18947.

Modahl LE, Macnaughton TB, Zhu N, Johnson DL, Lai MM. (2000). RNA-Dependent replication and transcription of hepatitis delta virus RNA involve distinct cellular RNA polymerases. *Mol Cell Biol* **20:** 6030-6039.

Moraleda G & Taylor J. (2001). Host RNA polymerase requirements for transcription of the human hepatitis delta virus genome. *J Virol* **75:** 10161-10169.

Naji S, Grunberg S, Thomm M. (2007). The RPB7 orthologue E' is required for transcriptional activity of a reconstituted archaeal core enzyme at low temperatures and stimulates open complex formation. *J Biol Chem* **282:** 11047-11057.

Naji S, Bertero MG, Spitalny P, Cramer P, Thomm M. (2008). Structure-function analysis of the RNA polymerase cleft loops elucidates initial transcription, DNA unwinding and RNA displacement. *Nucleic Acids Res* **36:** 676-687.

Naryshkina T, Kuznedelov K, Severinov K. (2006). The role of the largest RNA polymerase subunit lid element in preventing the formation of extended RNA-DNA hybrid. *J Mol Biol* **361:** 634-643.

Nesser NK, Peterson DO, Hawley DK. (2006). RNA polymerase II subunit Rpb9 is important for transcriptional fidelity in vivo. *Proc Natl Acad Sci U S A* **103:** 3268-3273.

Otwinowski Z & Minor W. (1997). Processing of X-ray diffraction data collected in oscillation mode. *Method Enzymol* **276:** 307-326.

Peng J, Schwartz D, Elias JE, Thoreen CC, Cheng D, Marsischky G, Roelofs J, Finley D, Gygi SP. (2003). A proteomics approach to understanding protein ubiquitination. *Nat Biotechnol* **21:** 921-926.

Poole AM & Logan DT. (2005). Modern mRNA proofreading and repair: clues that the last universal common ancestor possessed an RNA genome? *Mol Biol Evol* **22:** 1444-1455.

Potterton E, Briggs P, Turkenburg M, Dodson E. (2003). A graphical user interface to the CCP4 program suite. *Acta Crystallogr D Biol Crystallogr* **59:** 1131-1137.

Rackwitz HR, Rohde W, Sanger HL. (1981). DNA-dependent RNA polymerase II of plant origin transcribes viroid RNA into full-length copies. *Nature* **291:** 297-301.

Ratner JN, Balasubramanian B, Corden J, Warren SL, Bregman DB. (1998). Ultraviolet radiation-induced ubiquitination and proteasomal degradation of the large subunit of RNA polymerase II. Implications for transcription-coupled DNA repair. *J Biol Chem* **273:** 5184-5189.

Ribar B, Prakash L, Prakash S. (2006). Requirement of ELC1 for RNA polymerase II polyubiquitylation and degradation in response to DNA damage in Saccharomyces cerevisiae. *Mol Cell Biol* **26:** 3999-4005.

Rozenski J. (1999). Mongo Oligo Mass Calculator v2.06. http://library.med.utah.edu/masspec/mongo.htm.

Ruan W. (*in preparation*). *Dr. rer. nat. thesis*, Ludwig-Maximilians-Universität München.

Ruan W, Lehmann E, Cramer P. Evolution of two modes of intrinsic RNA polymerase transcript cleavage. *Manuscript submitted*.

Sakurai H, Mitsuzawa H, Kimura M, Ishihama A. (1999). The Rpb4 subunit of fission yeast *Schizosaccharomyces pombe* RNA polymerase II is essential for cell viability and similar in structure to the corresponding subunits of higher eukaryotes. *Mol Cell Biol* **19:** 7511-7518.

Salgado PS, Koivunen MR, Makeyev EV, Bamford DH, Stuart DI, Grimes JM. (2006). The structure of an RNAi polymerase links RNA silencing and transcription. *PLoS Biol* **4:** e434.

Schultz LD & Hall BD. (1976). Transcription in yeast: alpha-amanitin sensitivity and other properties which distinguish between RNA polymerases I and III. *Proc Natl Acad Sci U S A* **73:** 1029-1033.

Schwartz LB, Sklar VE, Jaehning JA, Weinmann R, Roeder RG. (1974). Isolation and partial characterization of the multiple forms of deoxyribonucleic acid-

dependent ribonucleic acid polymerase in the mouse myeloma, MOPC 315. *J Biol Chem* **249:** 5889-5897.

Sheu GT & Lai MM. (2000). Recombinant hepatitis delta antigen from E. coli promotes hepatitis delta virus RNA replication only from the genomic strand but not the antigenomic strand. *Virology* **278:** 578-586.

Sikorski RS & Hieter P. (1989). A system of shuttle vectors and yeast host strains designed for efficient manipulation of DNA in *Saccharomyces cerevisiae*. *Genetics* **122:** 19-27.

Sikorski TW & Buratowski S. (2009). The basal initiation machinery: beyond the general transcription factors. *Curr Opin Cell Biol* **21:** 344-351.

Somesh BP, Reid J, Liu WF, Sogaard TM, Erdjument-Bromage H, Tempst P, Svejstrup JQ. (2005). Multiple mechanisms confining RNA polymerase II ubiquitylation to polymerases undergoing transcriptional arrest. *Cell* **121:** 913-923.

Sosunov V, Sosunova E, Mustaev A, Bass I, Nikiforov V, Goldfarb A. (2003). Unified two-metal mechanism of RNA synthesis and degradation by RNA polymerase. *EMBO J* **22:** 2234-2244.

Studier FW. (2005). Protein production by auto-induction in high density shaking cultures. *Protein Expr Purif* **41:** 207-234.

Sydow JF, Brueckner F, Cheung AC, Damsma GE, Dengl S, Lehmann E, Vassylyev D, Cramer P. (2009). Structural basis of transcription: mismatch-specific fidelity mechanisms and paused RNA polymerase II with frayed RNA. *Mol Cell* **34:** 710-721.

Taylor JM. (2003). Replication of human hepatitis delta virus: recent developments. *Trends Microbiol* **11:** 185-190.

Toulokhonov I & Landick R. (2006). The role of the lid element in transcription by E. coli RNA polymerase. *J Mol Biol* **361:** 644-658.

Vassylyev DG, Sekine S, Laptenko O, Lee J, Vassylyeva MN, Borukhov S, Yokoyama S. (2002). Crystal structure of a bacterial RNA polymerase holoenzyme at 2.6 A resolution. *Nature* **417:** 712-719.

Wach A, Brachat A, Pöhlmann R, Philippsen P. (1994). New heterologous modules for classical or PCR-based gene disruptions in *Saccharomyces cerevisiae*. *Yeast* **10:** 1793-1808.

Wang D, Bushnell DA, Westover KD, Kaplan CD, Kornberg RD. (2006). Structural basis of transcription: role of the trigger loop in substrate specificity and catalysis. *Cell* **127:** 941-954.

Wassarman KM & Saecker RM. (2006). Synthesis-mediated release of a small RNA inhibitor of RNA polymerase. *Science* **314:** 1601-1603.

Weilbaecher RG, Awrey DE, Edwards AM, Kane CM. (2003). Intrinsic transcript cleavage in yeast RNA polymerase II elongation complexes. *J Biol Chem* **278:** 24189-24199.

Werner F & Weinzierl RO. (2002). A recombinant RNA polymerase II-like enzyme capable of promoter-specific transcription. *Mol Cell* **10:** 635-646.

Westover KD, Bushnell DA, Kornberg RD. (2004). Structural basis of transcription: nucleotide selection by rotation in the RNA polymerase II active center. *Cell* **119:** 481-489.

Whitehall SK, Bardeleben C, Kassavetis GA. (1994). Hydrolytic cleavage of nascent RNA in RNA polymerase III ternary transcription complexes. *J Biol Chem* **269:** 2299-2306.

Woudstra EC, Gilbert C, Fellows J, Jansen L, Brouwer J, Erdjument-Bromage H, Tempst P, Svejstrup JQ. (2002). A Rad26-Def1 complex coordinates repair and RNA pol II proteolysis in response to DNA damage. *Nature* **415:** 929-933.

Woychik NA. (1998). Fractions to functions: RNA polymerase II thirty years later. *Cold Spring Harb Symp Quant Biol* **63:** 311-317.

Yamaguchi Y, Filipovska J, Yano K, Furuya A, Inukai N, Narita T, Wada T, Sugimoto S, Konarska MM, Handa H. (2001). Stimulation of RNA polymerase II elongation by hepatitis delta antigen. *Science* **293:** 124-127.

Yamaguchi Y, Mura T, Chanarat S, Okamoto S, Handa H. (2007). Hepatitis delta antigen binds to the clamp of RNA polymerase II and affects transcriptional fidelity. *Genes Cells* **12:** 863-875.

Yuzenkova Y & Zenkin N. (2010). Central role of the RNA polymerase trigger loop in intrinsic RNA hydrolysis. *Proc Natl Acad Sci U S A* **107:** 10878-10883.

Zenkin N, Yuzenkova Y, Severinov K. (2006). Transcript-assisted transcriptional proofreading. *Science* **313:** 518-520.

Zhang J, Palangat M, Landick R. (2010). Role of the RNA polymerase trigger loop in catalysis and pausing. *Nat Struct Mol Biol* **17:** 99-104.

Zhang Y, Kim Y, Genoud N, Gao J, Kelly JW, Pfaff SL, Gill GN, Dixon JE, Noel JP. (2006). Determinants for dephosphorylation of the RNA polymerase II C-terminal domain by Scp1. *Mol Cell* **24:** 759-770.

Zubenko GS & Jones EW. (1981). Protein degradation, meiosis and sporulation in proteinase-deficient mutants of Saccharomyces cerevisiae. *Genetics* **97:** 45-64.

Zuker M. (2003). Mfold web server for nucleic acid folding and hybridization prediction. *Nucleic Acids Res* **31:** 3406-3415.

6 Abbreviations

5-FOA	5-fluoroorotic acid
°C	degree Celsius
Å	Ångstrom
Amp	ampicillin
APS	ammonium peroxodisulfate
ATP	adenosine 5'-triphosphate
b	base
bp	base pair
BSA	bovine serum albumin
ccc	clamp coiled coil
C-H$_6$	C-terminal hexahistidine tag
C-H$_{10}$	C-terminal decahistidine tag
CSM	complete supplement mixture
CTD	C-terminal domain
CTP	cytidine 5'-triphosphate
cv	column volume
Da	dalton
DdRP	DNA-dependent RNA polymerase
DNA	deoxyribonucleic acid
dNTP	deoxynucleoside triphosphate
DMSO	dimethylsulfoxide
DTT	dithiothreitol
E. coli	*Escherichia coli*
EC	elongation complex
EDTA	ethylene diamine tetraacetic acid
e.g.	for example [Latin: *exempli gratia*]
et al.	and others [Latin: *et alii*]
EtOH	ethanol
FAM	6-carboxyfluorescein
GTP	guanosine 5'-triphosphate
h	hour
HDAg	hepatitis delta antigen
HDV	human hepatitis delta virus
HEPES	2-[4-(2-hydroxyethyl)-1-piperazinyl]-ethanesulfonic acid
His	histidine
I	intensity
i.e.	that is [Latin: *id est*]
IPTG	isopropyl-β-D-thiogalactopyranoside
LB	lysogeny broth
Leu	leucine
l	litre
M	molar (mole/litre)
MES	2-(N-morpholino)ethanesulfonic acid
min	minute
MOPS	3-(N-morpholino)propanesulfonic acid

M_r	relative molecular mass
mRNA	messenger RNA
MWCO	molecular weight cut off
N-H$_{10}$-(SA)$_5$	N-terminal decahistidine-penta(serinylalanine) tag
NF	non-fluorescent
Ni-NTA	nickel-nitrilotriacetic acid
Nl	normal litre
nt	nucleotide
NTP	nucleoside triphosphate
OAc	acetyl-oxy
OD$_{600}$	optical density at 600 nm
ORF	open reading frame
p.a.	for analysis [Latin: *pro analysi*]
PCR	polymerase chain reaction
PEG	poly(ethylene glycol)
PI	protease inhibitor
PMT	photomultiplier tube
Pol	polymerase
Pwo	*Pyrococcus woesei*
R	residual index
RdRP	RNA-dependent RNA polymerase
RNA	ribonucleic acid
RNase	ribonuclease
Rpb	RNA polymerase B subunit
Rpb4/7	heterodimer Rpb4 and Rpb7
RNAi	RNA interference
rpm	revolutions per minute
rRNA	ribosomal RNA
RT	room temperature
SC	synthetic complete
S. cerevisiae	*Saccharomyces cerevisae* (baker's yeast)
SDS-PAGE	sodium dodecylsulfate polyacrylamide gel electrophoresis
SLS	Swiss Light Source
ssDNA	single stranded DNA
T	temperature
Taq	*Thermus aquaticus*
TB	transcription buffer
TBE	tris-borate-EDTA
TBP	TATA-binding protein
TCA	trichloroacetic acid
TCEP	tris(2-carboxyethyl) phosphine hydrochloride
TE	tris-EDTA
TEMED	N,N,N',N'-tetramethylethylenediamine
Tet	tetracycline
TF	transcription factor
TFB-I, TFB-II	transformation buffer I and II
Tris	tris-(hydroxymethyl)-aminomethane
tRNA	transfer RNA
Trp	tryptophane

U	unit
Ura	uracil
UTP	uridine 5'-triphosphate
v/v	volume per volume
w/v	weight per volume
× g	times gravity
YNB	yeast nitrogen base without amino acids
YP	yeast extract peptone
YPD	yeast extract peptone dextrose

Bases in nucleic acids:

A	adenine
C	cytosine
G	guanine
T	thymine
U	uracil

7 Curriculum vitae

Elisabeth Lehmann

Date of birth: 11th December, 1981

Place of birth: Dresden, Germany

Nationality: German

Marital status: unmarried

Education

1988–1992	Primary School
1992–2001	Secondary School Städtisches Bertolt-Brecht-Gymnasium, München Degree: *Allgemeine Hochschulreife* (general qualification for university entrance)
2001–2004	Studies in Chemistry and Biochemistry at the Ludwig-Maximilians-Universität München Degree: Bachelor of Science
2004–2006	Studies in Biochemistry at the Ludwig-Maximilians-Universität München Degree: Master of Science (equivalent to *Diplom-Biochemikerin*)
Nov 2006–	PhD thesis in the research group of Prof. Dr. Patrick Cramer, Gene Center of the Ludwig-Maximilians-Universität München

Publications

Kashkina E, Anikin M, Brueckner F, Lehmann E, Kochetkov SN, McAllister WT, Cramer P, Temiakov D (2007). Multisubunit RNA polymerases melt only a single DNA base pair downstream of the active site. *J Biol Chem* **282**(30)**:** 21578-21582. Erratum in (2009): *J Biol Chem* **284:** 22500.

Rippe K, Schrader A, Riede P, Strohner R, Lehmann E, Längst G (2007). DNA sequence- and conformation-directed positioning of nucleosomes by chromatin-remodeling complexes. *Proc Natl Acad Sci U S A* **104**(40)**:** 15635-15640.

Lehmann E, Brueckner F, Cramer P (2007). Molecular basis of RNA-dependent RNA polymerase II activity. *Nature* **450:** 445-449.

Andrecka J, Lewis R, Brückner F, Lehmann E, Cramer P, Michaelis J (2008). Single-molecule tracking of mRNA exiting from RNA polymerase II. *Proc Natl Acad Sci U S A* **105:** 135-140.

Cramer P, Armache KJ, Baumli S, Benkert S, Brueckner F, Buchen C, Damsma GE, Dengl S, Geiger SR, Jasiak AJ, Jawhari A, Jennebach S, Kamenski T, Kettenberger H, Kuhn CD, Lehmann E, Leike K, Sydow JF, Vannini A (2008). Structure of eukaryotic RNA polymerases. *Annu Rev Biophys* **37:** 337-352.

Brueckner F, Armache KJ, Cheung A, Damsma GE, Kettenberger H, Lehmann E, Sydow J, Cramer P (2009). Structure-function studies of the RNA polymerase II elongation complex. *Acta Crystallogr D Biol Crystallogr* **65:** 112-120.

Sydow JF, Brueckner F, Cheung AC, Damsma GE, Dengl S, Lehmann E, Vassylyev D, Cramer P (2009). Structural basis of transcription: mismatch-specific fidelity mechanisms and paused RNA polymerase II with frayed RNA. *Mol Cell* **34:** 710-721.

Ruan W, Lehmann E, Thomm M, Kostrewa D, Cramer P. Evolution of two modes of intrinsic RNA polymerase transcript cleavage. Manuscript submitted.